Advances in Colloid and Interface Science
78 (1998) 99–195

ADVANCES IN COLLOID AND INTERFACE SCIENCE

Structure, dynamics and transport properties of microemulsions

S.P. Moulik[a,*], B.K. Paul[b,*]

[a] *Centre for Surface Science, Department of Chemistry, Jadavpur University, Calcutta 700 032, India*
[b] *Geological Studies Unit, Indian Statistical Institute, 203 Barrackpore Trunk Road, Calcutta 700 035, India*

Abstract

The structure, dynamics and transport behaviors of microemulsions are physicochemically unique and need exploration for basic understanding of their formation, state of aggregation, internal interaction, and stability with reference to their probable uses. In this review, the structural characteristics of microemulsions and their dynamic and transport behaviors have been presented in detail. The underlying principles of the methodologies used for the above understanding have been concisely documented and discussed. An attempt has been made to maintain minimum overlapping of the contents of one section with another. As far as practicable, an effort has been made to include relevant references of the past and present works. Our apology to those authors whose works have escaped our notice.

Keywords: Dispersion; Structure; Diffusion; Conductance; Viscosity; Liquid membrane behavior

Contents

1. Introduction

Microemulsions [1] are compartmentalized liquids of potential current and future application prospects. They are dispersions of either 'water in oil' or 'oil in water' stabilized by pure or mixed amphiphiles, the latter is required for significant lowering of the oil–water interfacial tension by way of their interfacial adsorption, thus to help minimize the related positive free energy change of dispersion associated with surface formation [2–6]. The resultant microemulsions are isotropic, normally low viscous and thermodynamically stable solutions (dispersions) having a prolonged shelf-life [5,7,8]. Their, average particle size may fall in the range of 5–100 nm; they are polydisperse in nature and the polydispersity decreases with decreasing particle size. The microemulsions are physicochemically contrasted from macroemulsions (normally called emulsions), in the latter, the particle size is much larger, transparency is absent, stability is short and handling is restricted. Occasional homogenization–agitation is required to prevent macroemulsions from breaking (or phase separation). They are thus kinetically stable whereas microemulsions can be formed with expenditure of a very little energy (can be supplemented by the thermal energy of the system) and are thus thermodynamically stable. A mixture of the right composition of water, amphiphile and oil may spontaneously homogenize itself forming a microemulsion.

The water–oil microemulsion is topologically similar to reverse micelles [9–11] (where the polar heads of the amphiphiles are oriented inward and the non-polar tails orient towards the oil continuum); their description rests on the availability of free water in the core called the 'micro-pool'. The compositions yielding a rigid interior (or core) by immobilization of the water present, by way of hydration of the polar (or ionic) heads of the amphiphile and the counterions (when present) are termed 'reverse micelles'; compositions having mobile or free water in the core after satisfying the hydration requirements of the amphiphile head groups and counterions are called 'microemulsions'. The size of reverse micelles are thus normally restricted within 5 nm; a grown size smaller than 5 nm changes the status to microemulsion. Such a dimension dependent change of status may not hold for oil–water dispersions where the solvent dependent bound and free oil in the pool is of least physicochemical significance as in reverse micelles; of course normal micelles can consume oil and grow in size resulting o/w microemulsion. Pictorial representations of reverse micelles and microemulsions are given in Fig. 1.

It is important to clarify the nature and composition of the amphiphile used in the formation of microemulsion. A surfactant mixed with a cosurfactant in a certain proportion is most often convenient, and lower alkanols (like butanol, pentanol and hexanol), and amines (like butylamine, hexylamine) can be profitably employed for this purpose. It is considered that their presence in the interface

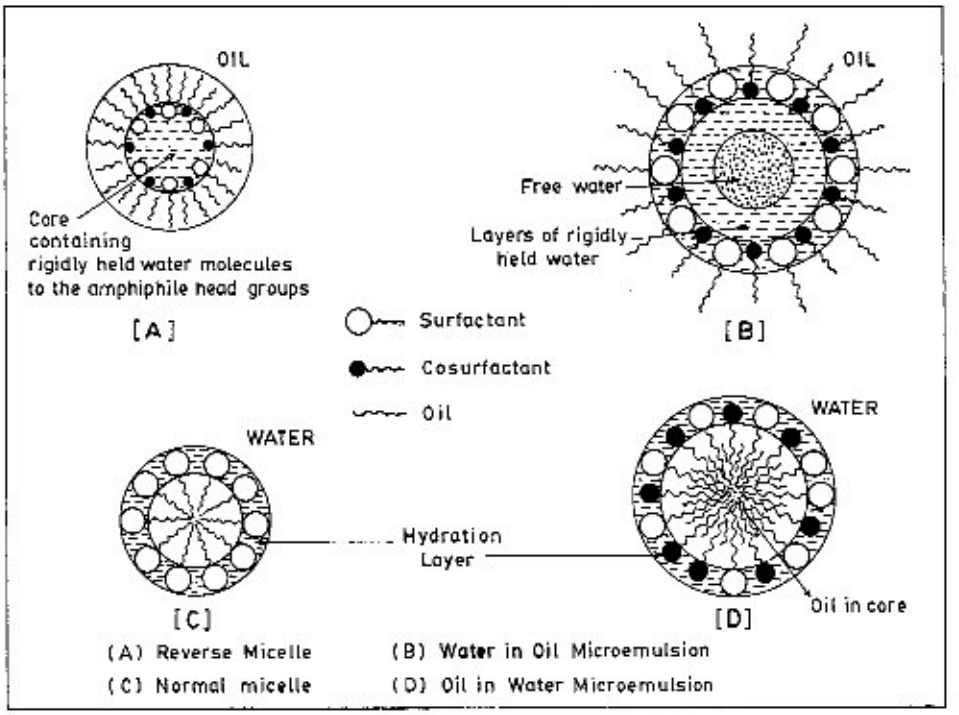

Fig. 1. Pictorial representations of reverse micelles and microemulsions.

between water and oil imparts flexibility, in addition to lowering the interfacial tension causing easier surface bending to energetically favored dispersion.

2. Phase manifestation

The ternary mixtures of water–amphiphile–oil or explicitly quaternary mixtures of water–surfactant–cosurfactant–oil can have different characteristic phase manifestations which was elaborately described by Winsor [12]. The concerned mixed systems may essentially fall into four categories:

1. dispersion of oil in water (o/w) in contact with essentially oil (Winsor I);
2. dispersion of water in oil (w/o) in contact with essentially water (Winsor II);
3. both o/w and w/o dispersions are simultaneously present in the same domain in mixed state in separate contacts with both oil and water (Winsor III); and
4. a homogeneous single phase of dispersion either o/w or w/o not in contact with any other phase (Winsor IV).

By adjusting the proportion of constituents, interconversion among the different classes (types) can be achieved. There are also scanty reports [13–15] of simultane-

ous presence of two microemulsion phases in contact with each other, and one in separate contact with water and the other with such a contact with oil. This may be considered as an extension of Winsor's classification forming the fifth category. A composite look of the above state of description is depicted in Fig. 2.

The experiences of workers have revealed that the phase forming behaviors [16–33] of ternary and quaternary microemulsion forming combinations depend on a number of factors, i.e. the types of polar medium (water, glycol, glycerol etc.), oils, amphiphiles, the presence of additive (especially electrolytes), the temperature, the pressure, etc. [34]. The extent of the phases and their internal structure are obviously influenced by the intrinsic and extrinsic factors mentioned earlier [35,36]. Both spherical and non-spherical forms of the dispersed state may aggregate forming chains, lamellae, mesophases, liquid crystalline states etc. Often gels of varying consistency are also formed. There higher states of aggregation are distinct departures from the genuine state of microemulsion. Pioneering works in this direction have been done by Ekwall and others [37–42]. The mixed water–amphiphile–oil systems can have complex phase intricacies, their identifications are painstaking but rewarding. In Fig. 3, phase manifestations on a triangular and tetrahedral representations are illustrated for two typical mixed systems.

3. Microemulsion structure

The internal structure of microemulsion may be complex and varied [43–49]. It is physicochemically conceived that on the lower side of water addition, the amphiphile requirement to augment dispersion is low, and on the average, a spherical dispersion of amphiphile-coated water nanodroplets exist in oil continuum (Winsor III). The situation is reverse for compositions with a low percentage of oil and a high percentage of water (Winsor I). The increasing dispersant concentration ends up with increased droplet dimension together with distortion of the spherical

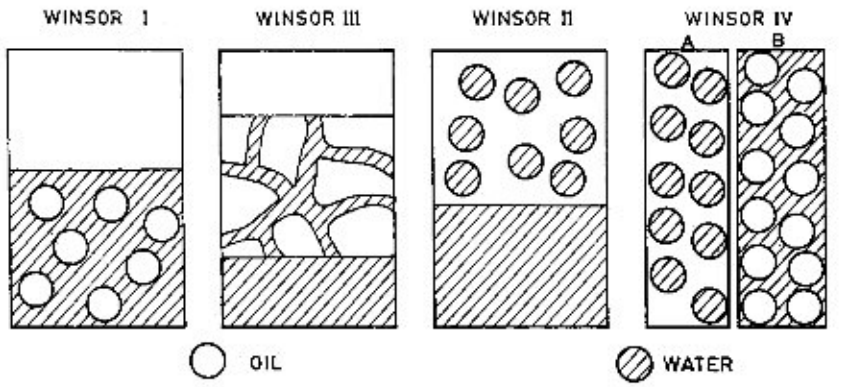

Fig. 2. Different phase-forming situations for water–amphiphile–oil mixtures.

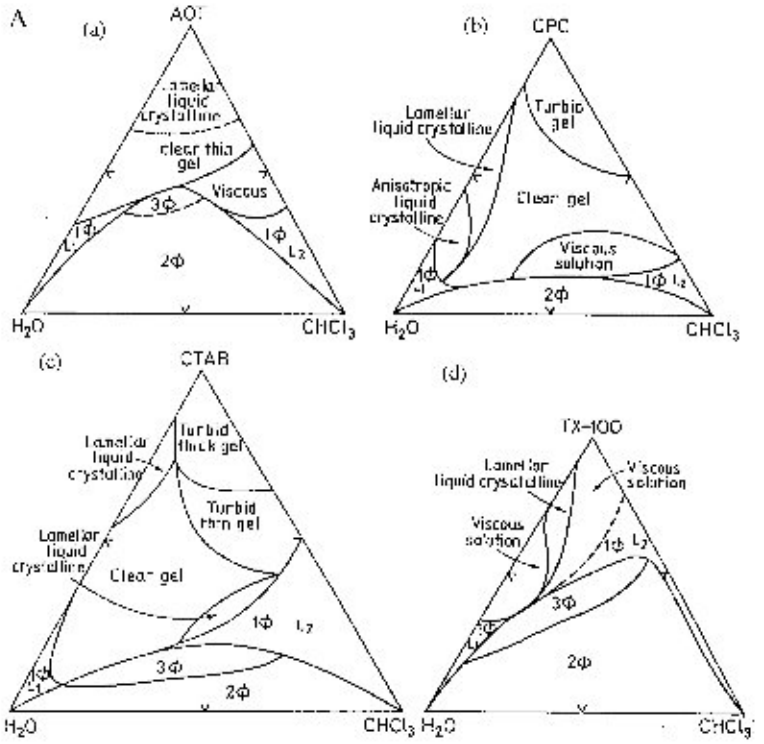

Fig. 3.

shape; at comparable proportions of water and oil, irregular dispersions of both oil and water may simultaneously exist. This is called the 'bicontinuous state' which is considered to be a sponge-like random network [50] (cf. Fig. 1, Winsor III); its demonstration by transmission electron microscopy (TEM) has been reported.

In Fig. 4, an outline of the composition dependent internal structures of a microemulsion system is illustrated. The self-diffusion coefficients of the components water and amphiphiles in microemulsion have been measured for structural information. The diffusion coefficients have been observed to increase with increasing amphiphile and water contents. This suggests either a bicontinuous structure or soft particle interface through which diffusion of species becomes faster.

The otherwise isolated spherical dispersions may show aggregation or clustering [51–54] after a threshold dispersant concentration as well as at an elevated temperature. This is of special importance in percolative preparations. Both regular and irregular clusters may be formed. Their consideration has importance in explaining the percolation of conductance and viscosity after a threshold temperature or droplet concentration for w/o microemulsions. The phenomenon will be discussed in detail in the 'Dynamics of microemulsions' section.

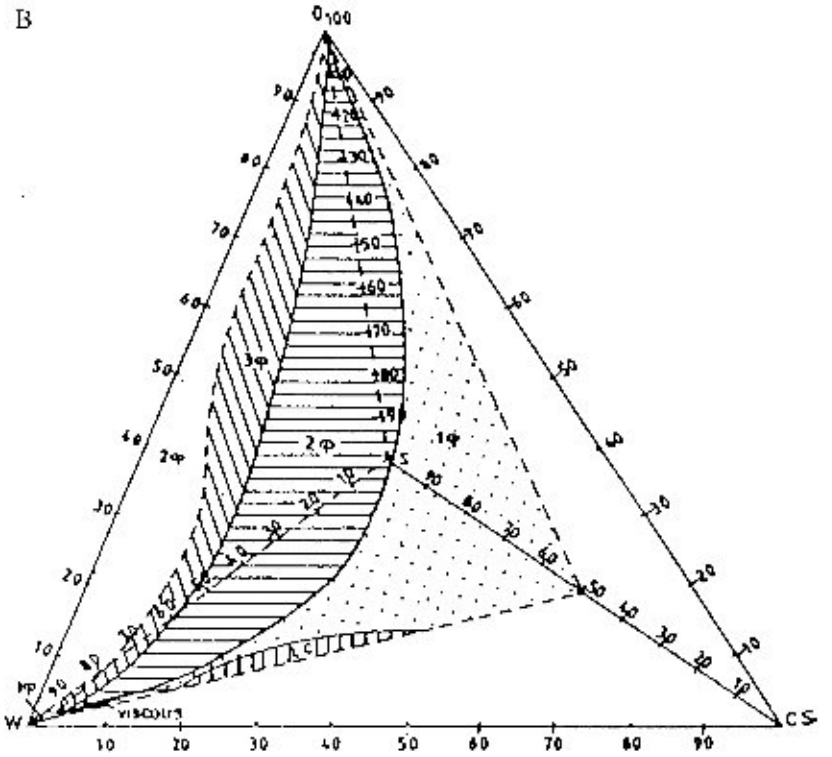

Fig. 3. (A) Ternary phase diagram for (a), H_2O–AOT–$CHCl_3$; (b) H_2O–CPC–$CHCl_3$; (c) H_2O–CTAB–$CHCl_3$ and (d) H_2O–TX100–$CHCl_3$ systems at 303 K. 1ϕ, single phase; 2ϕ, two phase; and 3ϕ, three phase (Mukherjee et al. [33]). (B) Terahedral representation of safola–AOT–hexylamine–water at S/Cos = 1 (w/w) at 303 K (Paul and Moulik [33]).

The bicontinuous structure and clustering phenomenon may have physical appearance of 'fractals' envisaged in colloidal aggregations [55–59]. Until detailed structural studies are available, this however, remains one of the various possible structural manifestations in microemulsions.

3.1. Structural models

Of the several structural models proposed, that of Lagues et al. [60] considers oil and water globules which are hard with a relatively sharp transition between them. Alternative layers of water, amphiphile and hydrocarbon in the form of a lamellar structure have been considered by Shinoda et al. [61], whereas Tamlon and Prager [62] have proposed randomly arranged hard hydrophobic and hydrophilic polyhedra. According to Scriven [63], the internal structure is a complex three-dimensional network with both hydrocarbon and water continuity. A random structure with varying curvatures has been proposed by Friberg et al. [64]. Lindman et al. [65]

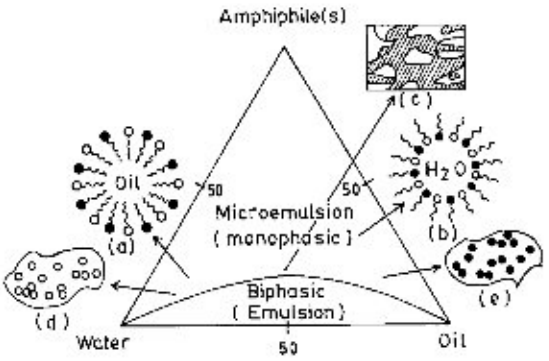

Fig. 4. A comprehensive ternary phase diagram showing probable interal structures: (a) o/w microemulsion; (b) w/o microemulsion; (c) bicontinuous dispersion; (d) isolated and aggregated o/w dispersion; and (e) isolated and aggregated w/o dispersion.

have proposed a hard and well-defined interface as in lamellar liquid crystals or micelles. A typical microemulsion has a polydispersity in aggregate size and shape; the size and shape of the aggregates very rapidly change, and the hydrophilic–hydrophobic interface maintains a relatively low order. Other workers [66–68] also bear similar ideas about the internal structures of microemulsions. The amphiphiles at the lower state of concentration reside in the interfacial region between oil and water domains; on incorporation of macroscopic amount of surfactant, the system may become anisotropic and liquid crystalline, generating globular or tubular structures [69].

3.2. Structure determination (techniques used)

The elucidation of the internal structure of microemulsion, although important, can be very complex, and sophisticated physical techniques are required for this purpose. Small angle X-ray scattering (SAXS), small angle neutron scattering (SANS), dynamic (or laser) light scattering (DLS), transmission electron microscopy (TEM), nuclear magnetic resonance (NMR), time resolved fluorescence quenching (TRFQ) methods have been in growing use over the last two decades. Other methods, i.e. conductance, viscosity, ultrasonic interferometry, ultrasonic absorption, dielectric permittivity, thermal conductivity, transient electrical birefringence, infrared spectroscopy, calorimetry, etc., are also in frequent use for the understanding of the internal physicochemical states of microemulsions. Noteworthy works in this direction are: Friberg et al. [64], Scriven [70], Cazabat and Langevin [71], Brunetti et al. [72], Roux et al. [73], Calje et al. [74], Chatenay et al. [75], Auvray et al. [76], Zana and Lang [77], Fang and Venable [78], and Moulik et al. [79]. For additional highlighting information, the articles by Bellocq et al. [20], Hansen [81], Nilsson and Lindman [82], Tabony [83], Lindman and Wennerstrom [84], Gradzielski and Hoffmann [85], and Bellocq et al. [85] may be consulted.

Throughout this article, more references of the above workers and others regarding the uses of the aforesaid methods in characterizing microemulsion systems can be found.

Of all the methods used for structure elucidation of microemulsions, the SANS, SAXS, DLS, TEM and NMR methods are most important and they can derive multiple data on microemulsion structure. Their applications are elaborated in detail compared to other methods.

3.2.1. SANS and SAXS methods

In scattering techniques, the waves scattered at a given angle by all points in the sample interfere with each other to produce one point in an interference pattern, which is then transformed to reconstruct an image of all correlations within the sample. For structural information, experiments must be designed which can measure distances on a scale comparable with the dimensions of the aggregates. For micelles and microemulsions, this can be profitably achieved by the use of neutron and X-ray radiations (wavelength < 1.0 nm) where measurements at low angles produce enough interference to derive information about the scattering species. In small angle scattering method the measured intensity is correlated with the number density of scatterers, the interparticle form factor, and interparticle structure factor to derive information on the particle size and structural correlation.

Thus, SANS and SAXS are powerful experimental techniques to study systems, their static structures, interactions, etc. Given an option, SANS becomes the method of choice for providing detailed structural information derived from a constant variation method. Over the whole range of colloidal dimensions (1–100 nm), the method is unique in determining particle size and interaction. The analysis of SANS data on microemulsions is capable of showing polydispersity of the droplet size and shape and their fluctuations. For simplified analysis, monodispersity and spherical shape are good approximations for the understanding of structural changes in the microdispersions [86–88]. Information on the correlation length of density fluctuations and isothermal compressibility can also be obtained from SANS measurements. Fractal analysis can also be made [89]. The microemulsion structure elucidation by SANS method has been advanced by a number of workers [90–94]. The morphology of porous glass and microemulsion can be analyzed by a recently developed level-wave model of Berk [95,96]. An alternative approach for analysis of SANS data is due to Chen et al. [97,98]. The salient features of the levelled-wave model are presented by Trevino et al. [99]. The studied triglyceride microemulsion (soybean oil–ethanol–water polyoxyethylene sorbitol hexaoleates) revealed the nature of the spatial distribution of water and oil in their low and high proportions. The work had produced convincing structural distinction of bicontinuous state of microemulsion, and dimensional simulation of their spatial distribution.

SANS method applied to water–didodecyl dimethyl ammonium bromide (DDAB)–cyclohexane w/o microemulsion aggregates at volume fractions of (water + amphiphile) less than 0.03 by Eastoe [100] has revealed polymer-like aggregates

water, phosphocholines (synthetic and natural) from soybean and cyclohexane has been reported by Eastoe et al. [112] using SANS measurements. For each surfactant and concentration, three different neutron contrasts (core–shell–drop) have been studied, and these data have been analyzed in terms of Schultz distribution of core–shell particles. Differences in film thickness and details of aggregating and dispersing behaviors have been reported.

Kellay et al. [113] have studied local properties of AOT monolayer at the oil–water interface by neutron scattering technique in mixtures of AOT–alkane–brine at low AOT concentrations and close to the optimal salinity. For octane and decane the film is lamellar. At the highest salinity it is an oil–brine bicontinuous phase. The rigidity of the surface film for dichain cationic surfactants *n*-alkyl–*n*-dodecyl dimethylammonium bromides $[R_1(C_{12}H_{25})N(CH_3)_2^+Br^-]$, with R_1 *n*-C_{10}, *n*-C_{14}, *n*-C_{16} and *n*-C_{18}, was studied systematically by Eastoe et al. [114] by SANS method to show that the film bending elasticity model is an appropriate description of the studied microemulsions. Eastoe et al. [115] have further studied the surfactant monolayers of o/w microemulsions with cyclohexane as oil and dichained surfactants of different tails, i.e. synthetic phosphatidylcholines, dialkyldimethyl ammonium bromides and AOT to establish that the oil penetration into the negatively curved monolayers on the whole depends on the surfactant alkyl chain structure. SANS study of the L_2-phase in cyclohexane has been made by Eastoe et al. [116] to understand the effects of replacing the Na^+ counterions of AOT for NH_4^+ and $(C_3H_7)_4N^+$. At a low volume fraction (0.025–0.075), spherical micelles are formed with both Na^+ and NH_4^+ counterions whereas $(C_3H_7)_4^+$ has produced cylindrical micelles at $\omega < 10$ and preferably spherical type at $\omega > 10$. Interesting SANS studies have been made by Eastoe et al. [117,118], where w/o microemulsions stabilized by surfactants of the type $M^{n+}(AOT)_n$, with counterions Na^+, Ca^{2+}, Mg^{2+}, Co^{2+}, Ni^{2+}, Cu^{2+}, Zn^{2+} and Cd^{2+} are considered. At low volume fraction (< 0.05) of the dispersed phase and at low water content ($\omega = 5$), spherical micelles are formed with Na^+ and Ca^{2+}, while rod-shaped dispersions arise with CO^{2+}, Ni^{2+}, Cu^{2+} and Zn^{2+}, and intermediate shapes have resulted with Mg^{2+} and Cd^{2+} ions.

Steytler et al. [119] have studied the effects of solidification of oil phase on the structure of colloidal dispersion in cyclohexane. Reversible liquid to solid transition of the continuous oil phase has been produced without affecting the colloid stability by changing the pressure or temperature. SANS results have indicated coexistence of solid alkane and a fluid cluster domain; at high pressure their merging can produce a porous spongy bicontinuous structure with respect to the particle aggregate and the solidified oil phase. The structural changes induced plastic crystal microemulsions as a function of pressure has also been investigated [120]; highly ordered microemulsion droplets of high concentration has been observed to coexist with a pure alkane plastic crystal. A high degree of compression of the surfactant layers also occurs under pressure.

SANS measurements by Eastoe et al. [121] have revealed a liquid-like non-penetrable surfactant layer of density 0.80 g cm^{-3} and thickness 1.1–1.2 nm in water–didodecyldimethyl ammonium bromide (DDDAB)–cyclohexane system. The

area per head group at the water interface is 0.56–0.61 nm^2, at the outer surface the area for the alkyl chains is 0.90–1.25 nm^2. The molecules in the film are tilted or conformationally disordered. The film rigidity has also been estimated from SANS and SLS measurements; SANS measurements on mixtures of D_2O–CO_2–ammonium carboxylate fluoropolyether surfactant as a function of pressure (192–287 bar) and D_2O composition (0.80–2.0 wt.%) have been taken by Zielinski et al. [122] to evidence water swollen inverted micelles in CO_2. The reduction in pressure at constant [D_2O] up to the phase boundary level has a little effect on the microemulsion structure.

The SAXS method has so far only been of limited use. Martino and Kaler [123] studied non-aqueous microemulsions of glycerol–propylene glycol–hydrocarbon–alkylpolyglycol ether system by SAXS method and demonstrated the presence of microstructures in the fluids and also structural similarities between aqueous and non-aqueous microemulsion systems.

The fluctuations of droplet shapes in microemulsions has been revealed by SAXS measurements [86,124]. Shioi et al. [125,126] reported cylindrical aggregates with polydispersed lengths and monodispersed cross-sectional diameters for oil-rich microemulsions with sodium bis(2-ethyl hexyl) phosphate by SAXS measurements. For water–alkane–*n*-dodecyl pentaethylene glycol microemulsions, Litcherfield et al. [127] and Teubner and Strey [128] observed sufficiently large structures by SAXS methods. The amphiphiles appeared to concentrate in the internal surface fixing the repeat distance to 50–80 nm. SAXS probing of microstructure of microemulsions was also done by North et al. [129] and Auvray et al. [130]. The latter workers suggested a 'filament'-like microstructure for formamide–CTAB–alkane systems. SAXS measurements on water–Triton X100–*n*-alkanol–CCl_4 microemulsions [131] revealed monodisperse anisotropic droplets.

The microstructure in concentrated didodecyl dimethylammonium bromide w/o microemulsions [volume fraction of (water + amphiphile) = 0.2] was studied by Barnes et al. [132] using SAXS techniques. The system is bicontinuous at low water content comprising disordered connected cylinders.

The SAXS method has been applied on water–pentaethylene glycol dodecyl ether–decane system containing one, four and six molecules of SDS per 100 molecules of the non-ionic surfactant [133]. With increasing charge density micellar cubic and hexagonal phases crystallize towards lower volume fractions. At higher temperature, reverse hexagonal and reverse micellar phases form in the presence of SDS and not in its absence. The cross-sectional area of the non-ionic surfactant has been found to be independent of the mixed surfactant composition. SAXS method applied to the water–octaethylene glycol mono *n*-dodecyl ether–*n*-pentanol–dodecane system by Regev et al. [134] has revealed different types of structures; spheres, lamellar, liquid crystals, stacks of surfactants, oil and water randomly oriented in space, etc.

The aggregation and structural changes in the L_2-phase in the water–sunflower oil monoglycerides–soyabean oil has been reported by Engström [135] using small angle X-ray diffraction. At a lower percentage of oil the L_2-phase is lamellar and monodisperse, the lamellar units stack to form discs. In a larger proportion of oil,

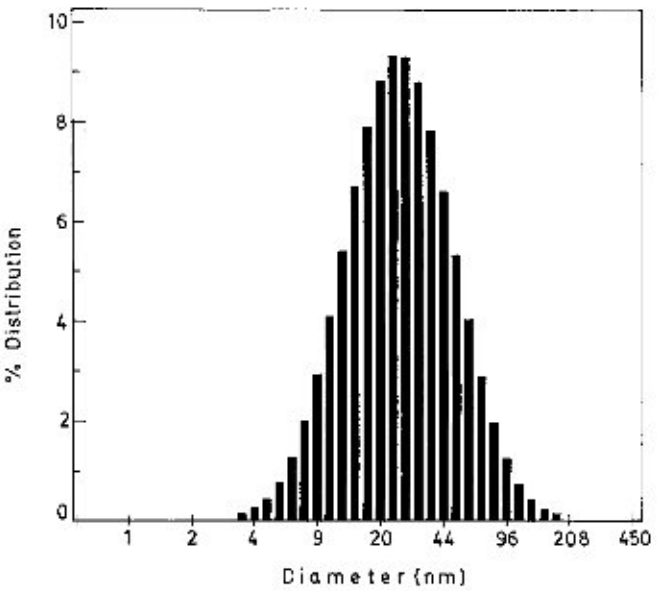

Fig. 5. Size distribution of water–AOT–heptane microemulsion system by DLS method. ω, 40.0; diffusion coefficient, 5.674×10^{-7} cm^2 s^{-1}; average diameter, 20.6 nm.

the size of the lamellar units decreases; at a very large proportion of oil, aggregation is insignificant. The study is unique in its features.

3.2.2. DLS method

Along with size determination, DLS is a good method for measuring the translational diffusion coefficient of microemulsion droplets (i.e. colloidal particles), and is useful in the investigation of concentrated dispersions [136–139]. When a coherent beam of light (as in lasers) interacts with colloidal particles with Brownian motion, the intensity correlation function provides information on the translational diffusion coefficient of the scattering particles and hence the hydrodynamics radius according to Stokes–Einstein equation. The diffusion coefficient can be related to a parameter called the 'correlation length' in a more general way than the diffusion coefficient because it can conveniently characterize discrete droplets as well as clusters, providing a scope for estimating inter-particle interactions. The method of DLS has thus gained potential importance in analysing particle size and related physical characteristics of microemulsions (and colloidal dispersions in general). A typical size distribution of water–AOT–heptane microemulsion system obtained by DLS method is presented in Fig. 5.

DLS measurements on water AOT–isooctane microemulsion by Zulauf and Eicke [66] and water–AOT alkanes by Clarke and Nicholson [140] evidenced hydrodynamic radii comparable with SANS measurements and the values follow a linear correlation with [water]–[AOT] mole ratio. With added electrolytes, the

droplet dependence on the chain length of the alkane was studied by Shah et al. [141]. According to them, increasing alkane chain length increased the droplet size. The dry reverse micelles of AOT (without water) was studied DLS in supercritical and near-critical ethane [142,143]. The stability of the system depended on pressure (solubilization of AOT needed a transition pressure of 200 bar) and approach of this pressure from higher values resulted increase in the 'correlation length' consistent with micelle–micelle interaction. The study of Eastoe et al. [144] on near critical propane and liquid alkanes revealed increase in 'correlation length' with increasing pressure at constant temperature. For higher alkanes, the 'correlation length' was found to be very sensitive to the bulk density at constant [water]–[AOT] mole ratio. Critical-like behavior was also shown by (water + NaBr)–CTAB–*n*-butanol-octane o/w microemulsions as revealed by DLS studies [145]. Lalanne et al. [146] reported rigid spherical droplets with weak interaction for water –AOT–CCl_4 system in the whole range of volume fractions. The critical behaviors of microemulsions formulated with SDS + pentanol and CTAB + butanol in the presence of NaBr, were also studied by several workers [147–149]. By changing the concentration of the dispersed phase, droplet interaction leading to microstructural variation can be assessed by DLS measurements. The interactions become attractive with increase in droplet size, decrease in alcohol (cosurfactant) chain length, change of oil and decrease in salinity [19,150,151]. The model proposed by Lamaire et al. [152] provides a good degree of agreement with experiments for w/o microemulsions.

The structural study of water–sodium bis(2-ethylhexyl) phosphate–benzene by Feng and Schelly [153] by DLS technique has revealed that the aggregates formed are rod shaped at $\omega < 3$; the dipolar crystallites successively dissolve with increasing water content, and at $\omega > 3$, non-dipolar, reverse micelles prevail.

DLS technique has been employed [154] to study droplet dimension of perfluoropolyether microemulsions [water–ammonium salts of carboxylic acid (surfactant)–perfluoropolyether (oil)]. The droplet formation has been augmented by the number of water molecules per polar head. A similar study by light scattering (DLS and SLS) has established aggregate attraction and water entrapment in a continuous network. The size of the aggregate increases with increasing water–surfactant ratio and molecular weight of the oil, whereas low water–surfactant ratio and high oil molecular weight induce stronger aggregate attraction.

3.2.3. TEM method

TEM technique has been limitedly but potentially used in the understanding of the microstructure of microemulsions under varied conditions of dispersant composition and concentration [48,155–158]. In the TEM technique, a direct imaging method was successfully employed for the first time for glass forming microemulsions [159]. The freeze-fracture electron microscopy (FFEM) employed by Jahn and Strey [160] can be of special mention in which the fracturing was done in vacuo and shadowing was made with Ta–W vapour. For water–*n*-octane–*n*-dodecyl pentaethylene glycol, the structure varied systematically with the water-to-oil ratio; at comparable water and oil content, a bicontinuous interwoven water and oil-rich

domains were demonstrated which can be considered as the first direct demonstration of bicontinuous structure. The FFEM applied to D_2O–*n*-decane–AOT system produced images in agreement with suggestion of water-in-oil droplets by others on the basis of SANS experiments [93]. For water–*n*-decane–*n*-hexanol–potassium oleate systems, water-in-oil droplet structures were also evidenced by the FFEM studies of Jahn and Strey [160]. Bicontinuous structures of water–*n*-octane–*n*-dodecyl pentaethylene glycol system was also reported by Kahlweit et al. [33]. The L_2-phase (microemulsion) in a ternary system (water–monoglyceride–triglyceride) studied by freeze-fracture technique [157] revealed oriented stacks of small smooth lamellae. By the FFEM technique, Fleischer et al. [161] have shown formation of dispersion of water in *n*-heptane continuum, bicontinuous as well as lamellar structure formation in water–Igepal CA-520–*n*-heptane system depending on composition.

Recently Pileni et al. [162] reported various structural transitions for water–copper (II) bis(2-ethyl hexyl) sulfosuccinate, $Cu(AOT)_2$–isooctane system with an increasing amount of water, and were characterized by transmission electron microscopy (TEM) and electron diffraction (ED). At a low water content, spherical and cylindrical reverse micelles are formed. By increasing the water content, a bicontinuous system appears. Further addition of water leads to the formation of planar and spherulite type lamellae. As more water is added only spherulite remain in tile phase. Still further addition of water leads to a reappearance of an interconnected network and then reverse micelles. They have also shown that the size and the shape of metallic copper particles can be partially controlled by the shape of the colloidal assemblies used as template.

3.2.4. NMR method

NMR spectroscopy based on physical properties of molecular spin is a very powerful method to study surfactant and self-organizing systems in solution. It provides a route to study molecular degrees of freedom. The method has been applied to determine micellar characteristics (i.e. critical micellar concentration (CMC), aggregation number, counterion binding, aggregate, shape, size and hydration, solution structure, solubilization equilibria, etc.).

The reverse micelles and microemulsions can be understood by the possibilities of determination of the self-diffusion coefficients of the constituting species; water, oil and amphiphile. The advantage of NMR method is that two- or three-phase characteristics can be monitored with single-phase domains on the micrometer scale. It also helps in finding out the degree of anisotropy and the presence of long-range discontinuities or continuities.

Using high resolution ^1H, ^2H and ^{13}C NMR techniques, intermolecular interaction and structural rearrangement of non-ionic and anionic amphiphile-aided microemulsions have been investigated [163–165]. The technique can directly reveal the nature of mono- and polydispersity, as well as particle anisotropy [107].

For microemulsion systems, self-diffusion studies of components by FT-NMR method have been extensively used [166], where the macroscopic self-diffusion of the constituents confined to droplets will be that of the droplets and will be low.

The self-diffusion characteristics (diffusion constant, D) can have the following distinctions:

1. w/o system: $D_{water} \ll D_{oil}$ and $D_{amp} \simeq D_{water} \simeq D_{droplet}$;
2. o/w system: $D_{oil} \ll D_{water}$ and $D_{amp} \simeq D_{oil} \simeq D_{droplet}$;
3. bicontinuous state: D_{water} and D_{oil} are both higher but D_{amp} is low because they exist in large aggregates.

The nature of the composition dependent self-diffusion coefficients of the constituents of saline water SDS–butanol–toluene determined by Guering and Lindman [167] is presented below in Fig. 6.

The bicontinuous structure of glycol, glycerol and propylene glycol, straight chain alkanes and pentaethylene glycol mono-*n*-ether microemulsion systems were studied by NMR method by Martino and Kaler [168]. The formulations dilute in oil showed microstructures. The existence of spherical aggregates in concentrated microemulsions of styrene–dodecyl trimethylammonium bromide–brine was also reported [169].

Jonströmer et al. [170] made NMR studies of three different surfactant–oil–polar solvent systems; the surfactants used were AOT, DDAB (didodecyldimethyl ammonium bromide and $C_{12}E_4$ (tetraethylene glycol dodecyl ether). At lower temperatures, closed isolated reverse micelles aggregated; at a higher temperature, structural changes towards a bicontinuous state occurred. The aggregate formation was not observed for DDAB and $C_{12}E_4$ systems. According to Das et al. [171,172] NMR probing revealed glycerol–SDS–hexanol system to be structureless.

The microstructure of four component microemulsions (water–octyldiglucoside–pentanol–decane) was studied by Parker et al. [173] using NMR technique. It has been realized that at 25% oil, increase in cosurfactant content causes a decrease in the mean curvature of the amphiphile film toward oil. The microstructure changes from o/w to w/o via a bicontinuous state. The diffusion of water is much less than

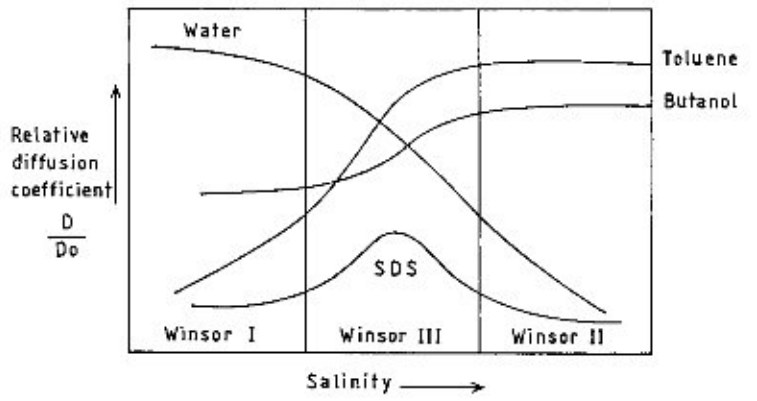

Fig. 6. Self diffusion characterstics in a microemulsion of water (NaCl)–SDS–*n*-butanol–toluene system (trend as in Guering and Lindman [167], drawn on an arbitary scale).

the octyldiglucoside in the w/o domain. The variable structure of water–octaethylene mono-*n*-dodecylether–*n*-pentanol–*n*-dodecane w/o microemulsion system was studied by the NMR method over and above the SANS method already discussed [134]. The L_2-phase (microemulsion) compound of water–sunflower oil monoglyceride–soybean oil triglyceride was studied by Gulik-Drzywicki and Larsson [157].

A number of other NMR probed microemulsion structure elucidation have appeared in recent literature. Jonströmer et al. [174] have used microemulsions with aqueous *N*-methylformamide or ammonium chloride as polar solvents, AOT, DDAB and tetraethylene glycol dodecyl ether as surfactants and isooctane as oil and have reported closed-isolated-reversed-micellar aggregates with AOT that changes to bicontinuous network at higher temperature. No dominating aggregate diffusion has been observed with DDAB and the non-ionic ether. The diffusion coefficients in water–SDS–pentanol and ammonium hydroxide–SDS–pentanol microemulsion systems studied by Olsson et al. [175] have established that replacement of water by ammonium hydroxide destabilizes the liquid crystalline phase and reduces the size of the colloidal association structures in the isotropic liquid part. The non-ionic microemulsions composed of heavy water (D_2O), pentaethylene glycol dodecyl ether and decane have evidenced [176] discrete oil-swollen micelles; the microemulsion fluid is in agreement with hard sphere model. By NMR self diffusion measurements in water–octylglucoside–pentanol–decane microemulsion system, Parker et al. [173] have reported a progressive decrease in the mean curvature of the surfactant film with addition of water at a constant oil content. The microstructure has been concluded to change from o/w to w/o via a bicontinuous microemulsion. According to Leaver et al. [177] prior to bicontinuous state limited growth from sphere to prolate (oil swollen) micelles occur in the water–pentaethylene glycol dodecyl ether–decane microemulsion studied by way of self diffusion measurements. Hendrikx et al. [178] studied the local properties of AOT monolayer for brine–AOT–*n*-alkane systems by NMR measurements and observed lamellar phase for alkanes with carbon numbers < 11 and bicontinuous or lamellar for longer chains depending on the salinity. The chains of the lower alkanes penetrate in the AOT monolayers, for higher alkanes the matter remains inconclusive.

The microemulsion, water–octaethylene glycol mono *n*-dodecyl ether–1-pentanol–*n*-dodecane, is considered a model for a fire-resistant hydraulic fluid and has been studied by the ^{1}H NMR method by Waysbort et al. [179]. From the study of the chemical shift data and inversion from w/o to o/w microemulsion has been found to occur with water in the range of 55–60 wt.% which agrees with the microviscosity obtained from T_1 (relaxation data) data. The T_1 data have also shown composition dependent distinction between the aggregated and free water in the formulations.

Microemulsion prepared with water, pentaethylene glycol dodecyl ether and mixed oil (cyclohexane + hexadecane 1:1 w/w) has been studied by Fourier transform pulsed gradient spin echo ^{1}H NMR technique by Olsson et al. [180]. The results suggest rapid fusion–fission of micellar aggregate at low oil content and at

low temperature, o/w microemulsion dominates in the system; a slight increase in temperature causes a significant growth in the micellar size.

Fleischer et al. [161] have studied the self-diffusion coefficients of water Igepal CA-520–*n*-heptane w/o microemulsion system with pulsed field gradient NMR to elucidate internal structure. At a composition of 40% water, 40% heptane and 20% (all wt./wt.) Igepal, the structure is bicontinuous; two Igepal fractions, one in the surfactant layers and the other in the *n*-heptane, have been observed. At higher water content, the transition of the microemulsion phase into lamellar phase was noticed. The existence of bicontinuous isotropic and lamellar phases have also been evidenced. The microstructure of the water in the aqueous pool of the droplets has been also examined by NMR self-diffusion studies; this is subsequently treated in a separate section.

3.2.5. Other methods

In addition to the methods described earlier, other methods, i.e. viscosity, conductance, thermal conductivity, dielectric permittivity, electrophoretic birefringence, ultrasonic interferometry, ultrasonic absorption, etc. although primarily employed for studying dynamics of microemulsions (to be discussed in a separate section) can also shed light in favor of internal microstructure. Such reports are fairly frequent in the literature.

Koper et al. [49] used dielectric permittivity, low shear viscosity and electrophoretic birefringence methods for understanding the aggregating behaviors of oil continuous water–AOT–isooctane microemulsions. At lower dispersion concentration, they observed the droplets to form chain like aggregates and the binding enthalpy was linearly dependent on droplet size. In the low droplet volume fraction region, the aggregation phenomenon strongly depends on temperature. Structural studies by dielectric permittivity and viscosity were also done in the past [181–184]. The viscosity and thermal conductivity studies of Lalanne et al. [146] on dilute w/o microemulsions of water–AOT–CCl_4 revealed rigid weakly interacting spherical droplets to exist. The dielectric permittivity method was also employed by Santhanalakshmi and Parameswari [131] to elucidate the microstructure of water–TX100–*n*-alkanol–CCl_4 microemulsion systems to be essentially monodisperse anisotropic droplets.

Lenz and Hoffmann [185] made structural investigations of ternary microemulsions composed of water–didodecyldimethyl ammonium bromide–dodecane system using flow and electric birefringence methods as well as with pressure jump–relaxation techniques and conductivity measurements. In the area of low water content, the system consisted very long interconnected channels and was bicontinuous. With increasing water content, after a critical stage, the system abruptly changed into the form of spherical aggregates yielding low viscosity and conductance. The behaviors fit into the model called 'disorder-open-connected-model' of Chen et al. [186]. Ellipsoidal shape of water-droplets for the studied microemulsion reasonably fitted the results. The lifetimes of both the globules and the channels were revealed to be short.

The laser-induced transient electric birefringence (optical Kerr effect) were

measured on w/o microemulsion (water–AOT–CCl_4) by Chen and Schelly [187] to decipher clustering behavior of the droplets. The laser electric fields jump was associated with two relaxations; the first is attributed to the collapse of the anisotropic structure and the second to the disintegration of the clusters. The disintegration of clusters was investigated as a function of AOT concentration, water content and temperature.

Das et al. [27] determined adiabatic compressibilities (by way of ultrasound velocity measurements) of saline water–xylene (or heptane) cholesteryl benzoate microemulsions by the ultrasonic interferometric method. The formation of structure upon mixing was observed, the heptane system evidenced a structural transition after 20% (w/w) of water addition. In comparison, the internal degree of flexibility was more for AOT-based microemulsion than TX100-based microemulsion with alkane as oil as understood from the excess compressibility measurements [29]. The structural implications of microemulsions in the presence of macromolecules in the aqueous phase was also examined by Das et al. [188] in the light of adiabatic compressibility. For structural understanding of the systems brine–Brij 35–*n*-propanol–heptane or nonane, water–Brij 35 + SDS or Brij 35 + Tween 20–heptane and water–SDS–*n*-propanol + *n*-hexanol–cyclohexane, Rakshit et al. [189–192] have also used adiabatic compressibility technique. The method of conductance has been successfully applied to estimate droplet dimension and density as well as their solvation (particularly for o/w systems) [78–80]; this will be elaborated in the 'Dynamics of microemulsion' section to be presented subsequently.

Positron annihilation spectroscopy (PAS) has emerged as a powerful technique for investigating structural changes, phase transitions and microenvironmental transformations in microemulsion systems as revealed from the works of Jain et al. [193]. They have carried out research using PAS technique in water–CTAB–hexanol, water–(TTAB + pentanol)–*n*-octane and water–AOT–isooctane microemulsion systems. Their measurements have helped to distinguish the boundary between the droplet like and bicontinuous structures in a well defined isotropic L_2-phase and the results have been supported by electrical conductivity measurements [194,195]. They have also suggested the existence of rotational isomerism in water–AOT–isooctane microemulsion system due to sudden change in the positron annihilation parameters, τ_1, τ_2 and I_2 on [water]–[AOT] i.e. ω for a fixed concentration of AOT [196] and these results have been supported by other conformational studies of AOT by Maitra et al. [197]. Recently, PAS has been applied to study the molecular association of TX100 in the non-aqueous medium of butanol–*n*-heptane [198].

In a water–surfactant–alkanol ternary system, an isotropic, low viscous L-phase appears covering the water-to-oil corner. The L-phase depending on the composition may contain lamellar liquid crystalline, cubic, hexagonal, etc., type of structures. With CTAB and SDS as surfactants and *n*-butanol, benzyl alcohol, *n*-hexanol, poly(propylene glycol), etc., as oils, the structures of the L-phases have been elucidated by the polarizing microscopic technique essentially by Rodenas et al. [199–201].

Dielectric time domain spectroscopy (TDS) has also been successfully applied to reversed micellar and microemulsion systems by several authors [202–205]. It has been shown that static permittivity is sensitive to geometrical changes of the aggregates and the dielectric relaxation is an indicator on interfacial polarization, counterion movements in the aggregates and spatial changes in the domain sizes. Finally, the conductivity which is also obtained from the dielectric spectroscopy experiment will give additional information about the mobility of the ions in the system. Recently, Sjöblom et al. [206] investigated the microemulsion system water (electrolyte)–DDAB–dodecane by means of TDS. The L_2-phase gradually decreases upon electrolyte addition until only a narrow channel exists. The original microemulsions are built up by closed aggregates and bicontinuous structures depending on the location of the L_2-phase. Dielectric parameters indicate that the electrolyte gradually changes the shape of the aggregates from elongated structures to spherical ones until the one-phase region vanishes and bicontinuous structures exist at a very low concentration of electrolyte.

The structure of water–AOT–ethane microemulsion under supercritical condition has been studied by Ikushima et al. [207] using high pressure FT-IR spectroscopy. The system has been found to maintain a single phase depending on pressure (P), temperature (T) and ω. The number of water molecules solubilized by AOT molecules can be 2.5 times more than that possible in ordinary organic liquids.

3.3. Polydispersity of particles

Although the consideration of linearly monomeric nanodroplets simplifies analysis and physicochemical characteristics of microemulsions, in reality, the systems are dimensionally polydisperse. The polydispersity narrows down with decreasing particle size (or increasing surfactant content for a fixed (not very high) amount of the dispersed phase; it widens with the increase in droplet size consequent upon higher proportion of the dispersed phase and/or lower proportion of the amphiphile [208]. The polydispersity of o/w microemulsions stabilized by non-aqueous amphiphiles (n-alkyl polyoxyethylene glycol ether) was studied by TRFQ and DLS methods [209]. The polydispersity was observed to increase with increasing temperature and decrease with increase in overall amphiphile chain length. In establishing the structural information, the TRFQ method is more accurate than DLS for small droplets, the former is more sensitive to the aggregate polydispersity than the latter. The polydispersity studies of microemulsions, particularly of o/w type, are infrequent [210]. The size and polydispersity of water–n-octane–AOT and water–dodecane–AOT microemulsions were studied by Almgren et al. [211] by TRFQ method. Ricka et al. [124] unambiguously demonstrated shape fluctuations and polydispersity in w/o microemulsions by SANS method.

The w/o microemulsion system studied by the DLS method in the authors' laboratory, and presented in Fig. 5, is typical example of a polydisperse system. Factors like, system composition, temperature, nature of amphiphile, presence of additives can have a reasonable effect on polydispersity. Elaborate studies in this direction have been undertaken.

The polydispersity of w/o microemulsion containing water–didodecyl dimethyl ammonium bromide–dodecane was also reported by Lenz and Hoffmann [185] using the method of electrical birefringence. With the advent of fourier transform pulsed-gradient spin-echo ^{1}H NMR technique, Olsson et al. [180] have studied water–pentaethylene glycol dodecyl ether–1:1 (w/w) mixture of cyclohexane and hexadecane system and have observed significant polydispersity in the micellar aggregates at low oil content.

3.4. Role of additives

The microstructural state of a microemulsion may be affected by the presence of additives. Full and Kaler [139] studied the polymerizable microemulsions containing styrene, dodecyl trimethyl ammonium bromide and brine by SANS and DLS methods, and observed swelling of microemulsion droplets with the addition of styrene. The self-diffusion coefficient of the droplets decreased with added styrene and the addition of salt did not affect the particle size but minimized interdroplet interactions. Such studies are important in the understanding of the polymerization kinetics and latex characteristics in microemulsion media [212,213]. The effect of additives (proteins and enzymes) on the waterpool size has been indicated by Pileni [214]. The structural effect of urea in water–AOT–*n*-hexane reverse micelles at $\omega = 10$ has been investigated by Amaral et al. [215] using light scattering (LS) and SAXS techniques as a function of ϕ for 3 and 5 mol dm^{-3} urea. LS results have indicated that the attractive intermicellar interaction becomes larger as urea concentration increases. They have further observed from Guinier's and Porod's analysis of X-ray data that AOT–*n*-hexane–water (urea) systems have maintained their structure and micellar dimension up to $\phi = 0.32$. Their results have indicated that the percolative transition has not occurred due to transition of spherical droplet state to a bicontinuous state, but from clustering of droplets at $\phi > 0.06$ due to interdroplet attractive interactions. The size of nanoparticles formed in w/o microemulsion has also been observed by Moulik et al. (unpublished results) to be larger than the droplet size without encapsulation of additives, i.e. $BaSO_4$ and $Cu_2[Fe(CN)_6]$. The observations of De and Maitra [36] and Maitra et al. [216] were also of similar kind. Growth of silica particles in microemulsion systems consisting of CTAB, sodium salicylate (NaSal), tetraethylorthosilicate (TEOS), and water has been investigated by Kurumada et al. [217] using static and dynamic light scattering (SLS and DLS), and the effect of micellar network structure has also been discussed. The diagram of composition has been given to show the region wherein a transient network-like structure has formed from CTAB micellar aggregates with cylindrical geometry. The SLS measurements have given smaller values of the structural correlation length while the silica particles have formed in the network medium than in a dispersed medium. The structural relaxation behavior obtained from the DLS measurements have shown a slowly decaying mode for the network-like medium, suggesting the retardation effect by the network-like structure of CTAB molecules. The network-like structure has effectively prevented the interminable growth of the silica particles by blocking their free motions.

Suarez et al. [218] used TRFQ method to study the effects of the nature, molecular weight and concentration of polymer on the droplet dimension, the interdroplet attractive interaction, and the rate of exchange of materials among the droplets in w/o microemulsions. The additive affected state of dispersion of microemulsions may influence their overall stability through interfacial interaction; the behaviors in bicontinuous dispersions may have interesting features and quality for future exploration. Similar to colloids, microemulsion droplets may be stabilized by interaction with polymer additives; aggregation is checked if the polymer molecules are adsorbed at the interface by way of attraction [219]. The polymers can also increase the inter-particle interaction leading to aggregation and ultimately to phase separation [220]. The modifications of w/o microemulsions by the addition of water soluble unchanged polymers was studied by Lianos et al. [221]. Joshi and Rakshit [222] have reported bicontinuous structure for water–CTAB–*n*-propanol–cyclohexane microemulsion in the presence of a water soluble polymer, PEG 400 in a wide range of temperatures. Nagarajan [223,224] has made elaborate studies on the transitions among the WI, WII and WIII microemulsions by the presence of non-ionic polymers which associate with the aggregates in microemulsions. The addition of polymers can then have potential possibility to manipulate microemulsion structures. A thermodynamic theory on non-ionic polymer-microemulsion has been also proposed [225].

Working on water–AOT–isooctane microemulsion in the presence of macromolecules (gelatin and block copolymer), Eicke et al. [226] have reported production of soft condensed microemulsion mediated polymer networks that can manifest fluidity displaying viscous flow. The formation of viscoelastic networks is also an important feature of such systems; dramatic influence of polymers on microemulsion stability and structure may also arise. This has been comprehensively presented in a recent short review by Kabalnov et al. [227] wherein important current references can be found. The structure and dynamic properties of ABA triblock copolymers in water–AOT–isooctane w/o microemulsions have been recently studied [228]. The investigated systems have evidenced transient network formation; DLS measurements have detected three diffusive processes for water molecules. The transient networks by ABA triblock copolymer [poly(oxyethylene)-b-polyisoprene-b-(polyoxyethylene)] has also been studied by Odenwald [229] by oscillatory shear measurements. Such systems are prone to viscoelastic behaviors. The adsorption of a polymer to a surfactant interface increases the interfacial elastic modulus that directly influences the temperature-induced droplet cluster formation in w/o microemulsion. Polymer molecules larger than droplet dimension can be dissolved in microemulsion solution causing polymer affected droplet clustering [230]. The w/o microemulsion system (water–AOT–isooctane) containing water soluble polymer, poly(oxyethylene) in the water droplets may cause an increase in the monolayer rigidity by the attractive interaction between the polymer and the surfactant leading to the polymer adsorption at the interface. This has been shown by Meier [231] from Kerr effect measurements.

The o/w (decane–pentaethyleneglycol mono dodecyl ether–water) microemulsion droplets have been used as a matrix by Meier [232] to form a new amphiphilic

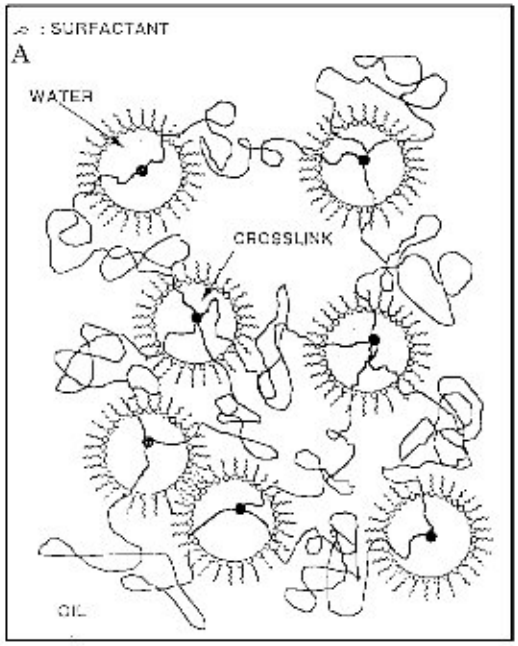

Fig. 7.

polymer network structure. Meier et al. [233] have very recently worked on the formation of microemulsion elastomers by covalently cross-linking ABA triblock copolymers containing polymerizable methylacrylate end groups in the droplet phases of w/o and o/w microemulsions. The formed microemulsion elastomers having solid state properties such as elasticity or stability in shape have been investigated by dynamic, mechanical and DLS methods. In Fig. 7, probable polymer containing/polymer linked microemulsion states are depicted. This field of polymer-contained microemulsion states seems to have future application prospects.

The solubilization ability of water–$CHCl_3$, and water–heptane mixtures stabilized by cetyltrimethylammonium ion with bromide and chloride counterions has been studied by Abuin et al. [234]. The effect of electrolyte on the structure of cosurfactant less microemulsion was also studied by Brun and Wade [235] by DLS and fluorescence polarization methods. The crystalline phase as well as liquid to solid transition behaviors of the AOT–cyclohexane phase as a function of temperature and pressure has been reported [69,236]. The study can be attended under the changing conditions of counterions for a better understanding of the intrinsic nature of microemulsion structure selected to variable environmental conditions.

4. Structure of micro waterpool

The structures of the interfacial water of both o/w and w/o microemulsion

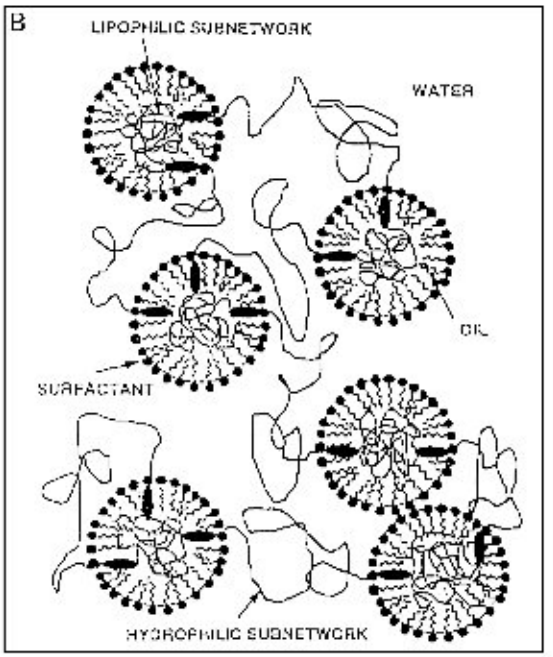

Fig. 7. Covalently cross-linked polymer network: (A) in w/o microemulsions; and (B) in o/w microemulsions [232,233].

systems are different from bulk water. In the micro-encapsulated domain of the latter, the presence of amphiphile head groups and the counterions (when present) may significantly affect the water mobility. According to reports [237–242] by various physical and thermodynamic methods, the amphiphile like AOT can attach six water molecules per SO_3^- group; the counter Na^+ ion also acquires its share. A similar physical state may also arise with sodium dodecyl sulfate (SDS) as the amphiphile. The interior water environment may become appreciably rigid or immobile. This is prominently manifested in [water]–[AOT] mole ratio of up to $\omega = 6$; thereafter, a graded structure of diminishing rigidity arises up to $\omega = 15$ beyond which bulk properties prevail. Three states of water have been demonstrated in w/o microemulsion system of water–AOT-isooctane by Zulauf and Eicke [66]. Two to six molecules per SO_3^- of AOT microemulsion have been reported from thermochemical measurements [243]. From calorimetric investigations it has been inferred that six water molecules are strongly bound to the SO_3^- group; NMR [237], ESR [237] and light-scattering [66] have also shown that up to 10–15 water molecules are structurally perturbed. Maitra [244] has proposed several regions of bound water in AOT reverse micelles. In a recent study, Moulik et al. [245] have reported the TX100 stabilized w/o microemulsion system in terms of free and bound water by calorimetric measurements. The knowledge of hydration and the environmental aqueous fluidity in the water droplets in w/o mi-

croemulsions is essential in understanding the dynamics of the physicochemical processes studied in them. The structure of various water species in AOT reverse micelles on replacement of Na^+ by Ca^{2+} and Zn^{2+} ions at very low water contents has been studied by FT-IR spectroscopy by Aliotta et al. [246]. The results have been explained on the basis of a two state model one 'tightly bound' to surfactant ions and one 'loosely bound' like bulk water in the micellar pool. The percentage of bound water during growth of micelles has been also estimated. The states of water in water–AOT–oil systems have been also examined by Boned et al. [247] using differential scanning calorimetry. Gu et al. [248] have pointed out that both the two-state and the three-state models have some problems. In order to elucidate these problems, they reported calorimetric measurements on sodium dodecylbenzenesulfonate (NaDBS)-based system with *n*-pentanol and *n*-heptane as a mixed apolar solvent and found that their thermal behavior is quite different from that of AOT-based systems.

There are only scanty reports on the states of water in w/o microemulsions using cationic surfactants. By proton-NMR, fluorescence and IR spectroscopic techniques [249] and SANS method [250,251], the behaviors with butyldodecyl dimethyl ammonium bromide in chlorobenzene and didodecyldimethyl ammonium bromide in cyclohexane have been examined at different ω values at various amphiphile concentrations. The existence of three types of water (bound, aggregated and free) in various proportions has been realized. Three states of water have also been supported from the high pressure FT-IR spectroscopic studies by Ikushima et al. [207] for a water–AOT–ethane microemulsion system under supercritical conditions. The relative extents of the states depend on ω, pressure and temperature. The solubilization of water and rotational isomerism of AOT are significantly influenced by the addition of salts.

The state of water has been also investigated by estimating microviscosity in the water pool of AOT stabilized microemulsion system by steady-state [252–255] and transient fluorescence depolarization [243,256]. The water pool at low ω has been understood to be highly viscous and the viscosity decreases with increasing ω up to 10, after which the decrease is gradual. The total fluorescence and fluorescence anisotropy study by Wittouck et al. [257] of AOT microemulsions in *n*-heptane and *n*-dodecane has also realized decreasing viscosity of the water pool with increasing ω. The polarity of water in the aqueous micropool also changes by the AOT environment leading to its higher basicity [258]. Using the viscosity sensitive fluorescence probe auramino, Hasegawa et al. [259,260] have reported rapid increase in waterpool microviscosity with decreasing size; even at higher range of ω, the pool viscosity has been found out to be greater than bulk viscosity.

Very recently, the state of water in the waterpool of reverse micelles (w/o microemulsions) has been elaborately investigated by a fluorescence probe technique by Hasegawa et al. [261] for water–AOT–*n*-alkanes (C_6–C_{12}), cyclohexane, isooctane, carbon tetrachloride, dichloromethane and chloroform using a viscosity sensitive fluorescence probe, auramine O and xanthene dyes for steady-state depolarization measurements. Up to $\omega = 10$, the microviscosity at the vicinity of AOT anionic head falls abruptly and then gradually decreases until the upper limit

of water tolerance. The heterogeneity of the waterpool has also been demonstrated by the fluorescence depolarization of xanthane dyes. The effects of temperature, surfactant concentration, solvent and counterion on the state of water in terms of microviscosity have also been explored. In addition, clustering of the reverse micelles has been supported from the fluorescence data which has been dealt with in the section, 'Dynamics of Microemulsion'. Silber et al. [262] reported that there are at least two types of water (structured and bulk) in the reverse micelles from the study of solvatochromic behavior of 1-methyl-8-solvatochromic betaine (QB) and $E_T(30)$ in AOT–*n*-hexane system.

From time- and space-resolved studies, Cho et al. [263] have investigated the ability of 'probe' molecules to undergo a fast non-radiative process that depends on a reorientational relaxation time of the water solvent which may become orders of magnitude slower for water near a surface. A direct dynamic competition between diffusion of the probe and non-radiative event can be understood by this spectroscopic method. In the studied reverse micelles of AOT, perturbation on the orientation of the solvent, as measured from fluorescent life times of the probe (anthracene sulfonate), has been found within a distance of 1.0–1.5 nm, beyond which water in the pool behaves as normal. Recently, Sarkar et al. [264] have studied picosecond time-resolved stoke's shift of the laser dye, coumarin 480(I) in water–AOT–heptane microemulsion medium to show that the relaxation of water in the waterpool is several orders of magnitude slower than ordinary water. The fluorescence decay becomes faster with increase in ω, which suggests that the water in the small pools is much structured and the mobility of the water molecules increases in the waterpool with an increase in ω. From the deuterium isotope effect on 4-amino phthalimide in neat water and reverse micelles Das et al. [265] have recently studied the state of water in the waterpool of water–AOT–*n*-heptane microemulsion. In the neat water, they have found that the solvation dynamics are too fast to be detected. But D_2O slows down appreciably and the initial component of the solvation dynamics in the case of D_2O is 1.5 times slower than in the case of H_2O. Thus a clear distinction between the states of residence of H_2O and D_2O in the waterpool of microemulsion is indicated.

Recently, the association of water with the amphiphiles has been studied by Friberg et al. [266] by performing evaporation measurements of water–AOT–cyclohexanone microemulsion. Seventy percent evaporation of the original weight takes place with an approximately constant water–oil ratio in the vapor and is independent of original water–oil ratio. At a low percentage of water in the sample, the oil–water ratio strongly increases in the vapor phase. Colloidal association and strong binding of the water molecules to the surfactant (AOT) at low water content is envisaged.

5. Effects of protein solubilization on the structure of w / o microemulsion

The w/o microemulsions (or reverse micelles) of amphiphilic compounds in organic solvents are able to solubilize large amounts of water and the state of the

water in the microcompartments has been dealt with in a preceeding section in detail. The w/o microemulsions afford the unique possibility for the enzymes and proteins to localize in a intracellular conformation required to maintain their activities. There are a number of papers on the investigation of proteins–enzymes in reverse micellar solutions using surfactants of different charge types (in which AOT comprises a sizeable numbers). References on this aspect can be available in recent review articles of De and Maitra [36] and Paul and Moulik [35]. But many fundamental questions for the complete understanding of the protein solubilization process in w/o microemulsion remain unanswered. For example, the nature of the protein–reversed micelle complex, in particular protein localization and size–shape perturbations induced in the reverse micelles by the insertion of protein is only poorly understood. However, a number of important papers by several groups, i.e. Luisi et al. [267–270], Chatenay et al. [271,272], Pileni et al. [273–277], Fletcher et al. [278], Levashov et al. [279], Hatton et al. [280–282], Bratko et al. [283,284], Hirai et al. [285] have appeared on solubilization of different proteins in AOT–oil (isooctane, heptane, octane, etc.) reverse micellar systems using different techniques, for example, ultracentrifugation, SANS, SAXS, DLS, fluorescence recovery after fringe photobleaching, pulse radiolysis, synchrotron X-ray scattering, etc. These studies have revealed that it is possible to utilize the degree of hydration, surfactant concentration and the protein concentration as effective variables for the optimization of enzyme activity in several micelles. Several review articles [286–289] in this are also available in the literature.

Based on the experimental observations, different models have been put forward for the structure of protein containing reverse micelles. Luisi and coworkers [268] have proposed a model called the 'water-shell' model in which the micellar volume with protein is the sum of the volumes of the empty micelle and that of the protein. But it has been demonstrated that the protein filled microemulsion droplet grows at the expense of the unfilled droplets. On the average, the size of protein free droplet is smaller, and protein contained droplet is larger than their size prior to protein addition. The size difference between filled and unfilled droplets vary with the protein, but is of the order of 2:1.

In an alternative to the 'water-shell' model, Levashov et al. [279] have proposed that if the micellar size exceeds that of the protein, there would be no alteration of the droplet radius (fixed size model); if the size of the protein molecule exceeds that of the micelle, the latter grows to accommodate the protein (induced-fit model). This model suffers from criticism as it violates the area and volume constraints imposed on the system by the predetermined water, protein, surfactant concentrations. The results of Levashov and coworkers could be due to artifacts in the analysis procedure [268,281,282]. A ^{13}C NMR study conducted on the chymotrypsin solubilization in the reverse micelle of AOT in isooctane [290] has demonstrated no change in micellar size upon protein solubilization.

The 'water-shell model', picturing the enzyme molecule residing in the interior of the droplet surrounded on all sides by water, should only apply to hydrophilic proteins which do not contain large hydrophobic domains. Many enzymes, including lipases, are surface active and interact strongly with o/w interfaces. Such

of water insoluble substrates is that of microemulsion-based organo-gels (MBG). It has been observed that under certain conditions, it is possible to transform reversed micellar solutions into rigid, optically transparent gel-like structures of extremely high viscosity. These gels serve to entrap proteins and enzymes with the advantage over conventional reverse micelles in that they facilitate enzyme reuse and easy product separation. The two distinct kinds of MBGs that have been reported are gelatin gels and lecithin gels.

The biotechnological potential of gel formation in microemulsions has sparked great interest in MBGs and in-depth studies have been conducted to elucidate the microstructure of the systems. Quellet et al. [301,302] and Luisi et al. [303–307] have proposed the first structural model of this system from extensive conductivity measurements, differential scanning calorimetry, light scattering, X-ray scattering, circular dichromism and pulsed-NMR studies. They have proposed the generation of nanogel structures in the waterpool of the microemulsions as an initial nucleation step in the gelation process. As soon as the nucleation is terminated, percolation of the nanophase forming infinite fractal clusters in the water droplets occurs. Gelatin is intimately involved in the percolation process in which its polypeptide segments form helices extending into the organic phase. Percolation is accompanied by a drastic change in the microstructure and a dramatic increase in the electrical conductivity. The final sol–gel transition step involves the formation of a three-dimensional network of nanogels interconnected by cross-linked bridges composed of gelatin helices. A conflicting structural model has been proposed by Atkinson and coworkers [308] based on SANS data in conjunction with tracer-diffusion studies, NMR and conductivity measurements of the organogels. Their model proposes the formation of an extensive network of rods containing gelatin and water which coexist with a surfactant shell of AOT in equilibrium with microemulsion droplets.

Recently, Atay-Guneyman et al. [309] have reported the transport of a divalent metal ion through the microemulsion-based ligand (murexide), and a metal-ion ligand complexation reaction has been observed.

7.1. Lecithin gels

The microemulsification of hydrocarbons by biological amphiphile (lecithin-based microemulsion) was first reported by Shinoda and Kaneka in 1988 [310] using soyabean lecithin as the amphiphile and hexadecane as oil. Scartazzini and Luisi [311] demonstrated that addition of small amounts of water to soybean–lecithin organic solvent reverse micelles causes a dramatic increase in viscosity and the formation of a rigid, optically transparent gel matrix. Solutions of lecithin in up to 50 different solvents are amenable to gelation upon the addition of small amounts of water which causes an increase in viscosity by a factor of 10^6. Since lecithin solutions do not contain any polymeric material, the formation of such highly viscoelastic solutions is intriguing. Recent studies have been aimed at elucidating the microstructure of lecithin-based microemulsions [312–315] and organogels [307] from extensive rheological, light scattering [307], conductivity and FT-IR

spectroscopic studies. Rheological studies have shown that the elastic-modulus of the gels is related to the lecithin volume fraction by a power law relation where the exponent is very similar to that in semidilute polymer solutions leading to 'polymer-like reverse micelles'. Viscosity and light scattering data suggest that the gelation process occurs in the system resulting from self association of lecithin molecules into a cylindrical reverse micelle. Since the viscosity increases upon the addition of water, the aggregation of lecithin molecules is water-induced. Recently, different authors [316–318] have reported that either discrete droplets or bicontinuous microemulsions are formed in the water–lecithin–alcohol–hexadecane system from viscosity and conductivity measurements. Aliotta et al. [319] presented some results from Brillouin scattering measurements on water–lecithin–cyclohexane reverse micellar system as a function of [water]–[lecithin] and temperature, and suggested a polymer-like network.

7.2. Interfacial water structure in lecithin–oil–water reverse micelles

The study of water organization at the lecithin–water interface is important in the understanding of the various activities and structures of biomembranes [320]. Recently, Maitra et al. [321] have investigated the water structures in lecithin reverse micelles using benzene, cyclohexane, *n*-octane and *n*-dodecane as oils by NMR and FT-IR techniques, and have found that water remains in three different states; water hydrated to monomeric lecithin, water bound to lecithin polar groups at the lecithin–water interface in the aggregates, and free water or weakly hydrated water in the aqueous core of the aggregates. The composition of each of the various states of water depends on the amount of water solubilized in the micelles. It has been estimated that the maximum amount of water bound per lecithin molecule is between 4 and 5 in the aggregated system. The effect of cholesterol (an important constituent of biological membranes) on the interfacial water structure at the lecithin–water interface has also been examined.

8. Dynamic processes in microemulsions

The formation of micelles and microemulsions are dynamic self-organizing phenomena where aggregating–deaggregating processes operate in conjunction. In their process dynamics, exchange of matters between different phases continuously occur resulting in an overall equilibrium. In the study of dynamics of microemulsions, the intrinsic operative phenomena need identification and quantification, a task of importance requiring the serious attention of research. Their flow under stress and the transport of ions and molecules through them are also of potential importance in the study of microemulsion dynamics. A comprehensive presentation of the intrinsic and derived processes in microemulsion systems are presented in the following text. Of the various processes to be discussed, the self-diffusion of the components (species) of microemulsion has been presented with a fair degree of

elaboration in the previous section in connection with the discussion of microemulsion structure by NMR technique. This phenomenon is not presented in this section.

8.1. Motion of the amphiphile chain in microemulsion

Both in the three component (water–surfactant–oil) and four component (water–surfactant–cosurfactant–oil) w/o microemulsion systems, the head group of the surfactant is the least mobile and the motion increases down the chain and maximum at its end as revealed from NMR measurements. This feature is common to both ionic and non-ionic surfactants; the terminal methyl group can freely orient in the oil phase [21,81,252]. AOT in reverse micelles in chloroform and benzene also extends similar behavior [322]. The addition of water on the other hand results in an increase in the motion of the carbon atoms particularly those close to the head groups, at a lower water content (where the water core is yet to form) the increase in mobility reaches its maximum [240,252,323]. This conspicuous behavior needs an explanation. As regards the motion of the cosurfactant molecule (normally lower alkanols), NMR spectra has not recorded equal symptoms, like the surfactants; a very fast exchange of the cosurfactant between the existing environments is anticipated. Experimental detection of the actual state of affairs remains to be explored.

The motion of the surfactant in the o/w microemulsion system by NMR relaxation measurements has been inferred to be restricted by the formation of the interfacial layer between oil and water and anchoring of the ionic head group at the interface. The behavior of the cosurfactant is again inconclusive due to its fast exchange between various environments [85,324].

8.2. Exchange of components between the existing environments

The processes comprise: (1) the exchange of water between the bound and free state; (2) the exchange of counterions between the ionic head groups of the surfactant and core water; (3) the exchange of cosurfactants among the interfacial film, the continuous phase and the dispersed phase (if soluble in the phase); and (4) the exchange of surfactants between the interfacial film and the aqueous phase. The investigations on these aspects are not exhaustive but sufficient for a general understanding of the overall dynamic behavior.

The exchange time ($< 10^{-4}$ s) between the 'bound' and 'free' water on NMR time scale is rapid [21,81,240] on the micelle surface, water has a nanosecond residence time. The water exchange behaviors of micelles and microemulsions are not of significant difference. The resident time of water in microemulsion (10^{-9} s) [325] is comparable with its residence time in the hydration shell of the counterions Na^+, K^+, etc. A water-separated ion pair and a contact ion-pair at low water content ($\omega < 4$) with a time in the range 10^{-7}–10^{-8} s for the above process has been observed by ultrasonic absorption of AOT solution in decane [326].

The dynamic behavior of water exchange between the free and bound forms

suggests dynamicity in the counterion association–dissociation in micelles and microemulsions [240]. Fast exchange (10^{-4} s) of Na^+ in the interfacial layer in w/o microemulsion has been evidenced from study of the temperature dependence of ^{23}Na line width in NMR spectra. On a competitive basis, the residence time of I^- in cetyl pyridinium iodide micelle in the stern layer has been reported to be 10^{-7} s.

The exchange of cosurfactants between various existing phases has been reported to be fast on NMR time scale, it is well below 10^{-4} s [21,81,85,324,327,328]. The alcohol exchange has been found to be slowed down in the presence of brine [327]. The relaxation time for the alcohol exchange in a number of microemulsions (both w/o and o/w types) has been found to be $< 10^{-8}$ s [329,330], which does not decrease with increasing alcohol chain length as expected [331–333]. The cosurfactant exchange relaxation time has shown dependence on its ratio with the surfactant to oil content, as well as its ratio with variable content of water [329], these phenomena need explanation.

The surfactant exchange between the interfacial film and the dispersed phase in o/w microemulsion has been explored by ultrasonic absorption study [329,330]; the relaxation time of the order of 10^{-8} s has been found for water–SDS–1-butanol–toluene system. The exchange of surfactants has not been clearly understood. The possibility of self-association of the cosurfactant (alcohol) in the oil phase having a relaxation time of the order of 10^{-8}–10^{-9} s can not be ruled out. The investigations by NMR [81,324] have suggested restricted residence of surfactants at the interface whereas ultrasonic absorption indicates rapid exchange. This difference may originate from the population difference required between the two studies; in NMR the states must be well populated by the surfactants whereas the ultrasonic absorption method can probe when the levels are thinly populated (the latter method is thereby much more sensitive than NMR).

8.3. Dynamicity of the interfacial film

The interfacial film between oil and water plays a key role towards the formation, stability and discreteness of the droplets of the microemulsions or its continuous state [334,335]. It is the features of the exchange of surfactants and cosurfactants that decide the interfacial flexibility. The fluidity of the film has been assessed from spin lattice relaxation time of the alkanol in quaternary microemulsion systems with SDS and potassium oleate [324,336–338]. The flexibility of the film decreases with the increasing chain length of the alcohol; the interfacial fluidity has a reasonable influence on the dielectric constant, conductivity and scattering properties of the microemulsion systems. The alkanols introduce more disorder in the interfacial film as their chain lengths increasingly differ from the surfactant [337,339]. The exchange of the alkanols between the film and the oil and water phases makes the film porous and hence more fluid [340]. The interfacial film spontaneously fluctuates, the molecules diffuse laterally [338], but this property does not essentially guide the flexibility features of the film only; slower diffusion may have a link with greater affinity of the alkanols for the interface and consequently offers a controlling factor on the dynamics of the film behavior.

8.4. Dynamics of droplet fusion and related behaviors

The dispersed droplets in a microemulsion are in constant motion and can collide and even transiently fuse and dissociate, as well as form clusters of variable size and shape. The above phenomena depend on droplet concentration and type, and also on environmental conditions. For w/o systems, such dynamics conspicuously manifest on the conductance behavior. The fusion process can be conveniently monitored by the TRFQ method. The conductance behavior of w/o microemulsions, essentially formed with ionic amphiphiles depending on composition and temperature, may show a significant increase of 100- to 1000-fold and the phenomenon is called 'percolation'. It will be seen in the subsequent section that viscosity of microemulsion may also exhibit a percolation type of behavior, but it is relatively less frequent than conductance percolation. In the following discussion the dynamics of droplet fusion and conductance percolation will be elaborated. It is to be understood that the phenomenon of fusion of droplets in o/w systems is effectively restricted by the repulsive interaction of the ionic amphiphiles (as the stabilizers); on a general basis, the droplets can come closer but remain separated, the fission–fusion process is least probable.

8.4.1. Dynamics of droplet fusion in w / o microemulsion

Experiments reveal that mass-exchange, mass transfer and chemical reactions can occur through interdroplet fusion in w/o microemulsions. For example two microemulsion solutions, one containing $BaCl_2$ and the other Na_2SO_4, on mixing immediately produce $BaSO_4$; the solution remains clear or turbid depending on ω and overall concentration of $BaSO_4$. Faintly or vanishingly colored $CuSO_4$ containing w/o microemulsion when mixed with colorless solution of $K_4[Fe(CN)_6]$ in the same microemulsion medium immediately produces a stable chocolate brown color solution of dispersed $Cu_2[Fe(CN)_6]$. This reaction and other similar reactions performed in w/o microemulsion media have clearly advocated fusion of droplets and their subsequent fission operative under dynamic conditions, enabling exchange and transfer of mass among the droplets. Otherwise, due to solubility restriction, water soluble materials can not cross the non-polar (oily) barrier (continuum) existing between the droplets to produce products by the process of mass exchange and mass transfer.

According to experimental evidences, the redistribution of components among droplets in microemulsions is fairly rapid which has been attributed to two distinct type of processes (Fig. 8):

A. Droplets collide, temporarily merge (fuse) into larger droplets and then break (fission) into smaller droplets. This dynamic process leads to reaction by way of mass exchange and transfer,
B. Droplets break with loss of fragments which subsequently associate or coagulate with other droplets. This dynamic process also helps in chemical reaction and mass distribution.

The rapid exchange of the content of the droplet has been experimentally

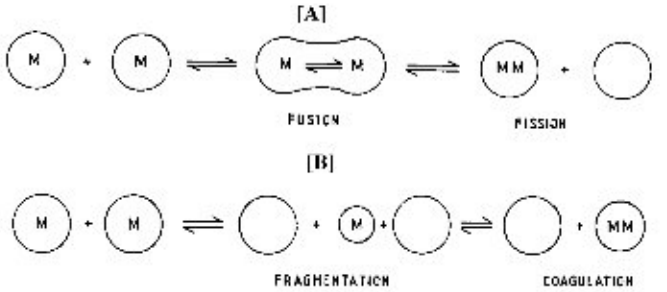

Fig. 8. (A) Collision, fusion and fission with mass transfer; and (B) fragmentation followed by coagulation causing mass transfer.

understood from the work of Menger et al. [341] who observed rapid hydrolysis upon the mixing of an ester taken from one microemulsion and the base in another. The authors suggested Scheme 1 as depicted in Fig. 8. Droplet collision and temporary merging phenomena were supported by the complexation study between Tb^{3+} and hydrophenyl acetic acid, which manifests large fluorescence enhancement [342]. Compared with micelles, the studied droplets have a much longer lifetime [343–345].

The rapid exchange of materials in the droplets has been supported by other studies in w/o microemulsions; behaviors of fluorescence probes, complex formation between water soluble reagents and the rate of dissolution of water in the water–SDS–1-pentanol–dodecane system were investigated [252,346,347]. For the chemical reaction to occur the following rate determining paths have been proposed as shown in Fig. 9.

The time for single fission in the above studies was estimated to be approx. 10^{-6} s and the rate constant for collision with merging approx. 10^{8} ms, but quantitative accounting of the rate constant could not be ascertained. In a model, Eicke et al. [348] proposed a transient dimer formation during collision between two droplets with opening of a water channel whereby exchange of materials occur by way of diffusion during the collision time.

Evaluation of the bimolecular exchange rate constant (k_e) has been attempted in

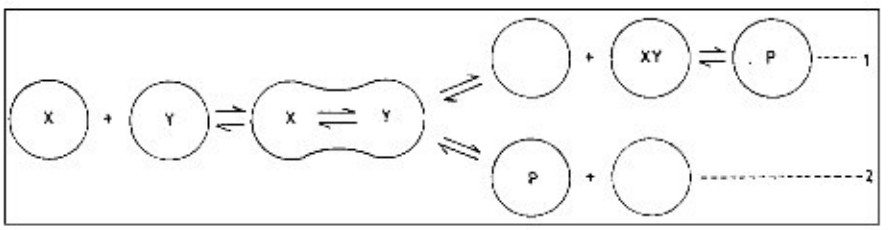

Fig. 9. Modes of reaction between X and Y forming the product P. (1) Droplet merging and splitting process (reaction slow). (2) Droplet merging and simultaneous reaction controlled process (reaction fast).

recent years, by a number of workers, using fast kinetics (stop-flow method), fluorescence and phosphorescence quenching and luminescence studies [349–352]. Of the several processes that occur, i.e. collision between two droplets, the opening of a water channel, the diffusion of reagents and their reaction and the dimer breakdown, the second step is considered to be rate-determining. k_e has been found to be of the order of 10^7 M^{-1} s^{-1} at 25°C, i.e. approximately one collision per thousand becomes fruitful in the transient merging of colloidal droplets forming a channel for reaction to occur. The process ends up with large entropy of activation required for the release of the amphiphile AOT from the interface and the required life time of the transient dimer is in microseconds. It has been anticipated that the splitting of the dimer may result in polydispersity of droplet size.

The bimolecular exchange rate constant k_e has been found to be extremely sensitive to the presence of additives. Thus benzyl alcohol (a cosurfactant) has been shown to increase k_e approx. 20-fold [353]. k_e is also very sensitive to the alkanol chain length. It has been presumed that the difference in the conductivities of w/o microemulsion systems with different alkanols essentially originates from the differences in their k_e values.

The effects of different parameters on the dynamics of w/o microemulsions have been systematically studied in recent years [354–358]. A comprehensive discussion of the results has been made by Lang et al. [359]. The droplet size and interdroplet interaction in w/o microemulsions have been elaborately assessed (by DLS and TRFQ methods, etc.) in terms of the type of oil, surfactant, alkanol chain length (and concentration), and temperature. The interdroplet attractive interaction (leading to fusion and mass exchange) and droplet size increase with increase in the alkane (oil) chain length and temperature, as well as with a decrease in surfactant and alkanol chain length and concentration. The rate constant, k_e, associated with the exchange of material between droplets upon collision with transient merging (Scheme 4) has been found to be $\geq (1–2) \times 10^9$ M^{-1} s^{-1}. Such high values of k_e have also been obtained by others [360–362] which suggest that the rate limiting step is not by the opening of the interfacial film but by the droplet diffusion (Fig. 10).

8.4.2. Time-resolved fluorescence quenching (TRFQ) method

The versatility and advantage of the method of TRFQ in the study of micellar

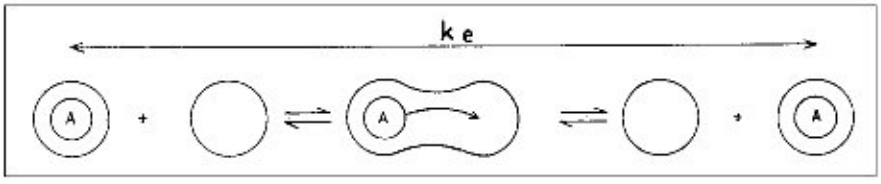

Fig. 10. Collision, transient merging, mass transfer and fission processes in w/o microemulsions. The overall rate constant of material exchange is k_e.

size and the kinetic process occuring in them have been elaborately discussed by Lang [363]. Extensive reviews on the results obtained with the TRFQ method also appear in the literature [364–366]. Bakale and Warman [367] have reported fast changes in the droplet size in the fusion–fission processes in water–AOT–isooctane systems by time-resolved microwave conductivity.

The fusion–fission processes are not favored in o/w microemulsions because of strong electrostatic repulsion to prevent droplet collision. Coagulation fragmentation (Fig. 8, Scheme B) does not contribute to the formation–dissolution of the droplet [368]. The absence of fusion–fission processes in o/w microemulsions has been also supported by stopped-flow study by Tondre and Zana [230] from the observation that the dissolution of oil in a dilute o/w emulsion is very slow. The injected oil absorbs the surfactants initially present in the system followed by electrostatic repulsion reducing the rate of collisions between injected oil droplets and the microemulsion droplets. The coagulation–fragmentation process in w/o microemulsion has also been probed with pyrene by the TRFQ method [366]. In mixed alcohol + surfactant solutions, rapid micellar exchange of micelle-solubilized pyrene has been observed by coagulation–fragmentation with a rate constant of the order of 10^5–10^6 s^{-1}. The addition of oil has increasingly decreased the interdroplet exchange of pyrene which stops at high oil content. In agreement with the chemical relaxation studies [368], fragmentation processes are less and less contributive to the dynamics of the o/w microemulsion as the dimension of the oil core builds up.

8.4.3. Principle of TRFQ method and results

In a homogeneous continuous medium the fluorescence of a probe compound is uniformly quenched by a quencher. The fluorescence decay of the probe with the quencher is enhanced and both of them follow linear correlations with time. In microheterogenous–compartmentalized environments (i.e. micelles, microemulsions, etc.), the probe and quencher molecules may reside either together or separately in the compartments, some of the compartments may also remain vacant, i.e. without the probe or the quencher. It is obvious that the compartmentalized probe with the quencher should exhibit rapid decay in the fluorescence by efficient quenching, and that containing only the probe should exhibit slow and normal decay. Thus the fluorescence decay pattern with time is initially rapid and slows after a time. This initial difference in fluorescence decay observed in compartmentalized liquids when analyzed in a rationalized way can help in obtaining information on the micellar aggregation number, size and bimolecular collision dependent mass exchange rate constant between the microemulsion droplets.

The fluorescence decay curves obey the following equations [369,370]:

$$I(t) = I(0) \exp\left[-A_2 t - A_3\{1 - \exp(-A_4)_t\}\right], \quad (1)$$

where $I(0)$ and $I(t)$ are the fluorescence intensities at time $t = 0$ and t, respectively following excitations, and A_2, A_3 and A_4 are time-independent parameters obtained with $I(0)$ using a non-linear weighted least-squares fitting procedure.

Table 1
The TRFQ results of the mass-exchange (transfer) rate constant by collision of w/o microemulsion droplets

System	Probe/quencher	$k_e \times 10^{-8}$ $M^{-1} s^{-1}$	Ref.
H_2O/AOT/Pn	$Rb(bipy)_3^{2+}/Fe(CN)_6^{3-}$	< 10	[359]
H_2O/AOT/Hp	$Rb(bipy)_3^{2+}/Fe(CN)_6^{3-}$	< 10	[359]
H_2O/AOT/Hp	$Rb(bipy)_3^{2+}/Fe(CN)_6^{3-}$	14	[353]
H_2O/AOT/*i*-Oc	Mg-teraphenylporphyrin/methyl viologen (MV^{2+})	19	[372]
H_2O/AOT/Dc	$Rb(biby)_3^{2+}/Fe(CN)_6^{3-}$	50	[359]
H_2O/AOT/Dodc	$Rb(biby)_3^{2+}/Fe(CN)_6^{3-}$	200	[359]
H_2O/SDS/1-hexanol/Tl	$Rb(biby)_3^{2+}/Fe(CN)_6^{3-}$	2.5	[353]
H_2O/SDS/1-hexanol/Hxdc	$Rb(biby)_3^{2+}/Fe(CN)_6^{3-}$	2.2	[346]
H_2O/SDS/1-hexanol/Hxdc	$Rb(biby)_3^{2+}/Fe(CN)_6^{3-}$	1.1	[346]
H_2O/CTAB/1-hexanol/Dodc	$Rb(biby)_3^{2+}/Fe(CN)_6^{3-}$	1.4	[353]
H_2O/CTAB/1-hexanol/Hx	1-methyl napthalene/KI	0.1	[353]
H_2O/DAP/cyclohexane	1-methyl napthalene/KI	13	[347]
H_2O/DBDAC/cyclohexane	$Rb(py)_3^{2+}$/methyl viologen(MV^{2+})	52	[359]
H_2O/TDBDAC/cyclohexane	$Rb(py)_3^{2+}$/methyl viologen(MV^{2+})	7	[359]
H_2O/HDBDAC/cyclohexane	$Rb(py)_3^{2+}$/methyl viologen(MV^{2+})	2	[359]

Pn, pentane; Hp, heptane; *i*-Oc, isooctane; Dc, decane; Dodc, dodecane; Tl, toluene; Hxdc, hexadecane; Hx, hexane; DAP, dodecylammonium propionate; DBDAC, dodecyl benzyldimethyl ammonium chloride; TDBDAC, tetradecylbenzyl dimethyl ammonium chloride; HDBDAC, hexadecyl benzyl dimethyl ammonium chloride.

With inter-droplet exchange of quencher (on the fluorescence time scale) which is our present interest,

$$A_2 = k_0 + k_e k_q [Q]/A_4,$$

$$A_3 = (k_q/A_4)^2 [Q]/[M],$$

$$A_4 = k_q + k_e [M],$$

and

$$N = \frac{[C]}{[M]} = \frac{[C]}{[Q]} (A_3 A_4 + A_2 - k_0)^2 / A_3 A_4^2,$$

where k_0 is the fluorescence decay rate constant, k_e is the mass exchange rate constant by collision (defined earlier), k_q is the pseudo-first order rate constant for interdroplet fluorescence quenching, $[Q]$ is the quencher concentration, $[M]$ is the micellar concentration, $[C]$ is the total surfactant concentration and N is the aggregation number.

By mathematical manipulation procedure,

$$[k_q] = A_3 A_4^2 / [A_3 A_4 + A_2 - k_0], \quad (2)$$

Table 2
A list of typical probes (P) and quenchers (Q) used in TRFQ studies of micellar and microemulsion systems

Surfactants	Normal micelles and o/w microemulsions
Anionic	Pyrene (P)
	Dodecyl pyridinium chloride (Q)
	Tetradecyl pyridinium chloride (Q)
	Hexadecyl pyridiniuin chloride (Q)
	$Ru(bipy)_3^{2+}$ (P)
	$Ru(bipy)_3^{2+}$ $(C_{17})_2$ (P)
	[1-methyl-1-tetradecyl-4-4′-bipyridinium]$^{2+}$ (P)
	Anthracene sulphonate (P)
Cationic	Pyrene (P)
	Hexadecyl pyridinum chloride (Q).
Nonionic	Pyrene (P)
	Hexadecyl pyridinium chloride (Q)
	Reverse micelles and w/o microemulsions
Anionic	$Ru(bipy)_3^{2+}$ (P)
	$Fe(CN)_6^{3-}$ (Q)
	Mg-tetraphenylporphyrin (P)
Cationic	$Ru(bipy)_3^{2+}$ (P)
	Methylviologen^{2+} (Q)
	1-methyl napthalene (P)

and

$$[k_e] = A_4(A_2 - k_0)/(k_q[Q]). \quad (3)$$

From the knowledge of N and necessary physical constants, the size of the microemulsion droplets can be estimated [366,371].

Further details of the principle and data manipulation method of TRFQ is beyond the scope of the present article, a comprehensive presentation of results would be quite revealing which is given in Table 1.

The probe (P) and quencher (Q) molecules employed for studying anionic, cationic and non-ionic micelles are to be wisely selected. In Table 2, the P and Q molecules used in micellar and microemulsion studies are listed.

8.4.4. Usefulness of the TRFQ method

The TRFQ method is versatile in understanding the dynamics of micellar as well as their other physicochemical characteristics, i.e. aggregation number, polydispersity, particle size, as well as the shape (spheres, ellipsoids, discs, etc.) [372–381]. The TRFQ method has been used for diffusion data on reactants in cylindrical micellar systems [382–384]. This is the only method that helps determination of the kinetics of micellar exchange of reactants and micellar fragmentation; dissociation and association of a member from a micelle and to a micelle can also be

determined. The method can give information on the distribution of the micellar size but such studies are only limited. The analysis of polydispersity and the exchange process in terms of fluorescence decay is rather difficult and has not been applied to real systems.

The TRFQ method is advantageous over other methods (i.e. dynamic light scattering, DLS) where dilute solutions are used to keep micellar interaction at a low level; in TRFQ, concentrated solutions can be used since the fluorescence decay of the probe is independent of the interactions between micelles.

In structural and dynamical studies of micelles and microemulsions, the TRFQ method is indeed versatile [18,19,385–390]. In this connection, the time-resolved phosphorescence and triplet absorption quenching measurements of Johnsson and Almgren [391] to monitor the cluster-structure of L_2-phase of water–AOT–*n*-octane or *n*-decane microemulsion systems can be referred. The frequency and activation energy of the droplet fusion have been measured at different droplet sizes; the fusion rate has decreased and the activation energy has increased with increased droplet size. But the magnitude of the two parameters have been found to be independent of the alkane chain length.

8.5. Conductance of microemulsion

The ionic conductance in o/w, w/o and bicontinuous microemulsions can be dramatically different. It is almost like a normal aqueous medium in o/w microemulsion, very low in w/o microemulsion and significantly high in a bicontinuous condition. In the second, the water content, as well as the temperature, are the controlling factors for the magnitude of conductance; the phenomenon of percolation (as discussed in the subsequent section) may arise. The conductance behavior of bicontinuous microemulsion is comparable with the percolation feature. In fact during percolation, the microemulsion system is viewed to pass through a bicontinuous-like stage.

The ternary systems of water–surfactant–alkanol or benzyl alcohol or poly(propylene glycol), etc., can produce isotropic, low viscous solutions ranging from water to the oil corner in the ternary phase diagram, called the L-phase. This phase exhibits distinct structural, viscous and conductivity behaviors. The area has been recently thoroughly explored by Rodenas and coworkers. The water–CTAB–benzyl alcohol [201] has produced an L-phase where at constant [CTAB] the specific conductance increases and passes through a maximum with increasing benzyl alcohol concentration, and the maximum shifts towards a higher alcohol concentration. Again, at different [CTAB]–[Benzyl alcohol] ratios, the specific conductivity virtually produces maxima at $\sim 50\%$ (w/w) water addition. The increase and decrease in the conductivity have been attributed to the increased ionization of CTAB by alcohol incorporation in the micelle and the formation of mixed reverse micelles. The changed shape of the aggregates has also contributed to the transport property. The conductance study of water–CPC–*n*-butanol [200] has produced similar results in the L-phase region. The regions of maxima are also comparable with the L-phase of water–CTAB–benzyl alcohol system. In a separate work,

Sierra and Rodenas [199] have studied the system, water–SDS–poly(propylene glycol). The physical nature of the L-phase formed is comparable with the L-phases produced by *n*-butanol and benzyl alcohol mentioned above. At constant amount of the surfactant, the conductivity initially increases with the polymer concentration until 5% (w/w), thereafter, it progressively decreases to very low values. Identical conductance behaviors have been observed for water–CTAB–poly(propylene glycol) system [392,393] and water–CTAB–*n*-butanol system [394]. Other comparable studies with the alkanols are also from the laboratory of Rodenas [395–397]. The initial rise in conductance in the studied cases has been again ascribed to increased ionization of the surfactant by polymer incorporation; the subsequent decline in conductance has been adduced to the mixed reverse micelle formation.

The low conductance of w/o microemulsion systems at lower volume fraction of water or at a state much below the percolation threshold has been explained on the basis of migration of statistically charged droplets and the quantitative charge fluctuation model [50,398–400]. The reasoning for percolation and its mechanism have been subsequently presented. In this context, the conductance behaviors of perfluoropolyether microemulsions may be a noteworthy addition. Chittofrati et al. [401] have made an elaborate investigation on the water–ammonium salt of perfluoropolyether carboxylic acid–perfluoropolyether microemulsion system with a comparable size surfactant and oil. The conductance of the system as a function of water content at different oil to surfactant mass ratio has shown a well-shaped maximum in the curve which shifts towards higher water content with an increasing o/s ratio. The conductivity as a function of water content at constant mass ratio of water to surfactant has exhibited a sharp rise and a tendency to level off. The observed conductance increase cannot be accounted for either by the charge fluctuation model or the percolation model. It has been proposed by Chittofrati et al. [401] that the initially added water solvates the polar heads, and the increase in conductance results from the increased dissociation of the counterions from the head groups. At the conductance maximum, water droplet formation starts and further addition produces closed ensembles, i.e. reverse micelles where the conducting ions are confined in the interior. The onset of droplet formation has been corroborated by the light scattering measurements. A working model for the above water dependent conductance profile has been performed by the authors and a quantitative analysis has been attempted; the parameters, i.e. molar and ionic conductances at infinite dilution, fraction of water in the droplet, etc., have been evaluated. The work qualifies a distinction, and has added insight to the mechanism of conductance in an off-the-trend microemulsion system.

In recent literature [402,403], there are reports of unexpected conductance behaviors of microemulsions. Ajith et al. [402,403] have studied water–Brij-35–*n*-propanol–alkane and water–SDS–*n*-propanol–cyclohexane microemulsions in the presence of NaCl, and have observed that for lower ω the conductance decreases with increasing temperature; a rare phenomenon in solution. The difficulty for ions to hop from droplet-to-droplet with increasing temperature has been suggested for the conductance decline at lower ω. At higher ω, formation of clusters at higher

temperatures has produced increase in conductance after an initial decrease. The conductance study of water–SDS–mixed alkanol–cyclohexane has also been made by John and Rakshit [192] to reveal that the binary mixtures of lower alkanols (cosurfactants) behave like alkanols of carbon chain lengths intermediate between the two individual components. The systems have exhibited a fair degree of percolation trend. They have also reported non-percolating microemulsion systems of brine–Brij 35–*n*-propanol–*n*-heptane or nonane and water–CTAB–*n*-propanol–cyclohexane [189].

Mixed surfactant (anionic–nonionic, cationic–nonionic and cationic–anionic) have been also used in microemulsion preparation by Seedher and Manik [404] and Li et al. [405,406] for structural and conductivity studies. For AOT–TX100 and acetylpyridinium bromide (CPB)–TX100 mixtures, the former authors have observed that the threshold volume fraction for percolation depends on the mixing ratio when heptane is the oil; it increases with an increased proportion of the ionic component. Li et al. [405,406] have used AOT–TX100, CTAB–TX100 and Na-oleate–CTAB combinations along with lower alkanols (*n*-butanol, *n*-pentanol and *n*-hexanol) and observed bicontinuous and birefringent phases using diesel oil and heptane. The conductance of these systems have exhibited conspicuous trends (not of the percolation type) with the variation of the surfactant weight percent which can act as a marker for the identification of different phase transitions that may occur in the system. Eicke and Meier [407] have studied the interfacial charge transport in w/o microemulsions with mixed surfactants (AOT + pentaethylene monododecyl ether) and *n*-octane, and have observed unusual conductance, producing a percolation type pattern in the conductance vs. temperature course. The diffuse double layer at the water–oil interface of the droplets has been considered to be highly compressed which accounts for reduced mobility and surface conductivity.

8.5.1. Percolation of conductance

The phenomenon of percolation of conductance has been known to occur in binary inclusions containing conductor and insulator. It has been found that after a threshold volume fraction (ϕ) of spherical particles of the conductors ($\phi \simeq 0.17$), the conductance increases sharply and then levels off. This phenomenon is known as 'static percolation' and has been critically studied and analyzed [53,408–415].

The phenomenon of conductance percolation in colloidal solution, i.e. w/o microemulsion, is equally interesting if not more so [416–422]. The droplets containing surfactant ions come to a threshold distance wherein transfer of charge between them occurs efficiently; they are physicochemically dynamic and can approach their neighbours by diffusion to transfer charge [423]. This is how 'dynamic percolation' arises after a threshold volume fraction (ϕ_t) at a constant thermal condition or temperature. The phenomenon can be augmented by the increase of temperature at a fixed droplet concentration. The w/o microemulsions formed with non-ionic amphiphiles containing soluble salts in the aqueous core can exhibit conductance percolation as well [424].

The w/o microemulsion systems exhibit well-formed percolation behaviors and

thorough studies in this field can be found in Refs [69,425–428]. The origin, nature and mechanistic behaviors of the different percolating systems, as well as quantification of results can be found in these works. It has been observed that the [water]–[amphiphile] mole ratio, ω plays an important role in the percolation process; the threshold volume fraction of the disperse phase (ϕ_t) corresponds to a particular value of ω below which conductance-increase with volume fraction of the disperse phase (ϕ) is but minimum.

Of course for temperature percolation lower values of ω than required for volume percolation may be effective, it is the threshold temperature that essentially determines the phenomenon. The ω, i.e. size dependent percolation are clearly found in the works of Mukhopadhyay et al. [429] and Alexandridis et al. [430].

8.5.2. Mechanism of percolation

It has been considered that for the transfer of charges between them, the droplets need to come close and the amphiphile chain length is an important guiding factor for the process. Both the amphiphile shell length and the volume fraction of the disperse phase determine the value of ϕ_t. For zero shell length and no interparticle attractive interaction, the randomly packed hard sphere model proposes $\phi_t = 0.65$. For overlapping spheres with large values of shell volume, $\phi_t = 0.35$. Strong attractive interaction radically decreases ϕ_t; it can drop to 0.10 from 0.65. The largest effect occurs at the critical point near which the concentration fluctuations are maximum [431]. But for large shell length strong interaction may increase ϕ_t, the topology becomes randomly close-packed.

As regards transfer of charges there are two distinct schools of thought; one in favor of transfer by the hopping of surfactant from one droplet to another [419,432–435] and the other by the mechanism of fusion, interfacial layer opening and ion-transfer [355,356,436]. From self-diffusion coefficient measurements by NMR, Maitra et al. [437] are in favor of the hopping mechanism, whereas Jada et al. [355,356] have suggested transient channel formation leading to counterion transport during droplet clustering by the TRFQ method. According to Feldman et al. [438], the conductivity and dielectric polarization below the percolation threshold arise from the motion of counterions through water-channels, and are not as a result of the hopping of ions; above the threshold, the same mechanism still dominates. Mukhopadhyay et al. [429] are also in favor of the transient fusion model. The formation of bicontinuous state by droplet association has also been suggested to augment percolation [75]. The concentrated microemulsions produced by the ternary water–AOT–oil system have evidenced a globular form of droplets by DLS, only to vouch against bicontinuity as an explanation for conductance percolation [93]. The scattering studies have also revealed maintenance of droplet structure beyond percolation threshold [90,93,439] and hardly any change in shape and size near the phase separation stage [440]. Monte Carlo simulations with strong interactions in the short range have been shown to produce percolation transition for spherical particles [420,432,435,441].

The study on the percolation of water–AOT–alkane (i.e. hexane, isooctane,

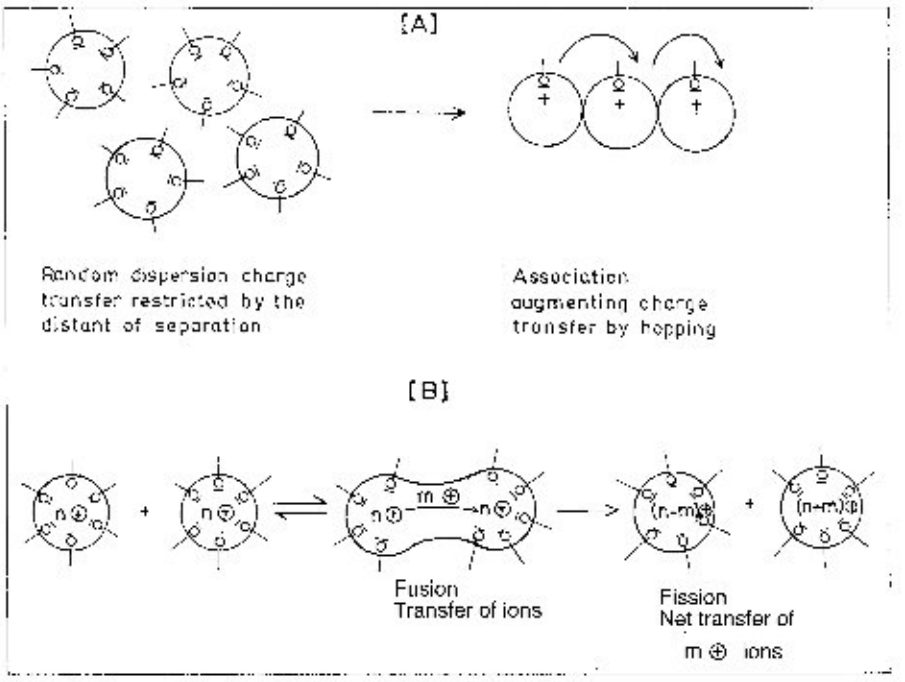

Fig. 11. (A) Hopping mechanism. Ions hop in the direction indicated by the curl heads (only one surfactant ion is shown to avoid a complex drawing). (B) Ion transport by fusion and fission. n ⊕ cations in the droplets. m ⊕ cations are involved in the transfer process.

decane, and dodecane) systems by Alexandridis et al. [430] is thorough with regard to [water]–[AOT] mole ratio (ω), and [oil]–[AOT] ratio (S) and temperature. Effective percolation has been observed at $\omega > 15$; the percolation temperature decreases with increasing ω and decreasing S. The increasing molar mass of the alkane has shifted the percolation threshold to a lower temperature. Similar ω-dependent percolation behaviors have also been reported by Mukhopadhyay et al. [429] for water–AOT–decane w/o microemulsion systems. The percolation phenomenon in this system appears to be distinct at $\omega \geq 12$, a value of 15 has been reported by Alexandridis et al. [430]. A schematic representation of the models of charge transfer is shown in Figs. 11A and 13.

8.5.3. Theory of percolation

The phenomenon of percolation is, on the whole, guided by scaling law [279,442–444]. At a constant temperature and in the percolation range, the conductance of conductor–insulator mixtures as in water droplets (with ionic amphiphiles or added electrolyte in the case of non-ionic amphiphiles) dispersed in oil in w/o microemulsions follows the relation,

$$\sigma = k(\phi - \phi_t)^{\mu},$$

or

$$\ln \sigma = \ln k + \mu \ln (\phi - \phi_t), \tag{4}$$

where σ is the conductance of the microemulsion system, and k and μ are constants of which k is related to the conductance of the dispersed phase. The exponent μ should be 1.9 for both static and dynamic percolation according to recent work [445].

At a constant composition (fixed ω), the scaling law for the temperature percolation [446–448] in w/o microemulsion is,

$$\sigma = P(\theta - \theta_t)^{n},$$

or

$$\ln \sigma = \ln P + n \ln (\theta - \theta_t), \tag{5}$$

where θ is the temperature corresponding to the conductance σ, θ_t is the threshold temperature for transition and n is an exponent. Both ϕ_t and θ_t required in Eqs. (4) and (5) are obtained from the plots between σ and ϕ, and σ and θ, respectively, as depicted in Fig. 12.

Like μ, the expected value of n is also 1.9 [445,446]. The values of μ and n realized from experiments in most cases are at odds with the expected value of 1.9. A pragmatic discussion on the values of the exponents μ and n will be made in a subsequent section on the 'effects of additives on percolation'.

8.5.4. Conductance theories of binary inclusions and their applications to percolation

The conductance of binary mixtures can be quantified by the effective medium theory (EMT) [278,279,410,415,449]. The EMT theory has been shown to be inadequate for microheterogenous dispersions of metals and metal oxides in a medium. Granqvist et al. [450] have recommended consideration of dipole–dipole

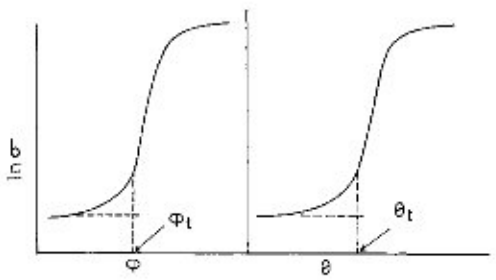

Fig. 12. Typical volume and temperature percolation diagrams. The procedure for getting ϕ_t and θ_t are indicated by arrow heads in the diagrams.

interaction among the dispersed entities naming EMT as EMTDD (DD stands for dipole–dipole interactions). The dipolar interactions may give rise to the formation of chains and clusters of spherical droplets. Bernasconi and Wiesmann [451] have also proposed a percolation equation of the conductance for microheterogenous dispersions of solids in suitable media.

Owing to Böttcher, the EMT equations, under practicable conditions, can assume the scaling equation,

$$\frac{\sigma - \sigma_c}{3\sigma} = \frac{\sigma_d - \sigma_c}{\sigma_d + 2\sigma}\,\phi, \tag{6}$$

where σ, σ_c and σ_d are the conductivities of the solution, the continuous medium and the disperse phase of spherical entities, respectively, and ϕ is the volume fraction of the dispersed phase.

When $\sigma_c = 0$, i.e. the continuous medium (oil, in case of microemulsion) is highly resistive, Eq. (7) takes the scaling form with exponent $\mu = 1$:

$$k = \frac{3}{2}\,k_d\left(\phi - \frac{1}{3}\right). \tag{7}$$

For non-spherical dispersions the threshold volume fraction $\phi_t < 1/3$, this can be conveniently explained on the basis of EMTDD.

The experimental determination of ϕ is difficult and by mass balance it takes the form [325]

$$\phi = \frac{\rho_s}{\rho_d}\,[W_s(1 + rM_{cs}/M_s) + W_{cs}' + W_w], \tag{8}$$

where ρ_d and ρ_s, are the densities of the dispersed phase and the solution, and W_s, W_{cs}' and W_w are the weight fractions of surfactant, cosurfactant (in the aqueous phase) and water, respectively, and M_s, and M_{cs} are the molar mass of the surfactant and cosurfactant, respectively, in the system, and r is the structural ratio i.e. N_{cs}/N_s, where N_{cs} and N_s represent the number of molecules of cosurfactant and surfactant in the interphase.

The radius of water droplets of the disperse phase (R_w) can be obtained by the relation [78]

$$R_w = \frac{3[M_s + rM_{cs} + \{(W_w + W_{cs}')/W_s\}M_s]}{N\rho_d(a_s + ra_{cs})}, \tag{9}$$

where the new terms a_s, a_{cs} and N represent the cross-sectional areas of surfactant, cosurfactant and Avogadro number, respectively.

The effective radius, R_e of the droplet (water core plus interphase) can be obtained by considering appropriate length of the surfactant or by the appropriate relation,

$$R_e = \left(\frac{3}{4\pi}\right)^{1/3}\left(\frac{4\pi R_w^3}{3} + \frac{A_s M_s}{\rho_s N} + \frac{A_{cs} M_{cs}}{\rho_{cs} N}\right)^{1/3}, \quad (10)$$

where the fresh terms A_s and A_{cs} represent the aggregation number of the surfactant and the cosurfactant molecules per droplet, and ρ_s and ρ_{cs} stand for the densities of the surfactant and cosurfactant, respectively. For the basis and detailed procedure of the above relations (Eqs. (4)–(10)) the works of Venable and Fang [78] and Bisal et al. [79,80] may be consulted. These reports uniquely show the power of the conductance method for the basic structural understanding of w/o microemulsions. The results of such an analysis for typical classes of microemulsion are presented in Table 3 (taken from Bisal et al. [79]).

The above results suggest that conductance–percolation can be a fruitful method of characterizing the water droplets in microemulsion systems. The role of the surfactant type in influencing the droplet size and amphiphile aggregation is apparent.

The EMTDD theory introduced by Granqvist and Hunderi [450] with dipole–dipole interaction and depolarizing factors leads to the equations,

$$\frac{1}{3}\phi\alpha + (1-\phi)(\sigma_c - \sigma_d)/(\sigma_c + 2\sigma_d) = 0, \quad (11)$$

where

$$\alpha = (\sigma - \sigma_d)/\left[\sigma_d + \frac{1}{3}(\sigma - \sigma_d)\right]$$

α is related with the polarizability (the depolarization factor for sphere is 1/3); σ_c,

Table 3
Dimensional characterstics of w/o microemulsions at $\sigma = 0.50$ and at constant weight fraction of water, $W_w = 0.2$ at 293 K

System	R_w (nm)	R_e (nm)	A_s	A_{cs}
CTAB/Hp/Bu	4.52	5.34	257	636
SDS/Hp/Bu	6.90	7.85	1360	612
AOT/Hp/Bu	5.80	6.61	523	340
CTAB/Dc/Bu	4.45	5.26	241	636
AOT/Dc/Bu	5.68	6.49	493	357
SDS/Xy/Bu	7.75	8.84	474	270
CTAB/Dc/HA	5.35	6.27	477	475
SDS/Dc/HA	6.30	7.25	1057	517
AOT/Dc/HA	5.56	6.38	474	270

Although AOT forms microemulsion without cosurfactants, they were used with AOT for a comparison with SDS and CTAB.
Hp, heptane; Dc, decane; Xy, xylene; Bu, butanol; HA, hexylamine.

σ_d and σ, are the conductances of the continuous medium, the dispersed phase and the mixture, respectively.

The general formula for randomly oriented ellipsoid is

$$\alpha = \frac{1}{3}\sum_{i-1}^{3}\frac{\sigma - \sigma_d}{\sigma_d + L_i(\sigma - \sigma_d)}, \tag{12}$$

where L_i stands for the triplet depolarization factor dictated by the axial ratios [450].

The aggregation of droplets in microemulsion can produce spheroidal geometry to which the EMTDD theory can be applied. The dipole–dipole interaction should result in a shift of the percolation threshold towards lower concentration; for $\sigma_c = 0$, the ϕ_t^{EMTDD} is equal to 0.271 for chains and 0.156 for clusters. For isolated spheres, the equivalent depolarization factors L_1, L_2 and L_3 are each equal to 1/3, which for single-stranded chains are 0.133, 0.435 and 0.435, respectively, and for a closed packed lattice the values are 0.0865, 0.0865 and 0.827, respectively. With $\sigma_c = 0$ and using L-values in Eq. (12) and inserting the results in Eq. (11) we get the following relations. For isolated spheres,

$$\sigma = \frac{3}{2}\sigma_d\left(\phi - \frac{1}{3}\right)$$

or the Böttcher equation. For chains,

$$\sigma = -0.1519\sigma_d[0.1566\phi + 1.7216\phi^2 - 0.729\phi^3]\phi_d. \tag{13}$$

For a cluster,

$$\sigma = -0.0984\sigma_d + [0.539\phi + 0.5679\phi^2]\phi_d. \tag{14}$$

Bernasconi and Wiesmann [451] have proposed an explanation of the EMT theory considering the clustering of droplets,

$$\sigma = 1.05\sigma_d(\phi - 0.157). \tag{15}$$

The threshold value, $\phi_t = 0.157$, is in exact agreement with the ϕ_t^{EMTDD} for clusters when $\sigma_c = 0$ as mentioned earlier. Eq. (15) is valid up to $\phi \leq 3/4$. For greater values of ϕ, the equation transforms into the form of EMT.

The application of the EMT and all the forms of EMTDD equation have been tested in detail by Paul et al. [80] considering the literature data of works by different authors [78,79,442,452,453]. Altogether 29 systems have been treated and for details the original paper [80] may be consulted. Table 4 is a concise presentation of the results.

The results in Table 4 support the invalidity of the EMTDD (cluster) and the Bernasconi–Wiesmann equation (Eq. (15)) on the systems considered. A good fraction of the systems have supported both EMT and EMTDD (chain) formula-

Table 4
Testing of the validity of percolation theories on different microemulsion systems

No.	System (wt. ratio)	r	Validity
1.	CTAB/Bu/Hp (20:60:20)	4.88 (4.89)	EMT and EMTDD (chain)
2.	CTAB/Bu/Hp (26.67:53.33:20)	2.48 (1.78)	EMT and EMTDD (chain)
3.	CTAB/Bu/Dc (26.67:53.33:20)	2.64 (1.77)	EMT and EMTDD (chain)
4.	SDS/Bu/Hp (20:60:20)	2.20 (0.97)	EMT and EMTDD (chain)
5.	AOT/Bu/Hp (20:60:20)	3.78 (2.98)	EMT and EMTDD (chain)
6.	CTAB/HA/Dc (26.67:53.33:20)	1.00 (0.13)	EMT and EMTDD (chain)
7.	CTAB/HA/Hp (26.67:53.33:20)	1.03 (0.10)	EMT and EMTDD (chain)
8.	SDS/HA (33.33:66.67)	2.0 (0.72)	EMT and EMTDD (chain)
9.	SDS/HA/Hp (20:60:20)	1.40 (0.74)	EMT and EMTDD (chain)
10.	SDS/HA/Hp (15:63.75:21.25)	3.5 (2.10)	EMT and EMTDD (chain)
11.	SDS/HA/Hp (20:50:30)	1.70 (0.61)	EMT and EMTDD (chain)
12.	SDS/HA/Hp (20:40:40)	1.80 (0.47)	EMT and EMTDD (chain)
13.	CTAB/Bu/Hp (26.67:53.33:20)	2.55 (1.93)	EMT and EMTDD (chain)
14.	CTAB/HA/Hp (26.67:53.33:20)	1.18 (0.32)	EMT and EMTDD (chain)
15.	AOT/HA/Hp (26.67:53.33:20)	1.14 (0.11)	EMT and EMTDD (chain)
16.	AOT/Bu/Hp (26.67:53.33:20)	1.14 (0.59)	EMT and EMTDD (chain)

Systems 1–7 at 293 K, 8–12 at 298 K and 13–16 at 303 K.
Non-parenthesized and parenthesized values in column 3 are according to EMT and EMTDD (chain), respectively. No. 8 is a ternary mixture of SDS/water/HA (as oil).
Bu, butanol; Hp, heptane; Dc, decane; HA, hexylamine.

tions. In Table 5, the essential results by the EMT and EMTDD (chain) theories are presented for comparison.

A correlative exercise between the EMT and EMTDD (chain) with respect to the r and σ_d values has also been attempted by Paul et al. [80]. The following least squares correlations have been reported,

$$r_{EMT} = 1.1 + 0.84 r_{EMTDD}\ (\text{chain}), \tag{16}$$

$$\sigma_d(\text{EMT}) = 0.22 + 0.750\sigma_d(\text{EMTDD} - \text{chain}). \tag{17}$$

It has been interestingly noted that the microemulsion systems that satisfy both EMT and EMTDD (chain) have $r_{EMT} \geq 1$, while those that do not satisfy them have $r_{EMT} \leq 1$. A probable mechanistic explanation of the phenomenon has been given by Paul et al. [80]. Their work has supported fitting of the conductance data of water-induced percolation phenomenon with EMT and EMTDD (chain) when microemulsion systems are formed with cosurfactants; without cosurfactants the results may fit to the EMTDD (cluster) as well as the BW theories identified by Paul et al. [80] for two systems only [452,453].

8.5.5. Effect of additives on conductance percolation

Like a normal solution, the ion-transport in w/o microemulsion is expected to be influenced by the presence of additives. In practice this has been demonstrated and the threshold concentration and temperature for percolation have been

Table 5
Comparison of results of EMT and EMTDD (chain) theories

System	σ_d (Sm^{-1})	R_w (nm)	R_c (nm)	A_s	A_{cs}
1.	1.14 (1.02)	4.05 (4.13)	4.81 (4.89)	139 (145)	679 (708)
2.	1.61 (1.69)	4.52 (5.01)	5.34 (5.87)	257 (367)	636 (653)
3.	1.14 (1.52)	4.45 (5.03)	5.26 (5.89)	241 (369)	636 (655)
4.	1.69 (1.95)	5.25 (6.86)	6.06 (7.76)	439 (1086)	965 (1054)
5.	0.65 (0.66)	4.55 (4.93)	5.29 (5.68)	182 (239)	686 (713)
6.	2.46 (2.92)	5.35 (6.69)	6.27 (7.69)	477 (1045)	475 (136)
7.	2.67 (3.23)	5.30 (6.74)	6.10 (7.75)	463 (1078)	476 (108)
8.	1.72 (2.10)	4.99 (6.78)	5.82 (7.72)	1010 (358)	784 (716)
9.	1.81 (2.24)	5.63 (6.74)	6.73 (7.68)	568 (1067)	795 (789)
10.	1.42 (1.76)	4.57 (5.59)	5.38 (6.45)	214 (449)	749 (942)
11.	2.28 (2.74)	5.27 (7.04)	6.13 (7.99)	450 (1241)	765 (757)
12.	2.56 (3.41)	5.17 (7.43)	6.03 (8.40)	420 (1488)	756 (892)
13.	1.46 (1.53)	4.48 (4.91)	5.30 (5.87)	1249 (340)	635 (656)
14.	2.86 (3.31)	5.13 (6.37)	6.04 (7.35)	414 (871)	487 (279)
15.	0.83 (0.99)	5.05 (6.24)	5.86 (7.08)	333 (694)	380 (76)
16.	0.76 (0.76)	5.32 (5.93)	6.11 (6.77)	393 (555)	448 (327)

System no.: as in Table 4.
Results in parentheses are according to EMTDD (chain).

observed to be conspicuously affected by certain types of additives. The works reported in this area are limited but they demonstrate the phenomenon well.

It has been demonstrated that butanol softens the interphase formed by the amphiphile + oil between water and oil [417], whereas cholesterol and its derivatives rigidify the interphase [454]. Toluene has been reported to block the passage of transfer of the charge carriers, thus to suppress the conductance enhancement [437]. The first detailed demonstration of the effects of additives on temperature percolation on water–AOT–decane microemulsion system has been due to Mukhopadhyay et al. [429]. Alkanols, cholesterol, esters of cholesterol, benzyl alcohol and a crown ether have been used as additives. Except benzyl alcohol and crown ether, the other additives have increased the percolation threshold (θ_t). The additives have also lowered the activation energy for percolation. The θ_t has been observed to increase with the chain length of the alkanol. The authors have supported the interdroplet exchange of charge carriers by 'transient fusion followed by fission' mechanism suggested by the TRFQ method discussed earlier. The rate constant for fruitful bimolecular collision in the absence of an additive has been shown to be 0.7×10^9 M^{-1} s^{-1} at 303 K; the result obtained by Jada et al. [355,356] has been $1–2 \times 10^9$ M^{-1} s^{-1}.

The combined effects of butanol and cholesterol on the percolation phenomenon of the water–AOT–xylene microemulsion system has also been reported [455]. Dutkiewicz et al. [437] have also reported the blocking effect of xylene, like toluene, for charge transport during conductance. In absence of butanol and cholesterol, the conductance increase is nominal; addition of cholesterol 14%

(w/w) suppresses the conductance. By increasing the proportion of butanol and decreasing the proportion of cholesterol, the conductance increases and the percolation tendency becomes prominent at 308 K. The conversion of non-percolating system to a percolating one by the presence of an alkanol (butanol) has been a unique demonstration of reduction of the self-blocking effect by the aromatic compound (xylene) like toluene.

In a subsequent study, Ray et al. [456] have investigated the effects of 29 additives (electrolytes, surfactants, and non-electrolytes) on the temperature as well as the volume percolation of conductance of the water–AOT–heptane microemulsion system in detail. The bile salts, sodium cholate (NaC) and sodium deoxycholate (NaDC) have evidenced diminution of both ϕ_t and θ_t values, whereas the other additives have shown no or mild enhancement of the threshold values. Eq. (4) has been tested and the exponent, μ has been evaluated. The θ_t values are all greater than 0.333 (required for Böttcher equation) and falling in the range of 0.357–0.477; the lower limit has been shown by bile salts NaC and NaDC. The values of the exponent (μ) have been observed to be $\simeq 1.0$, and less than the expected value of 1.9 [456]. The unique assisting effect of the bile salts has been explained on the basis of a special droplet fusion model by Ray et al. [447] and they have further extended the additive effects on the microemulsion system. In this study a demonstration of the unique effect of NaC to convert a non-percolating water–AOT–xylene system into a percolating one has been presented. The scaling laws of both volume and temperature percolation have been tested along with the activation energy for percolation (E_p). In Fig. 13, the effects of the bile salts NaC, NaDC and NaDHC (sodium dehydrocholate) and other additives on the temperature percolation have been presented for a ready understanding. The additive influenced parameters of the percolation process are presented in the Tables 6 and 7.

The sets of results presented above have again demonstrated that n- and μ values are rarely equal to the expected value of 1.9. In the presence of bile salts, μ values are on the lower side, i.e. < 1.9; it is equal to 1.9 only in the presence of TEAI (0.10 mol dm^{-3}), which is 1.8 without the additive, the rest are all above 1.9.

The proposed 'fusion–fission models' as influenced by the bile salts and aromatic compounds are presented in Fig. 14. Further works in this direction are required to establish the models on a firm basis.

The temperature induced conductance–percolation of H_2O–AOT–isooctane system has been studied by Eicke et al. [457] in the presence of triblock copolymer ABA (b-POE-b-PI-b-POE) as an additive. A thermodynamic model has been suggested to derive the variation of the percolation temperature as a function of the concentration ratio of copolymer and nanodroplets. The conductance–percolation study has been also presented by Meier [230] wherein the water–AOT–isooctane and water–pentaethylene glycol monododecyl ether–n-octane systems have been employed with polyoxyethylenes of varied molecular weights. Like Eicke et al. [457], Meier has also observed shift of the percolation threshold towards higher temperature with increasing polymer concentration. The influence of the polymer on the percolation phenomenon depends on polymer–surfactant interaction.

Table 6
Effect of additives on the temperature-induced percolation parameters for w/o microemulsion system[a]

Additive (mol dm^{-3})	ω	θ_t (°C)	ln P	n	E_p (kJ mol^{-1})
System: water–AOT–Hp					
0	33	35	2.00	1.80	1480
NaC(0.1)	33	9.0	1.70	2.50	1451
NaC(0.08) + 0.02 TEAI	33	14	0.43	3.01	882
TEAI (0.1)	33	43.0	2.10	1.90	379
NaC(0.08) + TEAI (0.02)	15	19.5	−2.31	2.78	295
TEAI (0.10)	15	35.5	−5.75	3.60	222
SDS (0.20)	33	33.5	−1.70	3.45	608
NaDHC (0.10)	33	34.0	1.20	2.57	1028
Xy 11% w/w in Hp	33	43.0	—	—	790
Xy 11% w/w in Hp + NaC (0.10)	33	17.5	—	—	867
Tl 11.23% w/w in Hp	33	46.5	—	—	532
Bz 11.37% w/w in Hp	33	46.5	—	—	532
Np 12.1% w/w in Hp	33	51.0	—	—	538
System: water–AOT–Xy					
NaC (0.50)	15	6.0	−3.53	2.56	147
NaC (0.50) + Ch (10% w/w) in Xy	15	20.0	−6.90	3.14	10.3
NaC (0.50) + Ch (14% w/w) in Xy	15	33.5	−4.70	3.01	119

[a] Taken from Ref. [447].
NaC, sodium cholate; Ch, cholesterol; NaDHC, sodium dehydrocholate; TEAI, tetraethylammonium iodide; Xy, xylene; SDS, sodium dodecyl sulfate; Tl, toluene; Bz, benzene; Np, napthalene.

Recently, Nazario et al. [458] have studied the temperature–percolation of the water–AOT–isooctane system in the presence of linear chained alkyl alcohols and poly(oxyethylene) alkyl ethers. In presence of alcohols, a shift in percolation to a higher temperature has been observed. The poly(oxyethylene) alkyl ethers have shown an opposite effect. The results have been interpreted in the light of a decrease in the fluidity of the interfacial layer.

Electrolytes, i.e. salts, HCl, NaOH, guanidinium chloride, etc have been found to

Table 7
Effects of bile salts on the volume percolation parameters of water–AOT–heptane microemulsion system at $\omega = 33$ and at 303 K

Additive (mol dm^{-3})	ln k	μ
NADC (0.18)	9.21	1.10
NADC (0.35)	12.47	1.96
NaC (0.10)	11.76	1.83
NaC (0.18)	10.86	1.76
NaC (0.20)	10.52	1.32
NaC (0.35)	9.79	1.22
NaC (0.70)	11.09	1.23

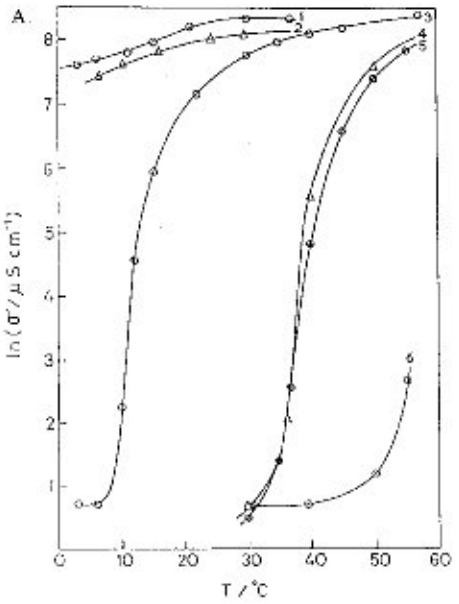

Fig. 13.

retard percolation of w/o microemulsion systems; they have been observed to decrease viscosity and capacity of water solubilization [459]. The additives like urea, thioureas, formamide and ethylene glycol have been observed to favor electrical percolation phenomenon even at low temperatures with a moderate concentration of additives. It has been suggested that the effect is related to the interfacial association of the additives with the AOT head groups. Binding of the additives at the interfacial layer has reduced the droplet surface curvature and helped in promoting attractive interdroplet attraction. Amaral et al. [215] have studied aqueous urea (3 and 5 M)–AOT–*n*-hexane microemulsion systems by LS and SAXS techniques to realize preservation of particle discreteness in the region of percolation. Preferential solubilization of urea at the interfacial region decreases its stiffness, consequently generating attractive interaction without formation of a bicontinuous phase. Conductance percolation thereby occurs by virtue of clustering of water microdroplets. Similar observations of preferential solvation of the surfactant head group in water–AOT–oil (hexane, isooctane, CCl_4) by urea inducing degree of dissociation of the head group leading to large conductance increment by way of droplet aggregation has been subsequently reported by Florenzano and Politi [460].

The solubilized macromolecules can even induce temperature percolation followed by a phase separation [214] favoring extraction of the products of reactions catalyzed by enzymes in w/o microemulsions, as has been reported by Papadimitriou et al. [294]. The enzymes chymotrypsin and trypsin have been used in

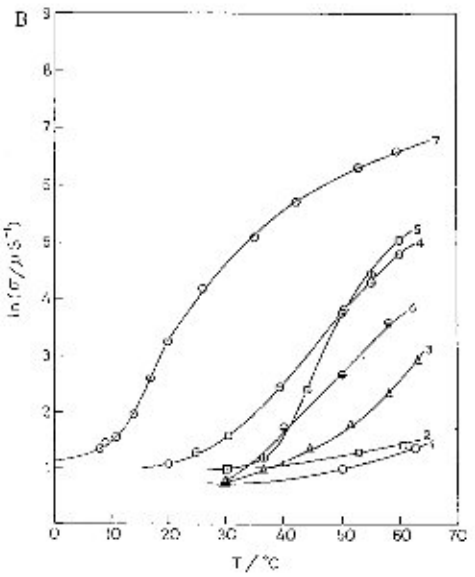

Fig. 13. (A) Effects of additives (NaC, NaDHC, SDS, and TMAI on the temperature induced percolation of H_2O–AOT–heptane microemulsion at $[H_2O]$:[AOT] = 33. Concentrations in mol dm^{-3} are given in parentheses: 1 — NaC (0.20); 2 — NaC(0.15); 3 — NaC (0.10); 4 — NaDHC (0.10); 5 — SDS (0.20); and 6 — TMAI (0.10) [447]. (B) Influence of NaC and cholesterol (Ch) on a non-percolative system H_2O–AOT–xylene at $[H_2O]$:[AOT] = 15. Concentrations in mol dm^{-3} are given in parentheses: 1 — without additive; 2 — NaCl (0.05); 3 — NaC (0.20); 4 — 10% w/w Ch. in Xy in the presence of NaC (0.50); 5 — 20% w/w Ch in Xy in the presence of NaC (0.50); and 6 — NaC (0.50) [447].

water–AOT–isooctane and water–CTAB–butanol–isooctane w/o microemulsions, and the percolation threshold has been observed to increase with increasing enzyme content. The electrical charge carriers are considered immobilized in the micro waterpool by the macromolecules to increase the threshold [461]. The bridging among the waterpools by the macromolecules can be another reasoning for the increased percolation threshold [462–465].

8.5.6. Pressure induced percolation of conductance

In volume percolation of conductance, at a constant amphiphile–oil level, the droplet size increases with addition of water which by the process of diffusion results in association and fusion, creating wider channels for efficient transfer of charges. An efficient percolating system then shows a rapid rise in conductance within a narrow width of ϕ. A similar explanation is also tenable for viscosity percolation. Effectively it is the association tendency of the droplets that initiates the percolation process causing changes in physical properties, i.e. conductance, viscosity and permittivity. At a constant composition (i.e. a fixed number of droplets) this dynamic percolation is augmented by the increased droplet motion leading to fusion if the droplet density is appropriate.

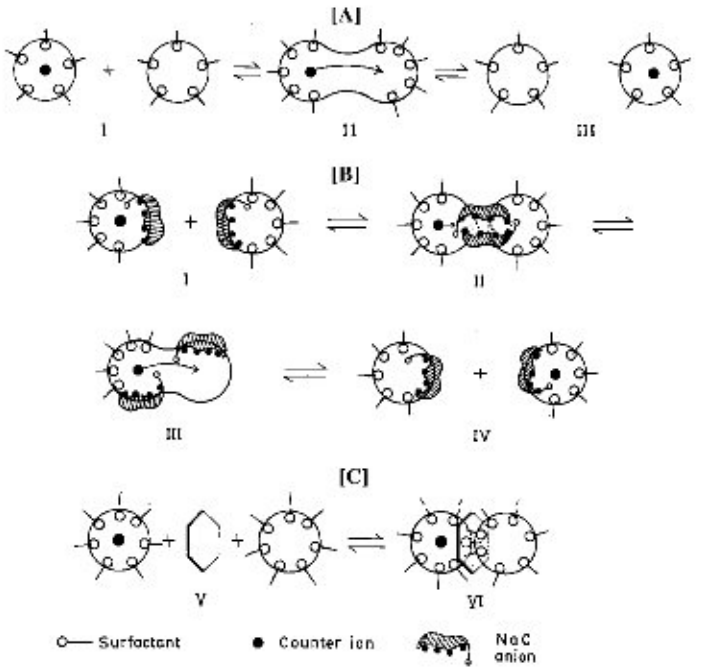

Fig. 14. Dynamics of events in percolation: fusion–fission process for mass transfer. (A) Without additive; (B) in the presence of bile salt (NaC), favored mass transfer or percolation; and (C) in the presence of an aromatic compound, etc., unfavored mass transfer or percolation [456].

At a constant composition, besides thermal energization at constant pressure, $P = 1$ bar that creates chances for droplet association, the process can also be initiated by changing pressure at a constant composition and at constant temperature. The droplet density required for pressure percolation can be different (normally lower) than that required for temperature percolation.

The effect of pressure on bicontinuous microemulsion formed with dodecyldimethyl ammonium bromide (DDAB)–water–super critical propane have shown conspicuous phase behavior due to pressure [466]. At pressures between 80–400 bar an 'antipercolation' behavior, i.e. decrease in conductance of three orders of magnitude has been observed; inter connecting channels in the bicontinuous microemulsion has been anticipated to breakdown into dispersed droplets. Comparable temperature and pressure effects on microemulsion has been witnessed; pairwise droplet attraction increases without affecting the droplet dimension [467]. The droplet size invariability has also been supported by other studies [468]. The SANS measurements of particle dimension as a function of pressure for the water–AOT–oil system have revealed strong interparticle interaction producing aggregates with almost unchanged particle size [469,470].

The work of Boned et al. [471] on the percolation of conductance and viscosity of water–AOT–undecane and glycerol–AOT–isooctane is of fundamental impor-

tance. They have varied pressure up to 1000 bar. The curves η vs. P and σ vs. P at constant ϕ and T, respectively, as well as η vs. ϕ and σ vs. ϕ at constant P and T, respectively, have been analyzed in the light of percolation theory. For the water–AOT–undecane system, the percolation threshold, ϕ_t has decreased with P which suggests increasing attractive interparticle interaction. For the glycerol–AOT–isooctane system, ϕ_t has varied insignificantly with P. The exponents of the scaling equations are 2 and −1.2 above and below ϕ_t irrespective of P. The forms of scaling equations considered are:

$$\left.\begin{aligned}\sigma &= C_1(P)\sigma_1(P)[K(P_t)(P_t - P)]^{\mu} \text{ for } P > P_t + \delta_P \\ \sigma &= C_2(P)\sigma_2(P)[K(P_t)(P - P_t)]^{-s} \text{ for } P < P_t - \delta'_P\end{aligned}\right\} \quad (18)$$

In Eq. (18), C_1 and C_2 are prefactors, σ_1 and σ_2 are conductances of the dispersed phase, P_t is the threshold pressure, K is the pressure derivative of ϕ_t and $(\delta P + \delta' P)$ is the 'cross-over regime' or the transitional interval which is of the order of $(\sigma_2/\sigma_1)^{1/(\mu+s)}$. The other terms have their usual significance. Similar forms of Eq. (18) are also obeyed by viscosity, η of microemulsion. It is a noteworthy point that the analysis of variations of σ as stated above is simple if K is independent of P_t and if σ_1, σ_2, C_1 and C_2 are also independent of P which is generally not so. If independent or the effects are negligible, then $\ln\sigma = f(\ln|P - P_t|)$.

The effect of pressure on the percolation phenomenon studied by Boned et al. [471] is not simple and further research is required. There has been limited study in this field and it obviously demands thorough and elaborate investigations for a number of systems of varied compositions and types.

To complete the discussion on the conductance of microemulsions, the behaviors of o/w systems need to be mentioned. This area has been little explored [472,473]. There is only one detailed study made by Bisal et al. [79] on 16 quaternary microemulsion systems using Tween 20 and TX100 as surfactants; butanol, hexanol and hexylamine as cosurfactants and hexane, heptane, decane, xylene and toluene as oils. The conductance behavior has been analyzed in the light of the EMT equations of Bruggeman [411], Böttcher [449] and Maxwell [474]. The Bruggeman equation provides the best fit. The hydration extent of the surfactant coated oil droplets has been estimated and found to depend on the types of surfactant and cosurfactant used. Since o/w microemulsion systems do not manifest percolation, it is beyond the scope of this review to make an elaborate presentation of their non-percolating conductance behaviors.

8.5.7. Thermodynamics of droplet clustering during percolation

It is considered that dispersed water droplets cluster during percolation by attractive interaction. In the clusters the droplets may even keep individual identities, in fact formation of bicontinuous structure may also result. The droplet clustering without coalescence has been established for AOT derived w/o microemulsions, and study of the energetics of the droplet clustering in them should

be worthwhile. Three important studies in this direction have recently appeared in literature [431,456,475]. Ray et al. [456] and Moulik et al. [475] have studied the water–AOT–heptane microemulsion system at different ω values for the temperature induced percolation process. They have considered the clustered state of droplets to be in a different phase (a pseudophase like surfactant micelles). The study of Gibbs free energy of cluster formation (ΔG_{cl}^0) has been obtained by the relation,

$$\Delta G_{cl}^0 = \mathrm{RT} \ln X_d, \tag{19}$$

where X_d is the mole fraction of the microdroplets corresponding to ϕ_t at constant ω. The enthalpy of clustering (ΔH_{cl}^0) has followed from the relation,

$$\frac{\mathrm{d}(\Delta G_{cl}^0)}{\mathrm{d}T} = \frac{-\Delta H_{cl}^0}{T^2}, \tag{20}$$

and the entropy of clustering has been obtained by the Gibbs formulation,

$$\Delta S_{cl}^0 = (\Delta H_{cl}^0 - \Delta G_{cl}^0)/T. \tag{21}$$

The thermodynamic parameters are in their standard states with ideal mixing of their components.

In the experimental design, dependence of the conductance of the microemulsion on ϕ (volume fraction of the dispersed phase) at a constant ω and temperature has been measured, and the experiment has been done at several temperatures. The estimation of ϕ_t has given $\Delta G_{cl}^0/T$, and the slope of the ΔG_{cl}^0 vs. T plot has produced ΔH_{cl}^0. The thermodynamic parameters for droplet clustering are presented in Table 8.

The results reveal that clustering is favored with increasing temperature; the process is also more spontaneous with increasing ω.

The ΔH_{cl}^0 values are all positive and also the ΔS_{cl}^0 values; both of them increase with increasing ω. The removal of the oil barrier surrounding the droplets and association of droplets are the two major processes in the percolation phenomenon of which the first is endothermic and contributes significantly compared with the second, making the overall process endothermic. The resultant, entropy is again positive owing to the major contribution of the former process associated with disorder. ΔH_{cl}^0 and ΔS_{cl}^0 compensate each other with a compensation temperature of 347 K vis a vis the experimental temperature of 303 K. ΔH_{cl}^0 obtained calorimetrically (the only report so far) are presented in parenthesis in column 4 of Table 8. They are comparable with those obtained by the application of Gibbs–Helmholtz equation at lower ω-values. The former ΔH_{cl}^0 (calorimetric) values are more accurate than the latter; the wide divergence at higher ω-values is noteworthy.

NaC and NaCl have made the clustering process (at $\omega = 40$) more spontaneous; enthalpy and entropy wise they are different without an additive (also at $\omega = 40$). Alexandridis et al. [431] have made a similar thermodynamic study in detail on

Table 8
ω-Dependent energetic parameters of clustering of water droplets in water–AOT–heptane microemulsion system at different temperatures[a]

ω	T (K)	$-\Delta G_{cl}^{0}$ (kJ mol^{-1})	ΔH_{cl}^{0} (kJ mol^{-1})	ΔS_{cl}^{0} (kJ mol^{-1})
10	303	13.6		
	308	14.0	16.3 (5.4)[b]	98
	313	14.6		
20	303	16.0		
	308	17.6	42.0 (47.0)[b]	191
	313	18.0		
30	303	17.8		
	308	19.6	77.9 (71.4)[b]	316
	313	21.0		
40	303	19.3		
	308	20.6	93.3 (117.4)[b]	391
	313	23.1		
40[c]	308	27.1	63.6 (123.3)[b]	294
	313	29.1		
40[d]	308	21.8	81.8 (155.2)[b]	336
	313	23.8		

[a] Results taken from Ref. [475].
[b] Values in parentheses are by calorimetric measurements.
[c] At 0.05 mol dm^{-3} NaC.
[d] At 0.01 mol dm^{-3} NACl.

water–AOT–alkane systems with respect to droplet size and concentration. ΔG_{cl}^{0}, ΔH_{cl}^{0} and ΔS_{cl}^{0} values obtained are of the same order and magnitude as obtained by Ray et al. [456] and Moulik and Ray [475]. The deformation of the surfactant monolayers upon droplet clustering, and the barrier of the activation energy for ion transport and/or water through the interface and the apolar continuum are considered reasons for the observed unfavorable clustering enthalpy. The free volume dissimilarity between the surfactant, tail or oil has been considered to manifest positive entropy. Similar to micellization, interdroplet interaction is considered to be entropic in origin. Endothermic and entropically driven clustering processes of the water–AOT–isooctane microemulsion system has been also reported by Nazario et al. [458].

Alexandridis et al. [431] have also comprehensively presented the other approaches in realizing the energy parameters for droplet clustering. Interfacial deformation, fusion and mass exchange models have been considered by different workers to rationalize the results. The concept of the activation barrier for the jump or exchange of charge carriers has been analyzed in the light of an Arrhenius type equation [430,454].

Activation energy has also been estimated by van Dijk et al. [476] from dielectric permittivity measurements. The clustering energetics have been again estimated

from viscosity and SAXS measurements [477–479]. All these results are of comparable order although based on specific but different assumptions.

The thermodynamics of clustering and the pseudophase existence of the aggregates envisioned by Ray et al. [456], Moulik and Ray [475] and Alexandridis et al. [430] is a more general framework to interpret the dynamic percolation phenomenon. By using the TRFQ method Johannson et al. [391] have estimated the activation energy for droplet fusion at different ω. Fletcher et al. [480] have derived the activation energy for droplet coalescence and solubilizate exchange by the stop-flow technique for a quaternary microemulsion system. The energy parameters have suggested the ternary AOT microemulsions to be more ordered. Further studies in this direction are needed for generalization of the thermodynamics of the percolation phenomenon.

8.6. Viscosity of microemulsions

In Section 3, viscosity derived structural information of microemulsions were briefly presented. An overall elaboration will be made in this section.

Among the fundamental physicochemical studies on colloidal dispersions, measurements of viscosity is of significant importance. It can provide first hand information on the internal consistency of the colloidal dispersions, as well as furnish knowledge on the overall geometry of the particles of the dispersed phase. The reported results from our laboratory and by others on the viscous behaviors of microemulsions have revealed variable features; both a rise and fall, as well as a viscosity maximum have been observed depending on the composition and environmental variations [26,27,29,33,481–488].

Since this transport property is a broad base, a comprehensive discussion in relation to other physical studies is presented.

8.6.1. Viscosity and microemulsion structure

Ekwall et al. [37] have made a fairly detailed investigation on binary (AOT–xylene) and ternary (water–AOT–xylene) systems adopting viscosity and other physical methods. The size and shape of micelles of reversed type have been found to depend on the amount of solubilized water, as evidenced from the measurements of intrinsic viscosity. The structure and properties of charged o/w microemulsions made up from a zwitterionic surfactant and hydrocarbon (which becomes charged upon the addition of either cationic or anionic surfactant) has been studied by Gradzielski and Hoffmann [85]. The systems have been characterized by means of light scattering, SANS, interfacial tension, conductivity and viscosity measurements. The light scattering results were corroborated by viscosity measurements as a function of concentration as opposed to the volume fraction of the 'dry' microemulsion aggregates. The microemulsions were shown to be composed of spherical aggregates consisting anisotropic particles and this observation was found to be in good agreement with the theoretical predictions for the viscosity of systems composed of spherical particles [489]. The difference in the values of relative viscosity, η_{rel} (between cationic and anionic systems) has been explained on

the basis of a higher effective volume fraction for an anionic system, i.e. a significantly larger effective hydration shell of the particles. As a result, the scattering properties of the anionic microemulsions were different from that of the cationic microemulsions. It has been found for the AOT–decane system that addition of NaCl decreases the relative viscosity of the solutions inducing a spherical geometrical form to the micelles [490]. The aggregation and shape of AOT micelles in *n*-hydrocarbons, benzene, toluene, carbon tetrachloride, dibromoethylene, *tert*-amyl alcohol and methanol were studied by ultracentrifugation, light scattering and viscometric techniques [491]. No micelle formation was obtained in methanol; the smallest micelle formation was observed in *tert*-amyl alcohol (micellar weight 2500). The AOT micelles essentially appeared to be monodisperse and slightly asymmetric in shape. The electrolytes, i.e. salts, HCl, NaOH, guanidium chloride, decreased both viscosity and water solubilization capacity of microemulsions. The cations associated at the water–oil interface, increased the natural negative curvature of the surfactant and hindered the exchange of materials between droplets by way of increasing the interfacial rigidity and decreasing mutual droplet interaction energy.

Rakshit et al. [402,403] studied the viscosity of the water–SDS–propanol–cyclohexane microemulsion system in the presence of NaCl along the single phase region at constant weight percent of the amphiphile. The rise in the viscosity with water addition has been ascribed to the increasing diameter of water filled conduits in the bicontinuous structure. The peak point in the viscosity–[water] profile denotes transition point of the w/o system to the o/w type. They have also reported that the viscosity of water–Brij 35–heptane or nonane microemulsion systems increases with the introduction of salinity. The heptane containing system has witnessed a larger increase as compared with the nonane system at all compositions, which means that the hydrophobicity of the system controls the functioning of NaCl. A similar effect has been observed in the cloud point studies; the same concentration of NaCl lowers the cloud point of a nonane derived microemulsion to a much lesser extent than a heptane system. The existence of the antagonistic effect of salinity and alkane chain length of the hydrocarbons has been envisaged. Similar conclusions were arrived at by Shah et al. [492]. Further reports on the viscosity of mixed alkane (heptane + nonane) microemulsions were due to Ajith et al. [189] indicating that the systems retain their bicontinuous structure as in pure alkane systems. Recently Joshi et al. [222] reported that the viscosity of the PEG 400 containing microemulsion system (water–CTAB–1-propanol–cyclohexane) is higher than those without PEG, and computed the activation enthalpy of the viscous flow using the Frenkel–Erying equation. The microemulsions exhibiting Newtonian viscosity behaviors and normal trends with component composition have also been reported from the laboratory of Rakshit [190,191]. According to Santhanalakshmi and Paramesari [158], a gradual increase of viscosity, conductivity and surface tension in the range of 0–20% (w/w) water content suggest that the dispersed phase, in all probability, is present in the form of droplets in water–TX100–*n*-alkanol–CCl_4 microemulsion systems. They have interpreted their results considering clustering of water droplets (with TX100 as the non-ionic

surfactant) by the formation of a mixed monomolecular layer of surfactant–cosurfactant couple.

The structure and properties of cationic surfactant derived microemulsions are little reported. Chen et al. [186] have reported partial phase diagram, conductivity and viscosity behaviors of cationic microemulsions formed from didodecyldimethyl ammonium bromide (DDAB) in different alkanes (i.e. C_6, C_8 C_{10}, C_{12} and C_{14}) with water. In the single phase region, the microemulsions were conducting at low water content and exhibited increased conductivity with increasing presence of water. A parallel viscosity behavior was also observed. At very high water content, the monophasic system becomes a rigid gel. A high and systematic degree of oil specificity was observed. The results were found to be consistent with simple pictures of microemulsion structure based on geometrical considerations. Langevin et al. [483] made a structural study of Winsor microemulsions formed with cationic surfactants (DDAB and CTAB) in comparison with earlier studies with anionic surfactants (SDS), and sodium hexedecyl benzene sulfonate (SHBS). They have explored the systems by way of composition analysis, structural analysis from viscosity measurements and quantitative structural characterization from SAXS experiments. It has been shown that the viscosity behaviors of the Winsor microemulsions can be correlated in terms of the Krieger formula [493], where a packing volume fraction has been taken into consideration. Inference on the bicontinuous microemulsion structure can be achieved by this approach. Bennett et al. [494] have observed two peaks in viscosity with increasing salinity, implying the existence of at least three microstructural regions: one before, one after and the other in between two peaks. According to them the maxima are indicative of the transition from a mono- to a bicontinuous structure. If the microstructure is observed as in liquid crystals, or is relatively difficult to break, as in gels, then the viscosity is expected to increase with increasing bicontinuity. The understanding of structural consistences in microemulsions has also been attempted from viscosity measurements by others [436,495,496]. The regular solution behavior has been observed for some systems, and some have shown specific behaviors.

The methods of steady state [252–255,497] and transient fluorescence depolarization [256,498] have been used to probe the microviscosity of reverse micelles, especially with AOT as the amphiphile. Very recently, Hasegawa et al. [259,260,499] have reported estimation of the microviscosity of the waterpool in the AOT reverse micelles as a function of $\omega(=[H_2O]/[AOT])$ by using a viscosity sensitive fluorescence probe (Auramino O, AuO). They have found that the waterpool is highly viscous in lower region of ω below 10, and then gradually decreases until the micellar solution becomes turbid above $\omega = 50$. But in the higher ω region, the microviscosity is considerably higher than the viscosity of ordinary (bulk) water. This has indicated that the solubilized water molecules are highly bound to the polar head groups of AOT. These results corroborate the results obtained with fluorescence depolarization studies with a cationic dye, rhodamine B. The fluorescence depolarization of xanthene dyes with different ionic characters demonstrates the heterogeneous nature of the waterpool. To obtain a more detailed picture of the static structure of AOT reverse micelles, the effects of temperature, am-

phiphile concentration, solvent and counterion on the micro-waterpool viscosity have been also examined. The dynamic fluctuation occuring near the vicinity of the phase separation in the cooling process of the microemulsion has been demonstrated by fluorescence depolarization measurements.

The surfactant sodium bis (2-ethylhexyl) phosphate (NaDHEP) in benzene and *n*-heptane can form crystallites, which with addition of water transform into reverse micelles [500]. This behavior has been corroborated by viscosity, DLS and other measurements. The crystallite formation takes place at $\omega < 3$. The study has shown that for this surfactant NaDHEP, a certain amount of water is required for reverse micelle formation otherwise crystalline rods are formed.

8.6.2. Non-Newtonian flow behaviors of microemulsions

Normally, the Winsor I and II microemulsion systems are low viscosity, Newtonian fluids. The Winsor III or the bicontinuous formulations may frequently exhibit non-Newtonian flow behavior and plasticity. Their flow under low and high shears may show distinct and specific features. Like all other fluids, rheology of non-Newtonian systems is complex and the microemulsions in this regard are no exceptions.

It has been reported that the problem of rheological behavior is a complex one and depending on the systems and experimental conditions, both Newtonian and non-Newtonian behaviors may arise. For example, Papaioannou et al. [501] observing variations of viscosity of quaternary systems as a function of their salt content, have reported a non-Newtonian behavior in favorable conditions. The same observation has been also made by Davis et al. [502] for microemulsions with equal water and oil contents. Recently, Hackett and Miller [503] have observed Newtonian behavior.

Chen and Warr [504] have investigated the flow of ternary microemulsions composed of water–DDAB–dodecane under shear in both cuvette and capillary viscometers, with an aim to study the relationship between structure and flow compositions and found it to be Newtonian up to very high shear rates ($\sim 3000\ s^{-1}$) although some indirect evidence for elasticity has been inferred from capillary viscometry. The densities and viscosities of AOT in heptane containing light and heavy water, as a function of the molar ratio ($\omega = [H_2O]/[AOT]$ or $[D_2O]/[AOT]$) have been measured at different temperatures (0, 5, 25 and 40°C) by D'Aprano et al. [505]. The difference in apparent molar volumes and viscosities have been explained in terms of the strength of the hydrogen bonding of H_2O and D_2O, and the intermicellar interactions mainly governed by the hydration of the head groups of AOT.

Recently, Berg et al. [506] have investigated the effects of droplet clustering on the shear viscosity by comparing the apparent viscosity of water–AOT–decane microemulsions flowing through thin membrane filters with well-defined pore sizes, with the viscosity measured in standard glass capillary viscometers. The apparent viscosity of microemulsions in pores differed from the viscosity measured in the capillary viscometer by less than 8–40% depending on the diameter of the pores. These differences are estimates of two effects: adsorption of droplets on the pore

wall and enhanced flow of suspensions near the wall. The absence of larger finite-size effects implies that clustering of droplets on the length scales of 0.1 μm or larger does not contribute substantially to the microemulsion viscosity.

Very recently, Mitra et al. [507] have observed that cinnamic alcohol can be a good cosurfactant and can itself behave like an oil, forming stable microemulsions with AOT. The vegetable oils, i.e. saffola, ricebran, sesame have been employed for the microemulsion preparation and their phase behaviors and flow properties have been studied. The shear viscosity method was used for overall understanding of the internal structure of microemulsions falling preferentially on the water side in the ternary phase diagrams. The viscosity has been observed to decrease with increasing shear rate (D) and levelled off at $D = 1620\ s^{-1}$ for sesame and saffola, whereas for ricebran oil, increases in viscosity with shear rate have been observed which also levelled off at $D = 1620\ s^{-1}$. The deformation of the dispersed entities under the shearing force has been envisaged. Later Ray and Moulik [508] have extended this study by using alkanols with carbon numbers 5–10 as oils and AOT as the amphiphile to generate microemulsions, and investigated their viscosity, conductance and thermodynamic behaviors. A fairly large region of the ternary phase diagrams, towards the higher amphiphile level, has been found to be quite viscous and obviously non-Newtonian in behavior. It has been reported that the viscosity increase with shear rate is more or less monotonic for w/o type (Winsor II), whereas it reaches a plateau for the bicontinuous type (Winsor III), as shown in Fig. 15.

The increase in viscosity with shear rate has supported the deformation of particle geometry and/or entanglement of the labile portions of the dispersed

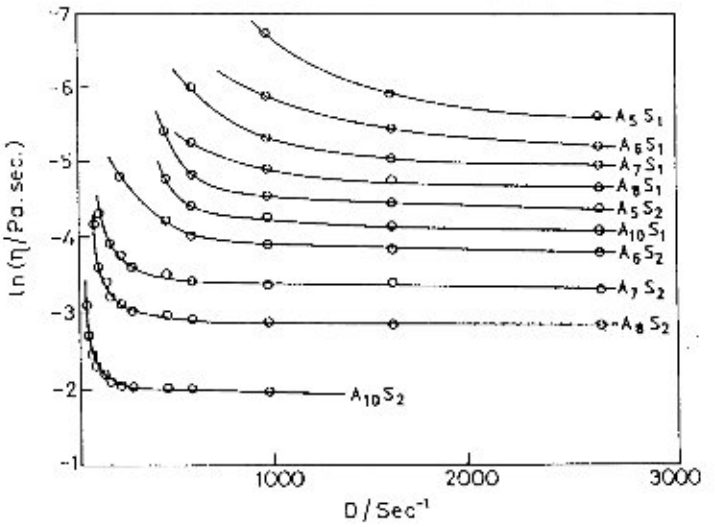

Fig. 15. Dependence of the viscosity of microemulsions with rate of shear at 303 K. Alkanol numbers are shown in tile curve. wt.% compositions of water–AOT–alkanol: S_1, 5:15:80; and S_2, 30:35:35 [508].

entities in the solution. The effect has intensified in the presence of a greater proportion of AOT in the preparation. The tails of AOT molecules present in the droplets of the reverse micelles have undergone mutual penetration forming linked microentities, and helped to maximize the viscosity making it independent of shear afterward. The element of particle deformation has operated in conjunction with the interparticle interaction effect. The samples studied have behaved like Bingham liquids, the property exhibited by many colloidal systems [509]. Those with a greater proportion of water have manifested less plasticity than the bicontinuous preparations. Kotlarchyk et al. [510] have investigated SAXS, dielectric relaxation, shear viscosity and DLS of dense water–AOT–decane microemulsions in order to substantiate the observed phase transitions, and further understanding of the structural and dynamic properties of an isotropic L_3-phase at a low temperature consisting of randomly connected lamellar sheets. They have witnessed the L_3-phase to exhibit Newtonian behavior up to a shear rate of 790 s^{-1} in contradiction to previous theoretical conclusions. The AOT–heptane–aqueous solution of polymers (i.e. polyethylene glycol, carboxymethyl cellulose, gelatin, starch, polyacrylamide) containing systems, studied by Kar and Moulik [30], have been found to be considerably viscous and non-Newtonian towards the higher amphiphile region. Application of shear has caused both thinning and thickening. In the viscous dispersion, the dispersed particles remain associated with the solvent, application of shear may desolvate them causing a thickening effect. Breakdown of chain type aggregates and orientation of stick like entities along the direction of shear may also cause a reduction in viscosity in pseudoplastic preparations. The systems studied by Kar and Moulik [30] were to some extent pseudoplastic. The increased viscosity with shear has suggested forced aggregation, deformation, as well as network formation in the system. John and Rakshit [192], from viscosity measurements of water–SDS–mixed alkanols (binary mixture), have highlighted the non-ideal behavior of mixing.

Sierra and Rodenas [199] have studied the rheology of the L-phase of the ternary system of water–SDS–poly(propylene glycol). At a shear stress > 20–60 s^{-1}, the samples have shown Newtonian behavior. Under this condition, the viscosity has increased with polymer concentration similar to the water–CTAB–PPG system [392]. The viscosity relative to the polymer solution at constant [SDS] has shown a decreasing trend with increasing polymer content which for the water–CTAB–PPG system has remained constant.

The first report on the rheological properties of inverse microlattices prepared by polymerization in non-ionic microemulsions was due to Candau et al. [511]. These microlattices consisted of sterically stabilized particles (diameter < 130 nm) of polyacrylamide and polymethylacrylate of trimethylaminoethyl chloride, swollen by high water contents ($\simeq 50\%$ water + 50% polymer) and dispersed in organic medium. The rheological behaviors of these materials followed quite closely that expected for hard-sphere suspensions. The data for the dependence of the high and low-shear limiting viscosities on volume fraction fitted the Krieger–Dougherty equation well [512]. But the dependence of the viscosity vs. the shear stress inferred that the microlattices are Newtonian in behavior extending up to a volume

fraction of approx. 50% in contrast to the limit of approx. 25% reported for conventional lattices. This difference has been accounted for by the partition of the disperse phase into polymer particles and small surfactant micelles.

8.6.3. Viscosity in relation to percolation of microemulsions

The phenomenon of percolation in microemulsion essentially involves droplet association (i.e. clustering) and fusion. It must, therefore, have a direct influence on the internal structure and hence viscosity.

A number of elaborate studies on the viscosity of both aqueous and non-aqueous (i.e. glycerol) microemulsions have been made in connection with the phenomenon of phase transition using AOT as the amphiphile, and isooctane, dodecane, undecane and cyclohexane as oils [220,436,495,496,513,514]. The influences of the volume fraction, ϕ, of the dispersed matter, the water (or glycerol)–amphiphile molar ratio, ω, temperature, salt content in the water and the nature of oil on the viscosity have been thoroughly examined. It has been concluded from the results that it is essential at first to identify the percolating and non-percolating nature of the studied systems. For a percolating system, the position of the maximum or the minimum (that may appear on the experimental curve) needs to be identified in relation to the 'percolation threshold'. If this has not been identified it is then essential to perform the measurements at a constant interaction level; otherwise false conclusions on the nature of structural changes will be drawn [513]. Eicke et al. [515] for the first time observed a pronounced similarity in the behavior of the self-diffusion coefficient, specific conductivity and viscosity of water–AOT–isooctane microemulsions. The results from dynamic and static experiments are consistent with a network structure model of microphases in the percolation range in which the droplets retain their discrete character. The temperature dependence of viscosity (increase of viscosity with temperature) is attributed to the increase in clustering of the droplets and subsequent network assembly supported by the electrooptic Kerr effect and DLS measurements [516]. They have further investigated [69] the structural inversion of the w/o microemulsion to the o/w type without any phase separation from the study of conductivity, viscosity and electrooptical Kerr effect, and confirmed the presence of two percolation processes for the water–AOT–decane system. The structural inversion takes place in two stages; with increasing oil content, the water-continuous microemulsion transforms into the bicontinuous form at roughly 20% (w/w) of oil (oil percolation threshold), and then at roughly 80% (w/w) of oil (water percolation threshold) the bicontinuous form transforms into the oil-continuous structure.

Like conductance, viscosity may also follow scaling type equations [513,514].

$$\eta = A(\phi - \phi_c)^{\mu'} \text{ if } \phi > \phi_c + \delta_1' \tag{22}$$

$$\eta = B(\phi_c - \phi)^{-s'} \text{ if } \phi < \phi_c + \delta_2' \tag{23}$$

where ϕ is the volume fraction of the dispersed matter (water and amphiphile), ϕ_c, is the percolation threshold, A and B are prefactors (cf. Eq. (18)), and μ' and s'

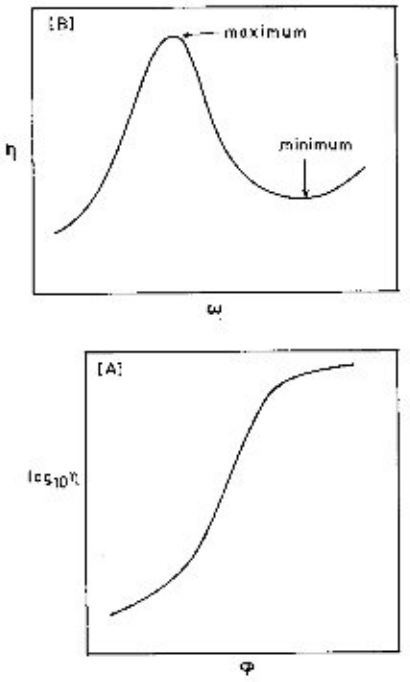

Fig. 16. (A) Variation of viscosity (η) with ϕ at constant ω and temperature of a percolating microemulsion system (arbitary scale); and (B) variation of viscosity (η) with ω at constant ϕ and at a constant temperature (arbitary scale).

are scaling exponents. By stepwise elimination of the experimental point closest to ϕ_c, until two straight lines are obtained in the two regimes ($\phi < \phi_c$ and $\phi > \phi_c$) for the $\log_{10}\ \eta = f(\log_{10}\ |\phi - \phi_c|)$ curve, the crossover regime δ_1' and δ_2' is obtained [514]. The width of crossover regime increases, when ω decreases. Variation of viscosity with volume fraction (ϕ) at constant ω, and with ω at constant ϕ at constant temperature for the percolating system are depicted in Fig. 16A,B.

The average values of μ' and s' are 2.0 and 1.20, respectively; these values are fairly near to the μ and s values 1.94 and 1.20, respectively [514], obtained for conductivity percolation. The s' value corresponds to the dynamic value of 0.7 obtained for static percolation. The scaling equations are much more favorable in waterless (i.e. with glycerol) microemulsions because $\eta_{oil} \ll \eta_{glycerol}$. For example with isooctane, $\eta_{isooctane}/\eta_{glycerol} = 5 \times 10^{-1}$ at 25°C and is even smaller at lower temperatures. The water–AOT–oil and glycerol–AOT–oil microemulsions behave in a broadly similar way provided that the conditions of application of dynamic percolation laws are satisfied. The percolation of conductivity is more clearly observed for the conductivity of water $\gg$ the conductivity of oil, but as η_{water} is not sufficiently different from η_{oil}, parallel manifestation of percolation of viscosity like conductance does not occur. Microemulsions produced by the dispersion of

polar and viscous non-aqueous solvents like glycerol and the low molecular weight polyethylene glycols, have the ability to show percolation of viscosity.

According to Chen and Huang [517], droplets of AOT dispersions exhibit an isothermal liquid glass transition at volume fraction, $\phi_g = 0.65$; the droplets are thus a randomly packed but close hard-sphere system [518]. The viscosity of such dispersions (for example D_2O–AOT–decane) can be fitted to a scaling type equation,

$$\eta = \eta_s(1 - \phi/\phi_g)^{-\alpha}, \tag{24}$$

where η_s is the viscosity of the continuous medium (i.e. oil) and α is a constant $\simeq 2$. This is in accordance with the mode–mode coupling theory of density fluctuations [519].

The increase in microemulsion viscosity with temperature, essentially for AOT derived systems, has been attributed to the phenomenon of percolation [495], but this needs further justification although droplet aggregation (clustering in random as well as a regular manner) may significantly add to the increase in viscosity of microemulsions.

Very recently, D'Aprano et al. [520] have compared the viscosity and the electrical conductance as a function of ϕ and have indicated that the process of momentum and charge transfer (even if related to the droplet cluster formation) are different. They have given evidence in favor of a viscoelastic phenomenon [521].

The dependence of the viscosities of waterless microemulsions (i.e. formamide–AOT–isooctane, ethylene glycol–AOT–isooctane and dimethyl formamide AOT–isooctane) on ω, ratio of [AOT] and [water] in the percolation range of conductance is presented in Fig. 17 [522].

The results suggest that clustering induced viscosity increase occurs for the systems (as mentioned earlier) at low ω. In terms of conductance, the phenomenon occurs at higher threshold volume fraction (ϕ_d^1); this cannot be induced by temperature. Although the low ϕ_d^1 in the viscosity profile and high ϕ_d^1 in the conductance profile are non-corroborative, the results have suggested the possibility of structure formation in a waterless microemulsion.

Mukhopadhyay et al. [484] have studied the viscosity of w/o microemulsion (water–AOT–decane) as a function of temperature in the percolation range in the presence of a good number of additives. A maximum in viscosity at a temperature of 40°C was observed in absence of the additives, which shifted towards a higher temperature in the presence of additives. A similar viscosity phenomenon was also reported by Borkovec et al. [69]. They suggested the rise in viscosity in the first step was as a result of percolation; but the decrease in viscosity in the second stage occurred as a result of the change in the overall droplet shape. The non-linear course of log η vs. T^{-1} plot has suggested progressive change in the activation energy for the viscous flow. The cluster formation and the change of its shape with temperature have contributed to the viscosity changes of the system.

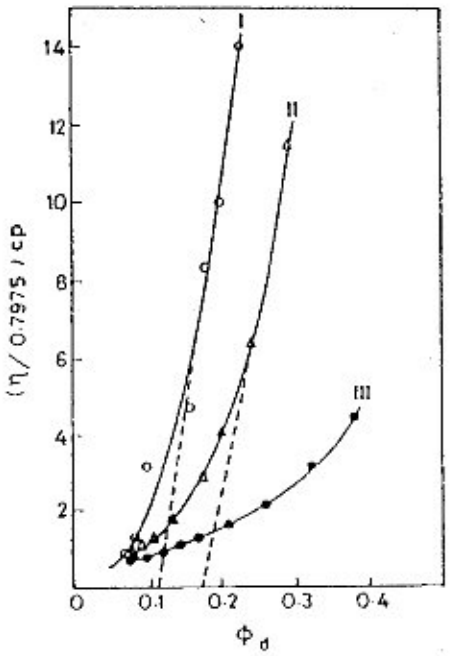

Fig. 17. The viscosity coefficient (η) vs. ϕ profiles for three microemulsion forming systems at 303 K: (1) FA–AOT–*i*-Oc at $\omega = 1.44$; (2) EG–AOT–*i*-Oc at $\omega = 1.85$; and (3) DMF–AOT–*i*-Oc at $\omega = 2.03$ [522].

8.6.4. Viscosity–conductance interdependence

In terms of normal understanding, the conductance of a well defined and less complex system shows inverse dependence on viscosity. For electrolyte solutions in media of variable viscosity this has been found to be so, and the rule of Walden (Walden product, i.e. $\lambda\eta$ = constant, where λ is the equivalent conductance of the electrolyte solution) has been observed to be more or less valid.

In a microemulsion medium this rule has been found to be very often violated, especially at the stage of percolation. Although conductance of microemulsion systems increases slowly or very rapidly either by increasing the volume fraction of the polar dispersed solvent (essentially water) at a constant temperature or the temperature at a constant composition, the corresponding viscosity may increase or decrease and it can pass through both maximum and minimum [26,27,29, 33,69,186,484]. It has also been reported that the maximum in viscosity, with respect to the volume fraction of the dispersed phase, may be independent of the type of alkanes used as oil, and it can depend on the temperature at the time of measurement [220]. The mean radius of the dispersed droplets may have a reasonable infuence in this regard, but it is difficult to explain the appearance of a sharp peak in the viscosity–volume fraction curve.

The formation of aggregates or infinite clusters of dispersed droplets providing

channels for enhanced ion conductance by either 'hopping' or a 'transient fusion and mass exchange' mechanism manifesting percolation, should result in increased viscosity (i.e. viscosity percolation). Paul and Moulik [33] have elaborately studied viscosity and conductance of biological microemulsions consisting of water–AOT–hexylene–saffola and have shown serious invalidity of the Walden product, $\lambda\eta$ = constant as mentioned earlier. This observation advocates complexity in the internal structural state of the studied w/o microemulsions. At a constant composition, increased temperature results in increased collision among the droplets providing greater scope for mass exchange i.e. temperature percolation of conductance; the process may not produce an onward increase in viscosity of the system (in fact increased temperature normally has a declining effect on solution viscosity). This finding may suggest weak dependence of membrane conductance on membrane viscosity; it is the channels that carry charges (ions) across it which are important. A porous dispersed body can favorably allow transport of ions (matter) through its water-filled pores. The increased viscosity imparted in the solution by the presence of the porous body may thus have an insignificant influence on the ion conductance in the solution. A word of caution is relevant at this point regarding the thermodynamic validity of the Walden product. According to the Curie–Pregogine principle of irreversible thermodynamics [523], forces and fluxes of different elements of symmetry should not couple. This seriously restricts coupling of λ with η, the product is thus essentially extrathermodynamic.

8.6.5. Testing viscosity equations

A good number of attempts to rationalize viscosity–concentration dependence of solutions in terms of empirical and semiempirical equations exist; for dilute non-interacting dispersions exact equations exist. Microemulsions are complex in nature, processing of viscosity data in the light of an unique approach is not expected. The reports in this direction are scanty. A brief discussion on the usefulness of viscosity relations for dilute and concentrated dispersions is, therefore, worthwhile. Since the rheological problems of microemulsions are by no means simple, attempts have been made to treat the experimental results using different fitting procedures with the help of adjustable interaction parameters. Baker et al. [524] and Tadros [525] have used the Mooney equation on the microemulsion system of water–NaDBS–hexanol–xylene,

$$\eta_r = \exp \frac{a\phi}{1 - k\phi}, \tag{25}$$

where η_r is the relative viscosity, ϕ is the volume fraction of water, and a and k are constants (a, is related to intrinsic viscosity of the dispersion and k is the so-called 'crowding factor' which takes into account interparticle interactions recommended for colloidal dispersions).

The measured viscosity results have shown the behavior normally encountered with concentrated dispersions, η_r increasing exponentially with ϕ_{H_2O} and [NaDBS];

the hydrodynamic volume of the dispersed droplets has thus continuously increased. This has been attributed to the increase in the ratio of the surfactant layer thickness to the droplet core radius with increased [NaDBS] in the system suggesting increased solvation of the microemulsion droplets.

The Mooney equation is of the same form as the equation of Vand [526],

$$\ln \eta_r = \frac{\nu\phi}{1 - Q\phi}, \tag{26}$$

where ν is the particle shape factor and Q is the interparticle interaction parameter. An equation of the same form differing only so far as in setting the interaction parameter Q in terms of two adjustable constants S and K' ($Q = SK'$) has been used by Robinson [527] for colloidal dispersions.

The viscosity of Winsor microemulsions prepared with cationic surfactants (CTAB and DTAB) and anionic surfactant (SDS), cosurfactant (butanol) and dodecane as the oil when tested as a function of salinity has been observed to pass through a broad maximum [483]. The viscosity can be related to their structural evolution by the Krieger formula [493,512]

$$\eta_r = \left(1 - \frac{\phi}{\phi_p}\right)^{-1/2}, \tag{27}$$

where ϕ_p is the packing volume fraction and other terms have their usual significance. The value of $\phi_p \simeq 0.75$ for compact cubic arrangements of spheres and $\simeq 0.65$ for a random arrangement of spheres. For the bicontinuous structure the following relation has been used.

$$\eta_0 = \eta_{aq}\phi_{aq} + \eta_{org}\phi_{org}, \tag{28}$$

where η_{aq} and η_{org} are the viscosities of the excess phases.

The packing fraction ϕ_p has been revealed from viscosity measurements to pass trough a maximum with wt.% of NaCl (or salinity) [483], the onset of droplet coalescence ($\phi_p = 1$) has been observed. For Winsor I and II, peaks in viscosity are not observed due to non-aggregation of the droplets by poor attractive interaction among the droplets. A good reason for coalescence, i.e. attractive interaction (the van der Waals force) increases with droplet sizes [528,529] in the Winsor III region.

Recently, Ajith et al. [191] have reported the use of Frenkel–Erying viscosity equation to calculate activation enthalpy of viscous flow for mixed surfactant microemulsion systems (Brij 35 + SDS)–1-propanol–heptane–water and (Brij 35 + Tween 20)–1-propanol–heptanol–water and the values are higher for the more viscous o/w systems. The free energy of solubilization of oil in water has been found to be a function of surfactant composition and the enthalpy is more or less independent of composition.

Detailed viscometric investigations on aqueous and waterless microemulsions using hexane, heptane, octane, isooctane, decane, cyclohexane, xylene and toluene

as oils and AOT as an amphiphile have been made by Ray and Moulik [522] and Ray et al. [530]. For the preparation of waterless microemulsions the polar solvents, i.e. formamide (FA), ethylene glycol (EG), propylene glycol (PG), dimethyl formamide (DAIF) and dimethyl acetamide (DMA) were used. The overall geometry and solvation of the droplets have been assessed; the dispersed water droplets have been observed to be close to spheres and their solvation by the oil is insignificant. In this evaluation Eiler's [531] semiempirical voluminosity equation has been considered,

$$\eta_r = \left(\frac{1 - 0.1\, V\phi_d}{1 - 1.35\, V\phi_d} \right)^2, \tag{29}$$

where V is the voluminosity defined as the ratio of the hydrated to anhydrous volumes of the droplets, and ϕ_d is the volume fraction of the anhydrous droplets. Ekwall et al. [37] have used this equation for AOT–xylene reverse micellar systems.

The viscosity of microemulsion systems referred to above and investigated by Ray and Moulik [522] and Ray et al. [530] have been examined in the light of the equations of Vand (Eq. (26)) [526], Thomas (Eq. (30)) [532] and Moulik (Eq. (32)) [533].

Thomas equation:

$$\eta_r = 1 + 2.5\phi + A\phi^2, \tag{30}$$

where A is the third virial coefficient.

A virial equation of the form,

$$\eta_r = 1 + 2.5\phi + 10.05\phi^2 + A' \exp(B\phi), \tag{31}$$

where A' and B are constants, has been also used by Thomas [532,534] for concentrated dispersions.

Moulik equation:

$$\eta_r^2 = I + M\phi^2, \tag{32}$$

where I and M are empirical constants ($1.5 < I > 1.0$ and M is large).

A striking validity of all three equations has been observed for the studied system at constant ω. A combined unified viscosity equation of the form [533],

$$(\eta_r/\phi)(1 - \eta_r/r\phi)^{1/2} = (12.5 - m/\nu)^{1/2} - (12.5m/\nu)^{1/2} Q\phi, \tag{33}$$

where the new terms $r = M/2.5$ and $m = A/(2.5)^2$, have fairly correlated the viscosity results. A representation of the validity of Eq. (33) is shown in Fig. 18.

The relation has been observed to be valid for $\phi > 0.05$. Except for octane and decane at $\omega = 7$, the slopes at lower ϕ are positive which have been also realized for electrolytes and carbohydrates [535].

Eqs. (29)–(33) have shown good validity at constant ω, but have failed to

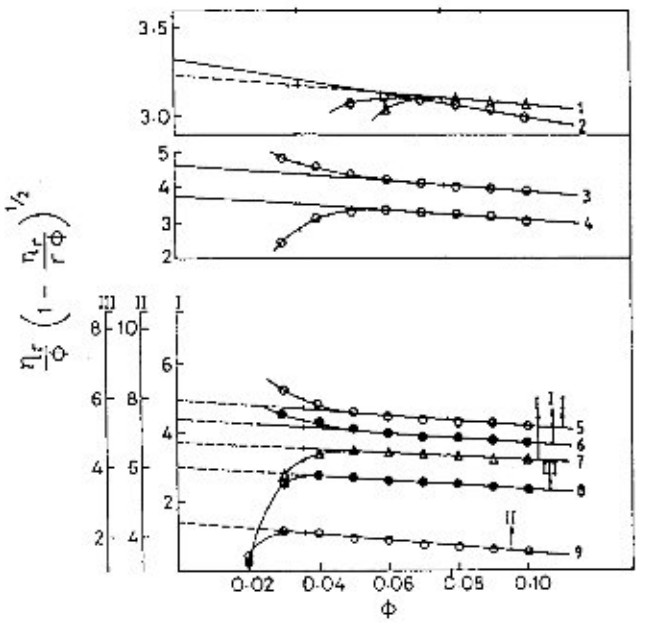

Fig. 18. $\eta_r/(1-\eta_r/r\phi)^{1/2}$ vs. ϕ profiles for w/o microemulsions at a constant ω at 303 K. Curves 1–9, Hp ($\omega = 15$); Hx ($\omega = 15$); Dc ($\omega = 15$); *i*-Oc ($\omega = 15$); Dc ($\omega = 7$); Oc ($\omega = 7$); Hx ($\omega = 7$); Hp ($\omega = 7$); and *i*-Oc ($\omega = 7$) [530].

corroborate results at variable ω. The correlation of the parameters (Q, M and A) of different equations with both the carbon number and the molar masses of the open chain hydrocarbon oils has been attempted. The results are exemplified in Fig. 19.

The effects of added salt (sodium cholate, NaC and NaCl) on the viscosity behavior of isooctane based microemulsions have also been reported; a distinct difference between the behaviors of microdispersions in open chain and cyclic hydrocarbon continuum has been observed.

The droplet geometry and solvation of w/o microemulsions has been understood with the help of the following equation [79,536]

$$[\eta] = \nu(\bar{v}_d + \delta\bar{v}_o), \tag{34}$$

where $[\eta]$ is the intrinsic viscosity of the microemulsion, and $\bar{v}_d$ and $\bar{v}_o$ are the partial specific volumes of the dispersed phase and dispersion medium (here oil), respectively, and δ is the gm/gm oil bound to the dispersed phase. The shape factor is $\nu = 2.5$ for spheres and is greater than 2.5 for spheroids.

Ray et al. [530] have observed negligible solvation of the water droplets by oil (viscosity is a dynamic way of probing, there may be solvation under static conditions). On the basis of $\delta = 0$, the calculated shape factor (δ) and axial ratio for spheroids (a/b, ratio of the major to the minor axis) are presented at different ω at a temperature of 303 K in Table 9.

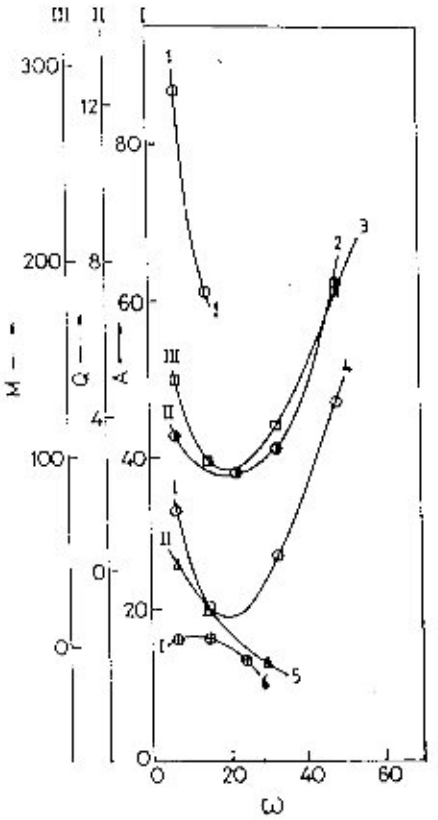

Fig. 19. M, Q and A vs. ω plots for w/o microemulsions at 303 K. Curves, 1, 2–4, 5, 6 are Dc, Hp, Hx and Cy, respectively [530].

The ν-values are only moderately higher than 2.5 (this is the maximum possible value for sphere) which suggests the droplet geometry to be minorily spheroidal.

Table 9
The shape factor (ν) and the axial ratio (a/b) of different AOT derived w/o microemulsions in different oils at four different ω values at 303 K

ω	ν, a/b					
	Hx	Hp[a]	*i*-Oc	Dc	Cy	Xy
7	2.71, 1.37	2.75, 1.43	2.63, 1.20	—	2.79, 1.47	2.66, 1.22
15	2.58, 1.12	2.63, 1.21	2.96, 1.78	2.32, —	2.86, 1.58	—
25	—	2.81, 1.47	—	—	2.79, 1.47	—
30	2.95, 1.67	—	3.11, 1.91	—	—	—

For Hp at $\omega = 15$, in 0.05 mol dm^{-3} NaC, $\nu = 2.78$ and $a/b = 1.47$, and in 0.05 mol dm^{-3} NACl, $\nu = 2.88$ and 1.58. For Hp at $\omega = 33$, $\nu = 2.90$ and $a/b = 1.66$

The dispersed droplets of FA, EG and DMF in waterless microemulsions (FA–AOT–*i*-Oc, EG–AOT–*i*-Oc and DMF–AOT–*i*-Oc) studied by Ray and Moulik [522] are also spheroidal in shape with low intrinsic viscosity and negligible solvation. The ν-values fall in the range of 2.8–4.9 (the values are comparatively higher than the tabulated values). The waterless microemulsions of the above type have also obeyed the viscosity equations of Eiler, Vand, Thomas and Moulik. Similar detailed report on viscosity of waterless microemulsions are rare in literature.

9. Interfacial transport in microemulsions

In recent years, increasing attention has been given to the development of novel surfactant mediated separation processes [537,538]. Among the various new methods, the application of microemulsions for the separation, concentration and purification of proteins, for the extraction of metals, as drug-delivery systems, etc. seems to be one of the most exciting and promising techniques [538,539]. The fundamental basis of extraction and separation with the help of microemulsion is interfacial solubilization and mass transfer. The processes are dynamic in nature across the oil–water interface. The trends of work in literature in the area can be broadly divided into two categories: (1) mass transport in relation to extraction by solubilization; and (2) mass transport with reference to a microemulsion acting as a liquid membrane.

9.1. Mass transport in relation to extraction by solubilization

In spite of a good number of publications about the extractional equilibria and the separation possibilities, the detailed mechanisms of the interfacial solubilization in the liquid–liquid system is not clear to date [538,539]. However, the basic principle of the equilibrium behavior of microemulsion as an extractant has been worked out. The interactions between enzymes and emulsion components are indeed complex and the reported results in this direction are not unambiguous. From this point of view, the amino acids, with their much simpler structure and properties, are promising solubilizates to investigate the partitioning of different substrates in the Winsor II system. The advantages of using amino acids as model compounds to investigate the mechanism of solubilization in w/o microemulsion systems have been comprehensively presented by Leodidis and Hatton [540]. Several authors, for example, Lifisi and coworkers [541], Furusaki et al. [542], Adachi et al. [543], Leodidis et al. [544], Fendler et al. [545], Dossena et al. [546] have investigated the solubilization of amino acids in the liquid–liquid system [541–544], as well as in the organic phase [545,546] and have stated that the electrostatic interaction is the main driving force for the solubilization and extraction of amino acids. The hydrophobic interaction has been considered as the other important factor by Leodidis and Hatton [540], Luisi et al. [541] and Adachi et al. [543]. They have also proposed the free energy of transfer (between water and

surfactant shell) of different amino acids as a new hydrophobicity scale similar to the Hansch parameter [547], or the Nozaki–Tanford [548] and Bull–Breese [549] scale. Generally, the hydrophilic amino acids are solubilized in the core of the water droplet while the hydrophobic representatives shelter mostly in the surfactant shell [540,543,544]. According to Fletcher et al. [550] as well as Leodidis and Hatton [551], the droplet curvature or size plays an important role in the partitioning of the solubilizate in the surfactant shell. The amino acids that preferentially solubilize in the shell of the reverse micelles are expelled from the interface with increasing curvature i.e. with decreasing droplet size. The process can de done by changing ionic strength, solvent type, etc.

Dynamics of transfer of amino acid (phenylalanine), metal ions, as well as enzymes from an aqueous phase towards the reverse micellar one in a stirred cell, have been reported by Nitsch and Plucinski [552–556] to understand that the solubilization of different species is an interfacial process, and the experimental results are explained on the basis of the three-step 'bud' mechanism [555]. In the first step, a w/o microemulsion drop from the bulk of the organic solution attaches itself to the macroscopic liquid–liquid interface and a so-called sticky collision [355] occurs. During the residence time of the micelle (bud) at the interface, in the second step, mass transfer (i.e. the incorporation of phenylalanine molecules into the AOT shell layer) occurs, and after a successful fusion of the surfactant monolayers in the neck of the bud. In the third step, the reverse micelles with the solubilizate diffuse towards the bulk of the organic phase [555]. The kinetics results also demonstrated the important role of the possible reorganization of the AOT molecules at the liquid–liquid micellar interface during the incorporation of phenylalanine molecules into the bud [555]. A general influence of the interfacial tension on the solubilization rate was found, i.e. a lower interfacial tension promoted the solubilization rate [555], possibly via increased thermal fluctuations of the bud.

All these works concerning amino acid solubilization have been performed with a pure water–AOT–oil system without cosurfactants. It is known that the addition of alcohols has strong influence on the elasticity and spontaneous curvature of the surfactant shell [334,557], which is also very important in the solubilization of amino acids [551]. In addition, the presence of alcohols decreases the aggregation number of the surfactant molecules and the diameter of the reverse micelles [558,559]; the changes depend on the alcohol hydrophobicity [558–560]. The literature regarding the influence of cosurfactants on the mass transfer between the aqueous and reverse micellar phases (i.e. in the Winsor II system) is, however, limited.

Recently Plucinski et al. [561] have reported that the addition of alcohols (C_nOH, where $n = 5–12$) to the micellar phase has no influence on phenylalanine partitioning between the micellar and aqueous phases in the water–AOT–isooctane system. The distribution coefficient of phenylalanine is independent of the alcohol type and concentration, and dependent on pH, showing the importance of electrostatic interactions in phenylalanine solubilization. Unlike the results of Leodidis et al. [551] and Fletcher [550], the change in the micellar droplet

curvature (i.e. the change of size) caused by the addition of alcohols or the change in the solvent type has no influence on the phenylalanine partitioning. It is concluded that the added alkanol molecules do strongly influence the hydrophobic lateral interaction during the solubilization of phenylalanine.

The kinetics results of phenylalanine solubilization have shown the importance of the structure of the interfacial surfactant layer on the dynamics of interfacial solubilization and has been discussed in the light of the three-step bud mechanism presented above [550]. The incorporation of the alcohols (cosurfactants) into the palisade AOT layer has a catalytic effect, i.e. it changes the dynamics of the solubilization without changing the equilibrium state. The short chain alkanols (pentanol, hexanol) accelerate the mass transfer and easy reorganization of AOT molecules during the phenylalanine incorporation, while the long chain alkanols ($n \geq 9$) retard the mass transfer from the aqueous to the micellar phase. These effects seem to be connected with the mechanical state i.e. fluidity of the surfactant–cosurfactant interfacial layer.

9.2. Dynamics of protein extraction

In biotechnology (genetic engineering for example) large-scale production of proteins adopting new techniques is much wanted. Selective protein extraction from fermenter liquids by reverse micelles (w/o microemulsions) is a new prospective recovery technique. The biopolymers (proteins and enzymes) have been shown to maintain their normal activities extracted by the liquid–liquid mass-transfer process. The literature on this topic is rapidly growing [562–601].

Salient important transfer phenomenon of typical biopolymer-extraction works are presented herein. Recently Dekker et al. [570] investigated the rate of mass transfer in the extraction of the enzyme, α-amylase between an aqueous phase and a reverse micellar (w/o microemulsion) phase in trioctyl methyl ammonium chloride (TOMAC)–isooctane, and have measured the mass transfer rate constants. The forward transfer (aqueous → non-aqueous for solubilization in the reverse micelles) has been found to be controlled by the diffusion of the enzyme in the aqueous phase boundary. The back (reverse) transfer (non-aqueous → aqueous for recovery after extraction) is the release of the enzyme from the micelles instead of boundary layer diffusion. The same mechanism is operative for the extraction and release of the enzyme ribonuclease with the anionic surfactant AOT. A detailed study of the extraction dynamics with a number of proteins, surfactants (TOMAC and Revopal H5), cosurfactant (octanol) and oil (isooctane) in relation to size, isoelectric condition and pH has been made by Wolbert et al. [571]. The maximal extraction has been mathematically correlated with the isoelectric point. Luisi and coworkers [563,581,582] have demonstrated that salt and buffer types are determinant factors in controlling the transfer across the organic phase; different salts impart different transfer efficiency. The said transfer process has been tested under varied environmental conditions using a great number of surfactants for the extraction of α-amylase [572]; only didodecyldimethyl, ammonium chloride and TOMAC are found to be effective. The extraction of the proteins, RNAase A and

also proposed [615–619]. The dependence of water uptake on electrolyte concentration in the external aqueous phase in Winsor II reverse micellar condition is now considered to be due to the changes in the electrostatic free energy of the double layer inside the waterpool of the reverse micelles.

9.4. Transport across a microemulsion functioning as a liquid membrane

Two immiscible liquid phases, one placed on both sides of another (taken in the middle) can form a liquid membrane system. Such a liquid membrane (middle phase) can act alone or with a porous support (supported liquid membrane) [620–622]. Transport is effected by way of either complexation or entrapment with suitable agents, thus the solute is transferred from one side called the 'source phase' (S) to the other called the 'receiving phase' (R). Microemulsions of Winsor I (o/w) and Winsor II (w/o) types can be considered as dispersed liquid membranes that can facilitate transfer of solutes (oil soluble compounds by Winsor I and water soluble compounds by Winsor II) across it by trapping them in the microdroplets for convenient uptake and subsequent release. Winsor I and II microemulsions are called 'bulk liquid membranes'.

The use of liquid membrane for separation is an established field and have importance in biology [623–631] as well as for developing practical separation processes [632–634].

The microemulsion or 'bulk liquid membrane' is a recent addition in the field of separation science and technology, and the bulk works for its introduction and prospect in the practical field have been advanced by Tondre and co-workers [635–646]. The fundamentals of the process have been worked out based on the transport studies of alkali metal picrates across w/o microemulsions [637–640]. It has been then extended towards the separation of metal ions, i.e. Ni^{2+}, Co^{2+} and Cu^{2+} [642–647]. A recent work demonstrates the separation of acetic acid from water by w/o microemulsion liquid membrane using non-ionic surfactant [648].

The investigations from the laboratory of Tondre have been elaborate and extensive in respect of cell design, solute choice, amphiphile (surfactant or surfactant + cosurfactant) selection, additive effects and data analysis with a pragmatic transport mechanism. They are also pioneers in the use of o/w microemulsions as a liquid membrane; the transport of lipophilic compounds, i.e. pyrene, perylene and anthracene across o/w liquid membrane, has been studied [637,638].

9.4.1. Experimental set-up and mechanism of transport

The experimental set-up to study separation by microemulsion as a liquid membrane can attain sophistication [646]. The basic design is described in the work of Derouiche and Tondre [642]. A schematic representative diagram is presented in Fig. 20A below.

The results of the transport of picrate ions using a Winsor II water–AOT–decane microemulsion by Derouiche and Tondre [642] are presented in arbitrary scale in Fig. 20B.

The formation of cluster, viscosity change, ion-concentration, etc. essentially

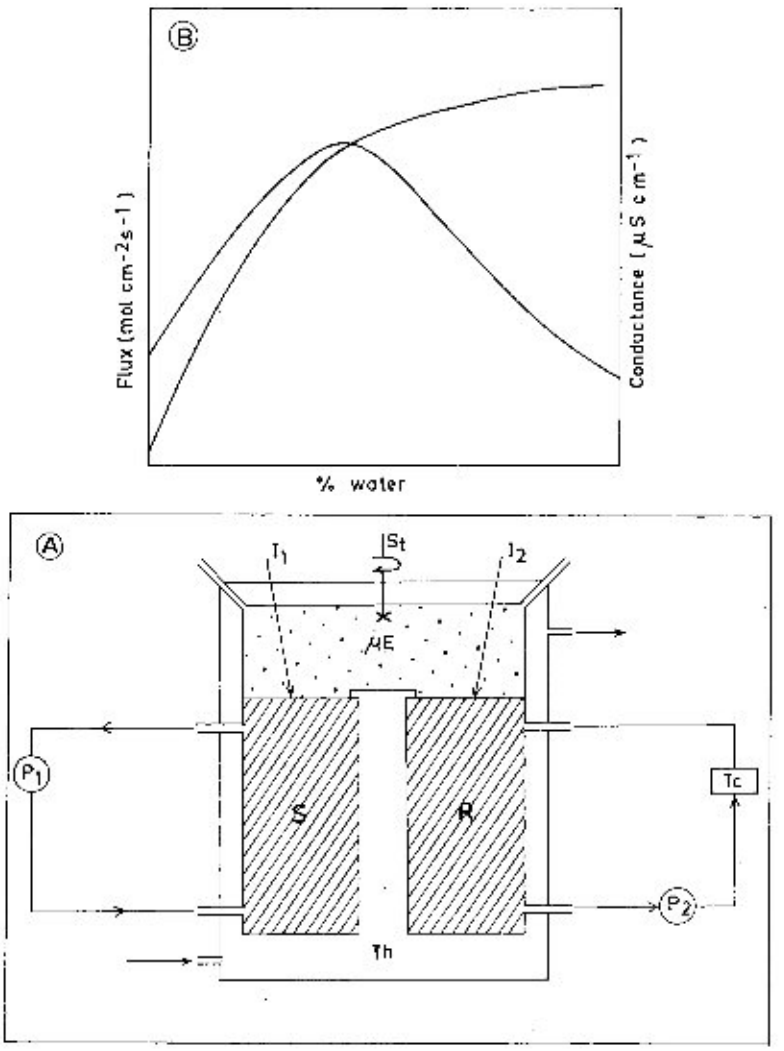

Fig. 20. (A) Schematic representation of the experimental set-up for transport experiment with w/o microemulsion (adapted from Derouiche and Tondre [642]). S, source of aqueous phase; R, receiving aqueous phase; μE, w/o microemulsion phase; S_t, stirrer; I_1, first interface; I_2, second interface; T_c, testing device; P_1, pumping device for circulation of the source phase; P_2, pumping device for circulation of the receiving phase. Note: for separation using the o/w microemulsion, the cell position is inverted. The S and R phase will be up and the μE phase will be down. (B) Dependence of picrate ion transport and conductance of the receiving (R) phase on % water in the Winsor II microemulsion (as trends shown in Derouiche and Tondre [642], drawn on an arbitary scale).

guide the transport process of the dynamic separating system. The droplet mobility can appreciably decrease in the post-percolation (clustering) stage. The analysis of the results may not be on the whole straightforward.

Table 10
Associated co-ion dependent transfer of Ni^{2+} by water–tetraethylene glycol dodecylether–hexanol–decane system

Anion	Transfer rate (ppm min^{-1})	10^{10} Flux (mol cm^{-2} min^{-1})
ClO_4^-	0.347	301.0
NO_3^-	0.0895	77.6
Cl^-	0.0741	32.4
$Acetate^-$	0.0341	29.6
SO_4^{2-}	0.0080	6.94

Taken from Derouiche and Tondre [642].

The separation of ions Ni^{2+}, Co^{2+} and Cu^{2+} [642–647], as well as the non-ionic compounds pyrene, perylene and anthracene [637,638] sharply increases with time. The separation of acetic acid from water [648] has also been observed to be sharp. Typical results of Ni^{2+} transport by w/o Winsor II liquid membrane are presented in Table 10.

Tondre and coworkers have proposed mechanisms for the transfer of hydrophilic and lipophilic substances by the microemulsion liquid membranes [638,642]. An outline of the suggested mechanisms is presented below.

A. Steps involved for transfer of salt:

1. The ions from S phase either cross I_1 and taken by the w/o μE droplet as an ion-pair or they are taken by the μE droplet by opening itself right at I_1.
2. The droplet with the ion-pair traverses through the aqueous membrane continuum to I_2.
3. The ion-pair is either released from the μE droplet near I_2 to cross it and dissociate in R phase, or the μE droplet releases the ion-pair by opening itself at I_2 to enter into R phase as dissociated.

B. Steps involved for transfer of lipophilic solute:

1. The solute in S phase crosses I_1, and is taken up by the o/w μE droplet.
2. The lipophile contained μE droplet traverses through the aqueous membrane continuum and is released near I_2.
3. The lipophile then crosses I_2 and enters into the R phase.

The picrate transport has been explained on the basis of facilitated diffusion model developed by Xenakis et al. [638] and Tondre and Xenakis [639]. The flux of transported solute (F) is given by the general equation,

$$F = \frac{DKC_G}{L}\left(\frac{[S]^n_{ss}}{1 + k[S]^n_{ss}}\right), \tag{35}$$

which applies to a neutral solute S (in this case $n = 1$), as well as to that of

uni–univalent electrolyte like alkali metal picrate (in this case $n = 2$). The subscript 'SS' stands for the operating concentration that exists in the source phase at steady state conditions. C_G, D and L are the carrier concentration (here droplet concentration), diffusion coefficient of the droplets and the cumulative thickness of the diffusion layers, respectively. K is either the extraction constant or the product of a partition constant times the equilibrium constant for solubilization inside the droplets.

The use of the above equation under varied experimental conditions has been tested and relevant mechanisms of transfer, as presented in Schemes A and B, have been invoked [646]. The flux measurements when compared with those reported from classical experiments involving direct contact have suggested that the presence of a membrane of pore diameter of the order of 2.4 nm, does not significantly affect the interfacial transfer mechanisms that occur in the microemulsion system.

For the transport of lyophilic materials through the o/w microemulsion, the following relation based on the reasonings of Ward [649] and Cussler [650] has been used by Xenakis and Tondre [638].

$$F = \frac{DKkC_D}{L}\left(\frac{C_{p^0}}{1 + kKC_{p^0}}\right), \tag{36}$$

where D is the diffusion coefficient of the microemulsion droplet, K is the equilibrium constant of binding of the solute with the droplet (this K is different from the K of Eq. (35)), k is the partition coefficient of solute between the oil phase and the continuous phase in microemulsion, C_D is the total droplet concentration, L is the thickness of the diffusion layers and C_{p^0} is the concentration of the solute outside the membrane.

C_{p^0} can be obtained from the partition coefficient of solute, k_p by the relation,

$$C_{p^0} = C_{p^i}\left[1/1 + \frac{1}{k_p}(V_M/V_S + V_R)\right], \tag{37}$$

where C_{p^i} is the solute concentration in the compartment S and V_M, V_S and V_R are the volumes of membrane, S and R compartments, respectively.

Apart from verification of the above relation, the transport of lipophilic compounds have given insight to the structural organization and percolation of oil droplets in a continuous aqueous phase. Besides, information on the thermodynamics of the solubilization–desolubilization processes of the solutes in a microemulsion droplet have also been obtained.

In the case of transition metal Ni^{2+} separation, Tondre and coworkers [643,646] have used 8-hydroxyquinoline and an industrial extractant Kelex 100 using water–SDS–butanol or pentanol–dodecane w/o microemulsion systems. The kinetics and mechanistic aspects of reaction occuring in the extraction of the metal ion have been thoroughly worked out. In a separate study [642] they have employed

microemulsion and crown ether or Kelex 100 to understand the coupled transport phenomenon. Synergistic effects for metal ion transport have been found in some cases but not in others; the results have been explored on the basis of diffusion of the carriers in the stagnant layers. Their works have also realized different mechanisms for non-ionic and ionic surfactant supported microemulsions discussed earlier [642]. The overall efficacy of microemulsion-based extraction of heavy metals (particularly mercury) from contaminated water involving oleic acid has been reported by Wiencek et al. [651] and successfully modeled [652] using experimentally determined equilibrium extraction, stripping, and the initial reaction kinetics. This model accurately predicts both the initial extraction kinetics and the final mercury extraction equilibrium. The good agreement between theory and experiment on the mechanism of extraction using microemulsion to that of coarse emulsions has been found. Furthermore, electrostatic coalescence and butanol addition have been evaluated as potential demulsification techniques for recovery of the components of mercury-rich microemulsions [653].

Recently, Hebrant et al. [654] have investigated the transport of amino acids (*p*-iodophenylalanine and tryptophan) by AOT–isooctane reverse micelles as liquid membranes. The rates of transport of the amino acids have been compared and discussed in relation to their partition coefficients between the water and AOT palisade layer. Different behaviors of the two amino acids have been shown. They have also investigated the rate of water uptake by the AOT reverse micelles, as well as the influence of the ionization state of amino acids on it. They have further attempted to perform enantioselective transports using chiral AOT. However, they have not succeeded in producing enantiomeric enrichments from these experiments and have suggested that the rigidity of the surfactant film has not been sufficient to permit chiral recognition in that case. Very recently, Tondre et al. [655] have reported the two ways of extracting copper ions in micellar particles: (1) association through ion exchange (anionic SDS micelles); and (2) complexation with micelle-solubilized hydrophobic extractants such as (CTAB–butanol–water–Kelex 100 microemulsions). They have compared for the first time the electrochemical behavior of copper ions whether they are simply bound to the micelle surface or more deeply embedded in the core of a microemulsion as a hydrophobic complex. However, they have concluded that the stability of Cu^{2+}–Kelex complexes is too high to recover copper metal by electrolysis from CTAB–butanol–water microemulsions.

9.4.2. Advantages of microemulsions as liquid membranes and their limitations

The microemulsions have several advantages over other types of membranes. Their low interfacial tension leads to easy formulation of smaller droplets, augmenting faster rates of transfer by way of increased surface area per unit volume. Their thermodynamic stability is a fundamental advantage over macroemulsions. Their easy emulsification and demulsification (such as with a change of temperature) helps favorably in transfer and recovery compared with complexing agents used in organic phases for facilitated transport. The rates of transfer by microemulsions are faster.

[19] A.M. Bellocq, J. Biais, P. Bothorel, et al., Adv. Colloid Interf. Sci. 20 (1984) 167.
[20] A.M. Bellocq, in: S. Safran, N. Clark (Eds.), Complex and Super-molecular Fluids, Wiley, New York, 1987, p. 41.
[21] C. Kumar, D. Balasubramanian, J. Colloid Interf. Sci. 74 (1980) 64.
[22] M. Kahlweit, E. Lessner, R. Strey, J. Phys. Chem. 87 (1983) 5032.
[23] M. Kahlweit, E. Lessner, D. Haase, J. Phys. Chem. 89 (1985) 163.
[24] M. Kahlweit, E. Lessner, R. Strey, J. Phys. Chem. 88 (1984) 1937.
[25] O. Ghosh, C.A. Miller, J. Phys. Chem. 91 (1987) 4528.
[26] S.R. Bisal, P.K. Bhattacharya, S.P. Moulik, J. Surf. Sci. Technol. 4 (1988) 121.
[27] M.L. Das, P.K. Bhattacharya, S.P. Moulik, Ind. J. Biochem. Biophys. 26 (1989) 24.
[28] M.L. Das, P.K. Bhattacharya, S.P. Moulik, Colloids Surf. 49 (1990) 247.
[29] S.R. Bisal, P.K. Bhattacharya, S.P. Moulik, Ind. J. Chem. 28A (1989) 55.
[30] P. Kar, S.P. Moulik, Ind. J. Chem. 34A (1995) 700.
[31] N. Mitra, P.K. Bhattacharya, S.P. Moulik, Ind. J. Biochem. Biophys. 33 (1996) 206.
[32] P.D.I. Fletcher, B.P. Binks, R. Aveyard, Langmuir 5 (1989) 1210.
[33] B.K. Paul, S.P. Moulik, Ind. J. Biochem. Biophys. 28 (1991) 174; K. Mukherjee, D.C. Mukherjee, S.P. Moulik, J. Colloid Interf. Sci. 187 (1997) 327.
[34] M. Khalweit, R. Strey, D. Hasse, et al., J. Colloid Interf. Sci. 118 (1987) 436.
[35] B.K. Paul, S.P. Moulik, J. Disp. Sci. Technol. 18 (1997) 95.
[36] T.K. De, A.N. Maitra, Adv. Colloid Interf. Sci. 59 (1995) 95.
[37] P. Ekwall, L. Mandell, K. Frontell, J. Colloid Interf. Sci. 33 (1970) 215.
[38] P. Ekwall, in: G.H. Brown (Ed.), Advance in Liquid Crystals, Academic Press, New York, 1975.
[39] M. Dovlaitzky, R. Ober, J. Billard, C. Taupin, J. Charvolin, Y. Hendricks, C.R. Acad. Sci. B292 (1981) 45.
[40] S. Safran, L. Turkevich, P. Pincus, J. Phys. Lett. 45 (1984) L–69.
[41] D. Roux, C. Coulon, J. Phys. 47 (1987) 1257.
[42] P. Stilbs, B. Lindman, J. Colloid Interf. Sci. 99 (1984) 290.
[43] K. Frontell, L. Hernqvist, K. Larsson, J. Sjoblom, J. Colloid Interf. Sci. 93 (1983) 453.
[44] P.L. Luisi, R. Scartazzini, G. Haering, P. Schurtenbarger, Colloid Polym. Sci. 268 (1990) 356.
[45] A. Shioi, M. Harada, K. Matsumoto, J. Phys. Chem. 95 (1991) 7495.
[46] F. Kern, R. Zana, S.J. Candau, Langmuir 7 (1991) 1344.
[47] M. Kahlweit, R. Strey, R. Schomaker, in: W. Knoche, R. Schomarker (Eds.), Reactions in Compartmentallized Liquids, Springer Verlag, New York, 1989, p. 1.
[48] E. Sjoblom, S. Friberg, J. Colloid Interf. Sci. 67 (1978) 16.
[49] G.J.M. Koper, W.F.C. Sager, J. Smeets, D. Bedeaux, J. Phys. Chem. 99 (1995) 13291.
[50] H.F. Eicke, H. Borkovec, B. Dasgupta, J. Phys. Chem. 93 (1989) 314.
[51] P. Guering, A.M. Cazabat, J. Phys. Lett. 44L (1983) 601.
[52] A.M. Cazabat, in: S. Safran, N. Clark (Eds.), Physics of Complex and Supermolecular Fluids, Wiley, New York, 1987.
[53] S. Kirkpatrick, Rev. Mod. Phys. 45 (1973) 574.
[54] D. Stanffer, Phys. Rep. 54 (1979) 1.
[55] R. Botet, R. Jullien, Aggregation and Fractal Aggregates, World Scientific, Singaporre, 1986.
[56] P. Meakin, Adv. Colloid Interf. Sci. 28 (1988) 2490.
[57] P. Meakin, in: F. Family, D.P. Landau (Eds.), Kinetics of Aggregation and Gelation, North Holland, Amsterdam, 1984.
[58] J. Feder, Fractals, Plenum Press, New York, 1988.
[59] P. Meakin, in: W. Knoche, R. Schomaker (Eds.), Reactions in Compartmentallized Liquids, Springer Verlag, New York, 1989, p 173.
[60] M. Lagues, R. Ober, C. Taupin, J. Phys. Lett. 39 (1978) 487.
[61] H. Saito, K. Shinoda, J. Colloid Interf. Sci. 32 (1970) 647; K. Shinoda, H. Saito, J. Colloid Interf. Sci. 26 (1968) 70.
[62] Y. Tamlon, S. Prager, J. Chem. Phys. 69 (1978) 517.
[63] L.E. Scriven, in: K.L. Mittal (Ed.), Micellization, Solubilization and Microemulsions, Plenum Press, New York, 2 (1977) 877.

[64] S. Friberg, I. Lapczynska, G. Gillberg, J. Colloid Interf. Sci. 56 (1976) 19.
[65] B. Lindman, N. Kamenka, B. Brun, P.G. Nilsson, in: I.D. Robb (Ed.), Microemulsions, Plenum Press, New York, 1982.
[66] M. Zulauf, H.F. Eicke, J. Phys. Chem. 83 (1979) 480.
[67] H.F. Eicke, J. Pure Appl. Chem. 52 (1980) 1349.
[68] R. Zana, J. Lang, in: E.J. Fendler, K.L. Mittal (Eds.), Solution Chemistry of Surfactants, Plenum Press, New York, 1984.
[69] M. Borkovec, H.F. Eicke, H. Hammerich, B. Dasgupta, J. Phys. Chem. 92 (1988) 206.
[70] L.E. Scriven, Nature 263 (1976) 123.
[71] M. Cazabat, D. Langevin, J. Chem. Phys. 74 (1981) 3148.
[72] S. Brunetti, D. Roux, A.M. Bellocq, G. Fourche, P. Bothorel, J. Phys. Chem. 87 (1983) 1029.
[73] D. Roux, A.M. Bellocq, P. Botherol, in: K.L. Mittal, B. Lindman (Eds.), Surfactants in Solution, Plenum Press, New York, 3 (1984) 1843.
[74] A.A. Calje, W.G.M. Agterof, A. Virj, in: K.L. Mittal (Ed.), Micellization, solubilization and Microemulsion, Plenum Press, New York, 2 (1978) 779.
[75] D. Chatenay, W. Urbach, A.M. Cazabat, D. Langevin, Phys. Rev. Lett. 54 (1985) 2253.
[76] L. Auvray, J.P. Cotton, R. Ober, C. Taupin, J. Phys. 45 (1984) 913.
[77] R. Zana, J. Lang, in: S.E. Friberg, P. Botherol (Eds.), Microemulsions CRC Press, Florida, 1987.
[78] J. Fang, R. Venable, J. Colloid Interf. Sci. 116 (1987) 269.
[79] S.R. Bisal, P.K. Bhattacharya, S.P. Moulik, J. Phys. Chem. 94 (1990) 350; J. Phys. Chem. 94 (1990) 4212.
[80] S. Pal, S.R. Bisal, S.P. Moulik, J. Phys. Chem. 96 (1992) 896.
[81] J.R. Hansen, J. Phys. Chem. 78 (1974) 256.
[82] P.G. Nilsson, B. Lindman, J. Phys. Chem. 86 (1982) 271.
[83] J. Tabony, A. Llor, M. Drifford, Colloid Polym. Sci. 261 (1983) 938; J. Tabony, M. Drifford, A. de Geyer, Chem. Phys. Lett. 96 (1983) 119.
[84] B. Lindman, H. Wennerstrom, in: K.L. Mittal, E.J. Fendler (Eds.), Solution Behaviors of Surfactants, Plenum Press, New York, 1 (1982) 3.
[85] M. Gradzielski, H. Hoffmann, Adv. Colloid Interf. Sci., 42 (1992) 149; A.M. Bellocq, J. Biais, B. Clin, P. Lalanne, B. Lemanceau, J. Colloid Interf. Sci. 70 (1979) 524.
[86] M. Kotlarchyk, S.H. Chen, J. Chem. Phys. 79 (1983) 2461.
[87] C. Toprakcioglu, J.C. Dore, B.H. Robinson, P. Chieux, J. Chem. Soc. Faraday Trans. 80 (1984) 13.
[88] R. Hilficker, H.F. Eicke, W. Sager, C. Stub, U. Hofmeier, R. Gehrke, Ber. Bunsenges Phys. Chem. 94 (1990) 677.
[89] A.N. North, J.C. Dore, A. Kartisikdes, J.A. McDonald, B.H. Robinson, Chem. Phys. Lett. 132 (1986) 541.
[90] M. Kotlarchyk, J.S. Huang, S.H. Chen, J. Phys. Chem. 80 (1982) 3273; J. Phys. Chem. 89 (1985) 4382.
[91] S. Muto, K. Meguro, Bull. Chem. Soc. Jpn. 46 (1973) 1316.
[92] B. Bedwell, E. Gulari, J. Colloid Interf. Sci. 102 (1984) 88.
[93] M. Kotlarchyk, S.H. Chen, J.S. Huang, M.W. Kim, Phys. Rev. Lett. 53 (1985) 941.
[94] N. James, E. Kaler, Langmuir 2 (1986) 184.
[95] N. Berk, Phys. Rev. Lett. 58 (1987) 2718.
[96] N.F. Berk, Phys. Rev. 44 (1991) 5069.
[97] S.H. Chen, S.L. Chang, R. Strey, Prog. Colloid Polym. Sci. 81 (1990) 30.
[98] S.H. Chen, S.L. Chang, R. Strey, J. Appl. Crystallogr. 24 (1991) 721.
[99] S.F. Trevino, R. Jonbran, N. Parris, N.F. Berk, Langmuir 10 (1994) 2547.
[100] J. Eastoe, Langmuir 8 (1992) 1503.
[101] J. Eastoe, R.K. Heenan, J. Chem. Soc. Faraday Trans. 90 (1994) 487.
[102] S.A. Safran, L.A. Turkevichand, P. Puicus, J. Phys. Lett. 45 (1984) L69; S.A. Safran, in: S.H. Chen, R. Rajagopalan (Eds.), Micellar Solutions and Microemulsions, Structure, Dynamics and Statistical Thermodynamics, Springer-Verlag, New York, 1990.
[103] J. Eastoe, J. Dong, K.J. Hetherington, D. Steytler, R.K. Henan, J. Chem. Soc. Faraday Trans. 92 (1996) 65.

[104] M.S. Leaver, U. Olsson, H. Wennerstrom, R. Strey, U. Wurz, J. Chem. Soc. Faraday Trans. 91 (1995) 4269.
[105] H. Bagger-Jörgensen, U. Olsson, K. Mortensen, Langmuir 13 (1997) 1413.
[106] D. Waysbort, S. Ezrahi, A. Aserin, R. Givati, N. Garti, J. Colloid Interf. Sci. 188 (1997) 282.
[107] N. Garti, R. Feldenkriez, A. Aserin, S. Ezrahi, D. Shapira, Lubracation Engg. 49 (1993) 404.
[108] U. Olsson, P. Schurtenberger, Prog. Colloid Interf. Sci., in press.
[109] U. Olsson, P. Schurtenberger, Langmuir 9 (1993) 3389.
[110] M.S. Leaver, U. Olsson, Langmuir 10 (1994) 3449.
[111] J. Eastoe, W.K. Young, B.H. Robinson, D.C. Steyler, J. Chem. Soc. Faraday Trans. 86 (1990) 2883.
[112] J. Eastoe, K.J. Hetherington, D. Sharpe, D.C. Steyler, S. Egelhaaf, R.K. Heenan, Langmuir (and references therein) 13 (1997) 2490.
[113] H. Kellay, Y. Hendrikx, J. Meunier, B.P. Binks, L.T. Lee, J. Phys. II France 3 (1993) 1747.
[114] J. Eastoe, D. Sharpe, R.K. Heenan, S. Egelhaaf, J. Phys. Chem. 101B (1997) 944.
[115] J. Eastoe, J. Hetherington, D. Sharpe, J. Dong, Langmuir 12 (1996) 3876.
[116] J. Eastoe, B.H. Robinson, R.K. Heenan, Langmuir 9 (1993) 2820.
[117] J. Eastoe, T.F. Towey, B.H. Robinson, J. Williams, R.K. Heenan, J. Phys. Chem. 97 (1993) 1459.
[118] J. Eastoe, G. Fragneto, D.C. Steytler, B.H. Robinson, R.K. Heenan, Physica B, 180 and 181 (1992) 555.
[119] D.C. Steytler, B.H. Robinson, J. Eastoe, K. Ibel, J.C. Dore, I. Macdonald, Langmuir 9 (1993) 903.
[120] J. Eastoe, B.H. Robinson, D.C. Steytler, J.C. Dore, Chem. Phys. Letts. 166 (1990) 153.
[121] J. Eastoe, K. Hetherington, J.S. Dalton, D. Sharpe, J.R. Lu, R.K. Heenan, J. Colloid Interf. Sci. 190 (1997) 449.
[122] R.G. Zielinski, S.R. Kline, E.W. Kaler, N. Rosov, Langmuir 13 (1997) 3934.
[123] A. Martino, E.W. Kaler, J. Phys. Chem. 94 (1990) 1627.
[124] J. Ricka, M. Borkovec, U. Hofmeier, J. Chem. Phys. 94 (1991) 8503.
[125] A. Shioi, M. Harada, M. Matsumoto, J. Phys. Chem. 95 (1991) 7495.
[126] A. Shioi, M. Harada, M. Tanabe, J. Phys. Chem. 97 (1993) 8281.
[127] F. Litcherfeld, T. Schmeling, R. Strey, J. Phys. Chem. 90 (1986) 5762.
[128] M. Teubner, R. Strey, J. Chem. Phys. 87 (1987) 3195.
[129] A.N. North, J.C. Dore, J.A. McDonald, B.H. Robinson, R.K. Heenan, A.M. Howe, Colloids Surf. 19 (1986) 21; E.W. Kaler, J. Phys. Chem. 94 (1990) 1627.
[130] X. Auvray, C. Peptipas, R. Anthora, et al., Colloid Polym. Sci. 265 (1987) 925.
[131] J. Santhanalakshmi, A. Parameswari, J. Surf. Sci. Technol. 8 (1992) 389.
[132] I.S. Barnes, S.T. Hyde, B.W. Ninham, P.J. Derian, M. Drifford, Th. Zemb, J. Phys. Chem. 92 (1988) 2286.
[133] V. Rajagopalan, H. Bagger-Jörgensen, K. Fukuda, U. Olsson, B. Jönsson, Langmuir 12 (1986) 2939.
[134] O. Regev, S. Ezrahi, A. Aserin, et al., Langmuir 12 (1996) 668.
[135] L. Engström, V.K.S. Shukla, G. Hølmer (Eds.), in Proc 15th Scandinavian Symp. on Lipids, Rebild Bakker, Skorping, Denmark (1989) 145.
[136] S.H. Chen, J.S. Huang, Phys. Rev. Lett. 55 (1985) 1888.
[137] Dynamic Light Scattering, R. Pecora (Ed.), Plenum, New York, 1985.
[138] J.H.R. Clarke, D. Brown, J. Phys. Chem. 92 (1988) 2881.
[139] S.J. Candau, in: R. Zana (Ed.), Surfactant Solutions: New Methods on Investigation, Surfactant Science Series, Marcel Decker, New York, 22 (1987).
[140] J.H.R. Clarke, J.P. Nicholson, in: K.L. Mittal, B. Lindman (Eds.), Surfactants in Solution Plenum, New York, 3 (1984).
[141] D.O. Shah, M.J. Hou, M. Kim, J. Colloid Interf. Sci. 123 (1988) 398.
[142] J.P. Blitz, J.L. Fulton, R.D. Smith, J. Phys. Chem. 92 (1988) 2707.
[143] J.P. Blitz, J.M. Tingey, J.L. Fulton, R.D. Smith, J. Phys. Chem. 93 (1989) 4198.
[144] J. Eastoe, B.H. Robinson, D.C. Steytler, W.K. Young, J. Chem. Soc. Faraday Trans. 86 (1990) 2883.
[145] R. Zana, J. Lang, O. Sorba, A.M. Cazabat, D. Langevin, J. Phys. Lett. 43 (1982) L829.
[146] J.R. Lalanne, B. Poullgny, E. Seln, J. Phys. Chem. 87 (1983) 696.

[147] A.M. Bollocq, P. Honorat, D. Roux, J. Phys. (Paris) 46 (1985) 743.
[148] R. Dorshow, F. de Buzzaccarini, C.A. Bunton, D.F. Nicoli, Phys. Rev. Lett. 47 (1981) 1336.
[149] C.M. Sorensen, Chem. Phys. Lett. 177 (1985) 606.
[150] A.M. Cazabat, in: V. Degiorgio, M. Corti (Eds.), Physics of Amphiphiles, Micelles, Vesicles and Microemulsions, North Holland, Amsterdam, 1985, p. 723.
[151] A.M. Cazabat, D. Langevin, in: V. Degiorgio, M. Corti, M. Gilio (Eds.), Light Scattering in Liquids and Macromolecular Solutions, Plenum Press, New York, 1980, p. 139.
[152] B. Lamaire, D. Roux, P. Bothorel, J. Phys. Chem. 87 (1983) 1023.
[153] K.I. Feng, Z.A. Schelly, J. Phys. Chem. 99 (1995) 17207.
[154] A. Sanguineti, A. Chittofrati, D. Lenti, M. Visca, J. Colloid Interf. Sci. 155 (1993) 402.
[155] J. Biais, M. Mereier, P. Bothorel, B. Clin, P. Lalanne, B. Lemanceau, J. Microsc. 121 (1981) 169.
[156] E.A. Hildebrand, I.R. McKinnon, D.R. MacFarlane, J. Phys. Chem. 96 (1986) 2784.
[157] T. Gulik-Krzywicki, K. Larsson, Chem. Phys. Lipids 35 (1984) 127.
[158] J. Santhanalakshmi, A. Parameshwari, Ind. J. Chem. 31A (1992) 630.
[159] J. Dubochet, H. Adrian, J. Texiera, et al., J. Phys. Chem. 88 (1984) 6727.
[160] W. Jahn, R. Strey, J. Phys. Chem. 92 (1988) 2294.
[161] G. Fleischer, K. Grätz, J. Kräger, H.W. Meyer, K. Quitzsch, J. Colloid Interf. Sci. 190 (1997) 9.
[162] M.P. Pileni, J. Tanori, A. Filankembo, Colloids Surfs., 1997, accepted.
[163] O.V. Vesetova, B.P. Nikolaev, A.M. Shlyakov, Kollid Zh. 47 (1985) 1027.
[164] J.S. Guo, M.S. Elasser, E.D. Sudel, H.J. Yue, J.W. Vanderhoff, J. Colloid Interf. Sci. 140 (1990) 175.
[165] C.L. Mesa, L. Coppola, G.A. Raniera, M. Terenzi, G. Chidichimo, Langmuir 8 (1992) 26.
[166] B. Lindman, P. Stilbs, in: S. Friberg, P. Bothorel (Eds.), Microemulsions, CRC Press, Boca Raton, Florida, 1986.
[167] P. Guering, B. Lindman, Langmuir 7 (1985) 464.
[168] A. Martino, E.W. Kaler, Langmuir 11 (1995) 779.
[169] A.P. Full, E.W. Kaler, Langmuir 10 (1994) 2929.
[170] M. Jonstromer, U. Olsson, W.O. Parker, Jr., Langmuir 11 (1995) 61.
[171] K.P. Das, A. Ceglie, B. Lindman, S.E. Friberg, J. Colloid Interf. Sci. 166 (1987) 390.
[172] K.P. Das, A. Ceglie, B. Lindman, J. Phys. Chem. 91 (1987) 2938.
[173] W.O. Parker, Jr., C. Genova, G. Carignano, Colloids Surfs. A 72 (1993) 275.
[174] M. Jonströmer, U. Olsson, W.O. Parker, Jr., Langmuir 11 (1995) 61.
[175] U. Olsson, K. Shinoda, B. Lindman, J. Phys. Chem. 90 (1986) 4083.
[176] U. Olsson, P. Schurtenberger, Langmuir 9 (1983) 3389.
[177] M. Leaver, I. Furo, U. Olsson, Langmuir 11 (1995) 1524.
[178] Y. Hendrikx, H. Kellay, J. Meunier, Europhys. Lett. 25 (1994) 735.
[179] D. Waysbort, S. Ezrahi, A. Aserin, R. Givati, N. Garti, J. Colloid Interf. Sci. 188 (1997) 282.
[180] U. Olsson, K. Nagai, H. Wennerstrom, J. Phys. Chem. 92 (1988) 6675.
[181] H.F. Eicke, J.C.W. Shepard, Helv. Chem. Acta 57 (1974) 1951.
[182] J. Sjoblom, B. Jonsson, C. Nylander, I. Lundstrom, J. Colloid Interf. Sci. 96 (1983) 504.
[183] J. Peyrelasse, C. Boned, J. Phys. Chem. 89 (1985) 370.
[184] M.A. Van Dijk, J.G.H. Joosten, Y.K. Levine, D. Bedeaux, J. Phys. Chem. 93 (1989) 2506.
[185] U. Lenz, H. Hoffmann, Ber. Bunsenges. Phys. Chem. 96 (1992) 809.
[186] S.J. Chen, D.F. Evans, B.W. Ninham, J. Phys. Chem. 88 (1984) 163.
[187] H.M. Chen, Z.A. Schelly, Langmuir 11 (1995) 758.
[188] M.L. Das, P.K. Bhattacharya, S.P. Moulik, Langmuir 7 (1991) 626.
[189] S. Ajith, A.K. Rakshit, J. Surf. Technol. 8 (1992) 365.
[190] S. Ajith, A.K. Rakshit, Langmuir 11 (1995) 1122.
[191] S. Ajith, A.K. Rakshit, J. Phys. Chem. 99 (1995) 14778.
[192] A.C. John, A.K. Rakshit, Colloids Surfs. A 95 (1995) 201.
[193] P.C. Jain, Adv. Colloid Interf. Sci. 54 (1995) 17.
[194] P. Hossein Khani, A.N. Maitra, P.C. Jain, J. De Phys. (IV) 3 (1993) 321.
[195] S. Roychowdhury, R. Yadav, A.N. Maitra, P.C. Jain, Mat. Sci. Forum 105/110 (1992) 1521.
[196] A.N. Maitra, M. Varshney, Colloids Surfs. 24 (1987) 119.

[197] M. Varshney, A.N. Maitra, Colloids Surfs. 96 (1995) 165.
[198] S.K. Das, B. Nandi Ganguly, J. Colloid Interf. Sci., 1997, accepted.
[199] M.L. Sierra, E. Rodenas, Langmuir 12 (1996) 573.
[200] I. Molinero, M.L. Sierra, E. Rodenas, J. Colloid Interf. Sci. 1998 (1997) 239.
[201] G. Montalvo, M. Valiente, E. Rodenas, J. Colloid Interf. Sci. 172 (1995) 495.
[202] R.H. Cole, G. Delbos, P. Winsor IV, T.K. Bose, J.M. Moreau, J. Phys. Chem. 89 (1985) 3338.
[203] J. Sjöblom, B. Jönsson, C. Nylander, I. Lundstrom, J. Colloid Interf. Sci. 96 (1983) 504; J. Colloid Interf. Sci. 100 (1984) 27.
[204] J. Sjöblom, B. Gestblom, J. Colloid Interf. Sci. 115 (1987) 535.
[205] B. Gestblom, J. Sjöblom, Langmuir 4 (1988) 360.
[206] J. Sjöblom, R. Skurtviet, J.O. Saeten, B. Gestblom, J. Colloid Interf. Sci. (and references therein) 141 (1991) 329.
[207] Y. Ikushima, N. Saito, M. Arai, J. Colloid Interf. Sci. 186 (1997) 254.
[208] S.P. Moulik, G.C. De, B.B. Bhowmik, unpublished data.
[209] P.D.I. Fletcher, R. Johannsson, J. Chem. Soc. Faraday Trans. 90 (1994) 3567.
[210] F. Sicoli, D. Langevin, L.T. Lee, J. Chem. Phys. 99 (1993) 4759.
[211] M. Almgren, R. Johannsson, J.E. Ericksson, J. Phys. Chem. 97 (1993) 8590.
[212] V.H. Perez-Luna, J.E. Puig, V.M. Castano, B.E. Rodriguez, A.K. Murthy, E.W. Kaler, Langmuir 6 (1990) 1040.
[213] J.E. Puig, A.P. Full, E.W. Kaler, ANTEC Conference Proceedings, 50th Meeting of the Society of Plastic Engineers, Detroit, MI, 2 (1992) 2587.
[214] M.P. Pileni, J. Phys. Chem. 97 (1993) 6961.
[215] C.L.C. Amaral, I. Rosangela, M.J. Politi, Langmuir (and references therein) 12 (1996) 4638.
[216] P. Ayuub, A.N. Maitra, D.P. Shah, J. Chem. Soc. Faraday Trans. 89 (1993) 3535; Physica C 168 (1990) 571.
[217] K. Kurumada, S. Itakura, S. Nagamine, M. Tanigaki, Langmuir 12 (1997) 3700.
[218] M.J. Suarez, H. Levy, J. Lang, J. Phys. Chem. 97 (1993) 9808.
[219] J.S. Huang, L.J. Fetters, W.D. Dozier, J. Sung, Stabiliz. Microemul. Polymer Polymeric Mat., Sci. Engng. 157 (1987) 965.
[220] J.S. Huang, J. Surf. Sci. Technol 5 (1989) 83.
[221] P. Lianos, S. Modes, G. Staikos, W. Brown, Langmuir 8 (1992) 1054.
[222] A.L. Joshi, A.K. Rakshit, Ind. J. Chem. 36A (1997) 38.
[223] R. Nagarajan, J. Chem. Phys. 90 (1989) 1980.
[224] R. Nagarjan, Langmuir 9 (1993) 369.
[225] R. Nagarjan, J. Chem. Phys. 90 (1989) 1980.
[226] H.F. Eicke, U. Hofmeier, C. Quellet, U. Zölzer, Prof. Colloid Polym. Sci. 90 (1992) 165.
[227] A. Kabalnov, B. Lindman, U. Olsson, L. Piculell, K. Thuresson, H. Wennerstrom, Colloid Polym. Sci. 274 (1996) 297.
[228] G. Fleischer, F. Steiber, U. Hofmeier, H.F. Eicke, Langmuir 10 (1994) 1780.
[229] M. Odenwald, H.F. Eicke, W. Meier, Macromolecules 28 (1995) 5069.
[230] W. Meier, Langmuir 12 (1996) 1188.
[231] W. Meier, J. Phys. Chem. 101B (1997) 919.
[232] W. Meier, Langmuir 12 (1996) 6341.
[233] W. Meier, A. Falk, M. Odenwald, F. Stieber, Colloid Polym. Sci. 274 (1996) 218.
[234] E.B. Abuin, M.A. Rubio, E.A. Lissi, J. Colloid Interf. Sci. 158 (1993) 129.
[235] A.M. Brun, W.H. Wade, J. Colloid Interf. Sci. 139 (1990) 93.
[236] D.C. Steytler, B.H. Robinson, J. Eastoe, K. Ibel, J.C. Dore, I. MacDonald, Langmuir 9 (1993) 903.
[237] H. Hauser, G. Haering, A. Pande, P.L. Luisi, J. Phys. Chem. 93 (1989) 7869.
[238] P.Q. Quist, B. Halle, J. Chem. Soc. Faraday Trans. 1 (1988) 1038.
[239] G. Haandrikman, G.J.R. Daane, F.J.M. Kerkhof, N.M. Van Os, L.A.M. Rupert, J. Phys. Chem. 96 (1992) 9061.
[240] M. Wong, J.K. Thomas, T. Nowak, J. Am. Chem. Soc. 79 (1977) 4730.
[241] M. Moran, G.A. Bowmaker, R.P. Cooney, Langmuir 11 (1995) 738.
[242] G. Giammona, F. Gofferedi, V.T. Liveri, G. Vassallo, J. Colloid Interf. Sci. 154 (1992) 411.

[243] A. Goto, S. Harada, T. Fujita, Y. Miwa, H. Yoshioka, H. Kishimoto, Langmuir 9 (1993) 86.
[244] A.N. Maitra, J. Phys. Chem. 88 (1984) 5122.
[245] S.P. Moulik, M.L. Das, A.R. Das, Langmuir 8 (1992) 2135.
[246] E. Aliotta, P. Migliardo, D.I. Donato, V.T. Liveri, E. Bardez, B. Larrey, Prog. Colloid Polym. Sci. 89 (1992) 1.
[247] C. Boned, J. Peyrelasse, M. Moha-Quchane, J. Phys. Chem. 90 (1986) 634.
[248] G. Gu, W. Wang, H. Yan, J. Colloid Interf. Sci. (and references therein) 167 (1994) 87.
[249] T. Kawai, K. Hamada, K. Kon-No, Bull. Chem. Soc. Japan 66 (1993) 2804.
[250] J. Eastoe, Langmuir 8 (1992) 1503.
[251] J. Eastoe, R.K. Heenan, J. Chem. Soc. Faraday Trans. 90 (1994) 487.
[252] H.F. Eicke, P.E. Zinsli, J. Colloid Interf. Sci. 65 (1978) 131.
[253] E. Kek, B. Valeur, J. Colloid Interf. Sci. 79 (1981) 465.
[254] H. Kondo, I. Miwa, H. Sunamoto, J. Phys. Chem. 86 (1982) 4826.
[255] K. Tamura, N. Nii, J. Phys. Chem. 93 (1989) 4825.
[256] P.E. Zinsli, J. Phys. Chem. 83 (1979) 3223.
[257] N. Wittouck, R.M. Negri, M. Ameloot, F.C. De Schryver, J. Am. Chem. Soc. 116 (1994) 10601.
[258] J. Nishimoto, E. Iwamoto, T. Fujiwara, T. Kumamaru, J. Chem. Soc. Faraday Trans. 89 (1993) 535.
[259] M. Hasegawa, T. Sugimura, K. Kuraishi, Y. Shinoda, A. Kitahara, Chem. Lett. (1992) 1373.
[260] M. Hasegawa, T. Sugimura, Y. Suzaki, Y. Shinoda, J. Phys. Chem. 98 (1994) 2120.
[261] M. Hasegawa, T. Sugimura, Y. Shindo, A. Kitahara, Colloids Surf. A 109 (1996) 305.
[262] N. Marianocorrea, M. Alicia Biasutti, J.J. Silber, J. Colloid Interf. Sci. 172 (1995) 71.
[263] C.H. Cho, M. Chung, J. Lee, et al., J. Phys. Chem. 99 (1995) 7806.
[264] N. Sarkar, K. Das, A. Datta, S. Das, K. Bhattacharya, J. Phys. Chem. 100 (1996) 10523.
[265] S. Das, A. Dutta, K. Bhattacharya, J. Phys. Chem. 101 (1997) 3249.
[266] S.E. Firberg, T. Young, R.A. Mackay, J. Oliver, M. Breton, Colloids Surfs. 100 (1995) 83.
[267] E.J. Bonner, R. Wolf, P.L. Luisi, J. Solid-Phase Biochem. 5 (1980) 255.
[268] G.G. Zampieri, H. Jaeckle, P.L. Luisi, J. Phys. Chem. 90 (1986) 1849.
[269] M. Caselli, P.L. Luisi, M. Maestro, R. Roselli, J. Phys. Chem. 92 (1988) 3899.
[270] P. Bruno, M. Caselli, P.L. Luisi, M. Maestro, A. Traini, J. Phys. Chem. 94 (1990) 5908.
[271] D. Chatenay, W. Urbach, A.M. Cazabat, M. Vacher, M. Waks, Biophys. J. 48 (1985) 893.
[272] D. Chatenay, W. Urbach, C. Nicot, M. Vacher, M. Waks, J. Phys. Chem. 91 (1987) 2198.
[273] M.P. Pileni, Chem. Phys. Lett. 81 (1981) 603.
[274] M.P. Pileni, T. Semp, C. Petit, Chem. Phys. Lett. 118 (1885) 414.
[275] J.P. Huruguen, M. Authier, J.L. Greffe, M.P. Pileni, J. Phys. Condens. Matter 3 (1991) 865.
[276] J.P. Huruguen, M. Authier, J.L. Greffe, M.P. Pileni, Langmuir 6 (1990) 243.
[277] F. Micheal, M.P. Pileni, Langmuir 10 (1994) 390.
[278] P.D.I. Fletcher, R.B. Freedman, J. Mead, C. Oldfield, B.H. Robinson, Colloids Surfs. 10 (1984) 193.
[279] A.V. Levashov, Y.L. Khmelnitsky, N.L. Klyachko, V.Y. Chernyak, K. Martinek, J. Colloid Interf. Sci. 88 (1982) 444.
[280] K.E. Goklen, T.A. Hatton, Sep. Sci. Technol. 22 (1987) 831.
[281] E. Sheu, K.E. Goklen, T.A. Hatton, S.H. Chen, Biotechnol. Prog. 2 (1986) 175.
[282] R.S. Rahaman, T.A. Hatton, J. Phys. Chem. 95 (1991) 1799; T.A. Hatton, S.H. Chen, Biotechnol. Prog. 2 (1986) 175.
[283] D. Bratko, A. Luzar, S.H. Chen, J. Chem. Phys. 89 (1988) 575.
[284] D. Bratko, A. Luzar, S.H. Chen, Bioelectrochem. Bioeng. 20 (1988) 291.
[285] M. Hirai, T. Takizawa, S. Yabuki, J. Chem. Soc. Faraday Trans. 91 (1995) 1981.
[286] P.L. Luisi, L.J. Majid, CRC Crit. Rev. Biochem. 20 (1986) 409.
[287] P.L. Luisi, M. Giomni, M.P. Pileni, B.H. Robinson, Biochem. Biophys. Acta 947 (1988) 209.
[288] E.B. Leodidis, T.A. Hatton, in: M.P. Pileni (Ed.), Structure and Reactivity in Reverse Micelles, Elsevier, Amsterdam, 1989, p. 270.
[289] A. Gupte, R. Nagarjan, A. Kilara, in: G. Charalambous (Ed.), Food Flavors: Generation, Analysis and Process Influence, Elsevier, 1995, p. 1.

[290] Y.E. Shapiro, N.A. Budanov, A.V. Levashov, N. Klyacho, Y.L. Khmelnitskii, K. Martinek, Collect. Czech. Chem. Commn. 54 (1989) 1126.
[291] A.M. Brozozowski, U. Derewenda, Z.S. Devewenda, et al., Nature 351 (1991) 491.
[292] M. Adachi, M. Harada, J. Phys. Chem. 97 (1992) 3631; J. Colloid Interf. Sci. 165 (1994) 229.
[293] K. Kawakami, M. Harada, M. Adachi, A. Shioi, Colloids Surfs. A 109 (1996) 217.
[294] V. Papadimitriou, A. Xenakis, P. Lianos, Langmuir 9 (1993) 912.
[295] S. Avramiotis, P. Lianos, A. Xenakis, Prog. Colloid Polym. Sci. 100 (1996) 286.
[296] S. Avramiotis, H. Stamatis, F.N. Kolisis, P. Lianos, A. Xenakis, Langmuir (and references therein) 12 (1996) 6320.
[297] N. Nguyen, J.B. Philips, V.T. John, J. Phys. Chem. 93 (1989) 8123.
[298] H. Nguyen, V.T. John, W.F. Reed, J. Phys. Chem. 95 (1991) 1467.
[299] A.M. Rao, H. Nguyen, V.T. John, Biotechnol. Prog. 6 (1990) 465.
[300] J.B. Philip, H. Nguyen, V.T. John, Biotechnol. Prog. 7 (1991) 43.
[301] C. Quellet, H.F. Eicke, Chimica 40 (1986) 233.
[302] C. Quellett, H.F. Eicke, R. Gehrke, W. Sager, Euro. Phys. Lett. 9 (1989) 293.
[303] G. Haering, P.L. Luisi, J. Phys. Chem. 90 (1985) 5892.
[304] G. Haering, P.L. Luisi, H. Hauser, J. Phys. Chem. 92 (1988) 3574.
[305] D. Capitani, A.L. Segre, G. Haering, P.L. Luisi, J. Phys. Chem. 92 (1988) 3500.
[306] P.L. Luisi, G. Haering, M. Maestro, G. Rialdi, Thermochimica Acta 162 (1990) 1.
[307] P.L. Luisi, R. Scartazzini, G. Haering, P. Schurtenberger, Colloid Polym. Sci. 268 (1990) 356.
[308] P.J. Atkinson, M.J. Grimson, R.K. Heenan, A.M. Howe, B.H. Robinson, Chem. Phys. Lett. 151 (1988) 494; J. Chem. Soc. Chem. Commun. 23 (1989) 1807.
[309] N.Z. Atay-Guneyman, F. Atadinc, Y. Kozluca, J. Colloid Interf. Sci. 169 (1995) 246.
[310] K. Shinoda, T. Kaneka, J. Disp. Sci. Technol. 9 (1988) 555.
[311] R. Scartazzini, P.L. Luisi, J. Phys. Chem. 92 (1988) 829.
[312] P. Schurtenberger, R. Scartazzini, P.L. Luisi, Rheol. Acta 28 (1989) 372.
[313] P. Schurtenberger, R. Scartazzini, L.J. Magid, M.E. Leser, P.L. Luisi, J. Phys. Chem. 94 (1990) 3695.
[314] D. Capitani, A.L. Segre, R. Sparapani, Langmuir 7 (1991) 250.
[315] G. Cavallaro, G. La Manna, V.T. Liveri, F. Aliotta, M.E. Fontanella, J. Colloid Interf. Sci. 176 (1995) 281.
[316] K. Shinoda, M. Araki, A. Sadaghiani, A. Khan, B. Lindman, J. Phys. Chem. 95 (1991) 989.
[317] J. Eastoe, B.H. Robinson, D.C. Steytler, F. Thorn-Lesson, Adv. Colloid Interf. Sci. 36 (1991) 1.
[318] S. Backlund, M. Rantala, O. Molander, Colloid Polym. Sci. 272 (1994) 1098.
[319] F. Aliotta, M.E. Fontanella, G. Squadrito, P. Migliado, G. La Manna, V.T. Liveri, J. Phys. Chem. 97 (1993) 6541.
[320] M.K. Jain, Introduction to Biological Membranes, Wiley Interscience, New York, 1988.
[321] A.N. Maitra, T.K. Jain, Z. Shervani, Colloids Surfs. (and references therein) 47 (1990) 255.
[322] M. Ueno, H. Kishimoto, Y. Kyogoku, J. Colloid Interf. Sci. 63 (1978) 131.
[323] C. Martin, I. Magid, J. Phys. Chem. 85 (1981) 3938.
[324] P. Lalanne, J. Biais, B. Clin, A.M. Bellocq, J. Chem. Phys. 75 (1978) 236.
[325] M. Eigen, Pure Appl. Chem. 6 (1963) 97.
[326] R. Zana, in: K.L Mittal (Ed.), Solution Chemistry of Surfactants, Plenum Press, New York, 1 (1979) 473.
[327] J. Biais, B. Clin, P. Lalanne, B. Lemanceau, J. Chim. Phys. 74 (1977) 1197.
[328] T. Nguyen, H. Hadj Ghaffarie, J. Chim. Phys. 76 (1979) 513.
[329] J. Lang, A. Djavanbakht, R. Zana, in: I.D. Robb (Ed.), Microemulsions, Plenum Press, New York, 1982, p. 233.
[330] J. Lang, A. Djavanbakht, R. Zana, J. Phys, Chem. 84 (1980) 145.
[331] S. Yiv, R. Zana, J. Colloid Interf. Sci. 65 (1978) 286.
[332] S. Yiv, R. Zana, W. Ulbricht, H. Hoffmann, J. Colloid Interf. Sci. 80 (1981) 224.
[333] J. Getting, H. Denver, P. Jobling, J. Rassing, E. Wyn-Jones, J. Chem. Soc. Faraday Trans. 74 (1978) 1957.
[334] P.G. De Gennes, C. Taupin, J. Phys. Chem. 86 (1982) 2294.

[335] C. Taupin, M. Dvolaitzky, R. Ober, Nuova Cimento 3D (1984) 62.
[336] G. Gilbert, H. Lehtinen, S. Friberg, J. Colloid Interf. Sci. 33 (1970) 40.
[337] V. Bansal, K. Chinnaswamy, C. Ramachandranm, D.O. Shah, J. Colloid Interf. Sci. 72 (1979) 524.
[338] J. Tabony, A. Llor, H. Drifford, Colloid Polym. Sci. 261 (1983) 938.
[339] P. Maelstaf, P. Bothorel, C.R. Acad. Sci. Paris 288 (1979) 13.
[340] J.M. Di Meglio, M. Dvolaitzky, C. Taupin, J. Am. Chem. Soc. 103 (1981) 1018.
[341] F. Menger, J. Donahue, R. Williams, J. Am. Chem. Soc. 95 (1973) 286.
[342] H. Eicke, J.C. Shepard, A. Steinemann, J. Colloid Interf. Sci. 56 (1976) 108.
[343] E.A.G. Aniansson, S. Wall, M. Almgren, et al., J. Phys. Chem. 80 (1976) 905.
[344] M. Kahlweit, J. Colloid Interf. Sci. 90 (1982) 92; Pure Appl. Chem. 53 (1981) 2069.
[345] E. Lessner, M. Teubner, M. Kahlweit, J. Phys. Chem. 85 (1981) 3167.
[346] B.H. Robinson, D. Steytler, R. Track, J. Chem. Soc. Faraday Trans. 1 (1979) 481.
[347] C. Tondre, R. Zana, J. Disp. Technol. 1 (1980) 179.
[348] H.R. Eicke, J.C. Shepard, A. Steinemann, J. Colloid Interf. Sci. 56 (1976) 168.
[349] P.D.I. Fletcher, A. Howe, N. Perrins, B.H. Robinson, C. Toprakcioglu, J. Dore, in: K.L. Mittal, B. Lindman (Eds.), Surfactants Solution, Plenum Press, New York, 3 (1984) 1745.
[350] B.H. Robinson, P.D.I. Fletcher, Ber. Bunsenges. Phys. Chem. 85 (1981) 863.
[351] S. Atik, J.K. Thomas, Chem. Phys. Lett. 79 (1981) 351.
[352] S. Atik, J.K. Thomas, J. Am. Chem. Soc. 103 (1981) 3543.
[353] S. Atik, J.K. Thomas, J. Phys. Chem. 85 (1981) 3921.
[354] J. Lang, A. Jada, A. Malliaris, J. Phys. Chem. 92 (1988) 1946.
[355] A. Jada, J. Lang, R. Zana, J. Phys. Chem. 93 (1989) 10.
[356] A. Jada, J. Lang, R. Zana, J. Phys. Chem. 94 (1990) 381.
[357] A. Jada, J. Lang, R. Zana, R. Makhloufi, E. Hirsch, S.J. Candau, J. Phys. Chem. 94 (1990) 387.
[358] J. Lang, G. Mascolo, R. Zana, P.L. Luisi, J. Phys. Chem. 94 (1990) 3069.
[359] J. Lang, R. Zana, N. Lalem, in: D.M. Bloor, E. Wyn-Jones (Eds.), The Structure, Dynamics and Equibilibrium Properties of Colloidal Systems, Kluwer Academic Publishers, The Netherlands, 1990, p. 253.
[360] P. Lianos, J. Lang, A.M. Cazabat, R. Zana, in: K.L. Mittal, P. Bothorel (Eds.), Surfactants in Solution, Plenum Press, New York, 1986.
[361] E. Gelade, F.C. De Schryver, J. Photochem. 18 (1982) 223.
[362] E. Gelade, F.C. De Schryver, J. Am. Chem. Soc. 106 (1984) 5871.
[363] J. Lang, in: D.M. Bloor, E. Wyn-Jones (Eds.), The Structure, Dynamics and Equilibrium Properties of Colloid Systems, Kluwer Academic Publishers, The Netherlands, 1990, p. 1.
[364] R. Zana, in: R. Zana (Ed.), Surfactants in Solutions, New Methods of Investigation, Marcel Decker, New York, 1987, p. 241.
[365] F. Grieser, C.J. Drummond, J. Phys. Chem. 92 (1988) 5580.
[366] J. Lang, N. Lalem, R. Zana, Colloids Surf. 68 (1992) 199.
[367] G. Bakale, J. Warman, J. Phys. Chem. 88 (1984) 2928.
[368] J. Lang, in: K.L. Mittal, P. Bothorel (Eds.), Surfactants in Solution, Plenum Press, New York, 1986.
[369] P.P. Infelta, M. Grötzel, J.K. Thomas, J. Phys. Chem. 78 (1984) 190.
[370] M. Tachiya, Chem. Phys. Letts. 33 (1975) 289.
[371] S.P. Moulik, S. Pal, Tenside Detergents 32 (1995) 1.
[372] J.M. Furois, P. Brochette, M.P. Pileni, J. Colloid Interf. Sci. 97 (1984) 552.
[373] A. Yekta, M. Aikawa, N.J. Turro, Chem. Phys. Lett. 63 (1979) 543.
[374] R. Zana, C. Weill, J. Phys. Lett. 46 (1985) L953.
[375] M. Almgren, J.E. Löfroth, J. Phys. Chem. 76 (1982) 2734.
[376] J.E. Löfroth, M. Almgren, in: K.L. Mittal, B. Lindman (Eds.), Surfactants in Solution, Plenum Press, New York, 1984, p. 627.
[377] G.G. Warr, F. Greiser, J. Chem. Soc. Faraday. Trans. 1 (1986) 1813.
[378] J.M. Chen, T.M. Su, C.Y. Mou, J. Phys. Chem. 90 (1986) 2418.
[379] G.G. Warr, L.J. Majid, E. Caponetti, C.A. Martin, Langmuir 4 (1988) 813.
[380] J. Lang, J. Phys. Chem. 94 (1990) 3734.

[381] N. Boens, H. Luo, M. Van de Auweraer, F.C. De Schryver, Chem. Phys. 146 (1988) 337.
[382] M. Almgren, J. Alsnis, E. Mukhtar, J. van Stam, J. Phys. Chem. 92 (1988) 4479; Prog. Colloid Polym. Sci. 76 (1988) 68.
[383] M. Van der Auweraer, S. Reckmans, N. Boens, F.C. De Schryver, Chem. Phys. 134 (1989) 91.
[384] M. van Auweraer, F.C. De Schryver, Chem. Phys. 111 (1987) 105.
[385] A. Malliaris, J. Lang, R. Zana, J. Chem. Soc. Faraday Trans. 1 (1986) 109.
[386] R.C. Doorance, T.F. Hunter, J. Chem. Soc. Faraday Trans. 1 (1974) 1572.
[387] P.K.F. Koglin, D.J. Miler, J. Steinwandel, M. Hauser, J. Phys. Chem. 85 (1981) 2353.
[388] M.A.J. Rodgers, M.F. Da Silva e Wheeler, Chem. Phys. Lett. 53 (1978) 165.
[389] Y. Croonen, E. Gelade, M. Vander Zegel, M. Van der Auweraer, H. Vandendriessche, F.C. De Schryver, J. Phys. Chem. 87 (1983) 1426.
[390] F. Grieser, Chem. Phys. Lett. 83 (1981) 59.
[391] R. Johannsson, M. Almgren, Langmuir 9 (1993) 2879.
[392] M.L. Sierra, E. Rodenas, Langmuir 10 (1994) 4440.
[393] M.L. Sierra, E. Rodenas, J. Phys. Chem. 97 (1993) 12387.
[394] M. Valiente, E. Rodenas, J. Colloid Interf. Sci. 127 (1989) 52.
[395] M. Valiente, E. Rodenas, Colloid Polym. Sci. 271 (1993) 494.
[396] E. Rodenas, M. Valiente, Colloids Surfs. 62 (1992) 289.
[397] E. Rodenas, E. Perez-Benito, J. Phys. Chem., 95 (1991) 4542, 9496.
[398] A. Jada, J. Lang, S.J. Candau, R. Zana, Colloids Surfs. 38 (1984) 251.
[399] D.G. Hall, J. Phys. Chem. 90 (1990) 429.
[400] N. Kallay, A. Chittofrati, J. Phys. Chem. 94 (1990) 4755.
[401] A. Chittofrati, A. Sanguineti, M. Visca, N. Kallay, Colloids Surfs. A 63 (1993) 219.
[402] S. Ajith, A.C. John, A.K. Rakshit, J. Pure Appl. Chem. 66 (1994) 509.
[403] A.C. John, A.K. Rakshit, Langmuir 10 (1994) 2084.
[404] N. Seedhar, M. Manik, J. Surf. Sci. Technol. 9 (1993) 81.
[405] X. Li, G. Zhao, E. Lin, J. Disp, Sci, Technol. 17 (1996) 111.
[406] X. Li, E. Lin, G. Zhao, T. Xiao, J. Colloid Interf. Sci. (and references therein) 184 (1996) 20.
[407] H.F. Eicke, W. Meier, Biophys. Chem. 58 (1996) 29.
[408] H. Scher, R. Zallen, Chem. Phys. 53 (1970) 3759.
[409] R. Blanc, E. Guyon, in: G. Deutcher, R. Zallen, J. Adler (Eds.), Percolation Structures and Processes, Annals of the Israel Physcial society, Israel Physical Society, Jerusalem, 5 (1983) 229.
[410] D.A.G. Bruggeman, Ann. Phys. (Leipz.) 24 (1935) 636; Ann. Phys. (Leipz.) 24 (1935) 665.
[411] R. Landauer, J. Appl. Phys. 23 (1952) 779.
[412] S. Kirpatrick, Phys. Rev. Lett. 27 (1971) 1722.
[413] J. Bernasconi, Phys. Rev. B 7 (1973) 2252; Phys. Rev. B 9 (1974) 4575.
[414] R.J. Elliot, J.A. Krumhansl, P.L. Leath, Rev. Mod. Phys. 46 (1974) 465.
[415] D. Stroud, Phys. Rev. B 12 (1975) 3368.
[416] H.F. Eicke, R. Kubick, R. Hasse, I. Zschokke, in: K.L. Mittal, B. Lindman (Eds.), Surfactants in Solution, Plenum Press, New York, 1984, p. 1533.
[417] A.M. Cazabat, D. Chateney, F. Guering, D. Langevin, J. Meunier, D. Sorba, J. Lang, R. Zana, M. Paillette, in: K.L. Mittal, B. Lindman (Eds.), Surfactants in Solution, Plenum Press, New York, 1984, p. 1737.
[418] A.M. Cazabat, D. Langevin, J. Meunier, A. Pouchelon, J. Phys. Lett. 43 (1982) L89.
[419] M.W. Kim, J.S. Haung, Phys. Rev. A34 (1986) 719.
[420] A.L.R. Bug, S.A. Safran, G.S. Grest, I. Webman, Phys. Rev. Lett. 55 (1985) 1896.
[421] S. Bhattacharya, J. Stokes, M.W. Kim, J.S. Huang, Phys. Rev. Lett. 55 (1985) 1884.
[422] M.A. Van Dijk, Phys. Rev. Lett. 55 (1985) 1003.
[423] S.A. Safran, G.S. Grest, A.L.R. Bug, in: H.L. Rosano, M. Clausse (Eds.), Microemulsion Systems, Marcel Decker, New York, 1987, p. 235.
[424] H.F. Eicke, W. Meier, H. Hammerick, Langmuir 10 (1990) 2223.
[425] S. Friberg, I. Lapczynaska, G. Gillberg, J. Colloid Interf. Sci. 56 (1976) 19.
[426] C. Cametti, P. Codastefano, P. Tartaglia, S.H. Chen, J. Rouch, Phys. Rev. A 45 (1992) R5358.

[427] H.F. Eicke, S. Geiger, R. Hilfiker, F.A. Sauer, H. Thomas, in: R. Pynn, T. Riste (Eds.), Time Dependent Effects in Disordered Materials, Plenum Press, New York, 1987, p. 219.
[428] M. Lagues, J. Phys. Lett. 40 (1979) L331.
[429] L. Mukhopadhyay, P.K. Bhattacharya, S.P. Moulik, Colloids Surf. 50 (1990) 295.
[430] P. Alexandridis, J.F. Holzwarth, T.A. Hatton, J. Phys. Chem. 99 (1995) 99.
[431] S.A. Safran, L.A. Turkevich, Phys. Rev. Lett. 50 (1985) 1930.
[432] G.S. Grest, I. Webman, S.A. Safran, A.L.R. Bug, Phys. Rev. A33 (1986) 2842.
[433] J.S. Haung, S.A. Safran, M.W. Kim, G.S. Grest, M. Kotlarchyk, N. Quirke, Phys. Rev. Lett. 53 (1984) 593.
[434] R. Hilfiker, H.F. Eicke, S. Geiger, G. Furler, J. Colloid Interf. Sci. 105 (1985) 378.
[435] J. Peyrelasse, M. Moha-Quchane, C. Boned, Phys. Rev. A 38 (1988) 904.
[436] E. Dutkiewicz, B.H. Robinson, J. Electroanal. Chem. 251 (1988) 11.
[437] A. Maitra, C. Mathew, M. Varshney, J. Phys. Chem. 94 (1990) 5290.
[438] Y. Feldman, N. Kozlovich, I. Nir, et al., J. Phys. Chem. 100 (1996) 3745.
[439] J.S. Haung, M. Kotlarchyk, Phys. Rev. Lett. 57 (1986) 2587.
[440] M. Kotlarchyk, S.H. Chen, J.S. Huang, M.W. Kim, Phys. Rev. A 29 (1984) 2054.
[441] S.A. Safran, I. Webman, G.S. Grest, Phys. Rev. A 32 (1985) 506.
[442] B. Lagourette, J. Peyrellase, C. Boned, M. Clausse, Nature 281 (1979) 60.
[443] M. Lagues, R. Ober, C. Taupin, J. Phys. (Paris) Lett. 39 (1978) L487.
[444] M. Clausse, J. Peyrellase, C. Boned, J. Heil, L. Nicolas-Morgantini, A. Zradha, in: K.L. Mittal (Ed.), Solution Properties of Surfactants, Plenum Press, New York, 3 (1983) 1583.
[445] Y. Feldman, N. Kozlovich, I. Nir, N. Garti, Phys. Rev. E51 (1995) 478.
[446] C.D. Miteseu, M.J. Musolf, J. Phys. Lett. (Paris), L-679 (1983).
[447] S. Ray, S. Paul, S.P. Moulik, J. Colloid Interf. Sci. 183 (1996) 6.
[448] S. Ray, S.R. Bisal, S.P. Moulik, Proc. Natl. Conf. Physical and Chemical Aspects of Organised Biological Assemblies, Jadavpur Uni. (Calcutta, India), 1991, pp. 85–89.
[449] C.J.F. Böttcher, Recl. Trav. Chim. 64 (1945) 47.
[450] C.G. Granqvist, O. Hunderi, Phys. Rev. B 18 (1978) 1554.
[451] J. Bernasconi, J.J. Wiesmann, Phys. Rev. B 13 (1976) 1131.
[452] M.T. Clarkson, S.I. Smedly, Phy. Rev. A 37 (1988) 2070.
[453] M. Moha-Quachane, J. Peyrelasse, C. Boned, Phys. Rev. A 35 (1987) 3027.
[454] C. Mathew, P.K. Patanjali, A. Nabi, A.N. Maitra, Colloids Surfs. 30 (1988) 253.
[455] L. Mukhopadhyay, P.K. Bhattacharya, S.P. Moulik, Ind. J. Chem. 32A (1993) 485.
[456] S. Ray, S.R. Bisal, S.P. Moulik, J. Chem. Soc. Faraday Trans. 1 (1993) 3277.
[457] H.E. Eicke, M. Gauthier, H. Hammerick, J. Phys. II France 3 (1993) 255.
[458] L.M.M. Nazario, T.A. Hatton, J.P.S.G. Crespo, Langmuir 12 (1996) 6326.
[459] L. Garcia-Rio, J.R. Leis, J.C. Mejunto, M.E. Pena, Langmuir 10 (1994) 1676.
[460] F.H. Florenzo, M.J. Politi, Brazilian J. Med. Biol. Res. 30 (1997) 179.
[461] P. Lianos, S. Modes, G. Staikos, W. Brown, Langmuir 8 (1992) 1054.
[462] J.P. Huruguen, M.P. Pileni, Eur. Biophys. J. 19 (1991) 103.
[463] J.P. Huruguen, M. Autheir, J.L. Greffe, M.P. Pileni, Langmuir 7 (1991) 243.
[464] P. Brochette, C. Petit, M.P. Pileni, J. Phys. Chem. 92 (1988) 3505.
[465] M.P. Pileni, J.P. Huruguen, C. Petit, in: D.M. Bloor, E. Wyn-Jones (Eds.), The Structure Dynamics and Equilibrium Properties of Colloidal Systems, Kluewer Academic Publishers, The Netherlands, 1990, p. 355.
[466] J.M. Tingey, J.L. Fulton, D.W. Matison, R.D. Smith, J. Phys. Chem. 95 (1991) 1145.
[467] J. Eastoe, B.H. Robinson, D.C. Steytler, D. Thron-lesson, Adv. Colloid Interf. Sci. 36 (1991) 1.
[468] E.W. Kaler, J.F. Billman, J.L. Fulton, R.D. Smith, J. Phys. Chem. 95 (1991) 458.
[469] J. Eastoe, W.K. Young, B.H. Robinson, D.C. Steytler, J. Chem. Soc. Faraday Trans. 86 (1990) 2883.
[470] R.D. Smith, J.P. Blitz, J.L. Fulton, ACS Symp. Ser. 406 (Super Critical Fluid Sci. Technol.) 165 (1989).
[471] C. Boned, Z. Saidi, P. Zans, J. Peyrelasse, Phys. Rev. E 49 (1994) 5295.

[472] R.A. Mackay, C. Hermansky, R. Agarwal, in: M. Kerker (Ed.), Colloid and Surface Science (Aersol Emulsions and Surfactants), Academic Press, New York, 2 (1976) 289.
[473] C. Burger-Guerrisi, C. Tondre, Colloid Polym. Sci. 73 (1987) 30.
[474] J.C. Maxwell, Electricity and Magnetism, 3rd ed., Oxford University, London, 1 (1892) 314.
[475] S.P. Moulik, S. Ray, Pure Appl. Chem. 66 (1994) 521.
[476] M.A. Van Dijk, E. Broekman, J.G.H. Joosten, D. Bedeaux, J. Phys. 47 (1986) 727.
[477] J. Smeets, J.P.M. Van der Ploeg, G.J.M. Koper, D. Bedeaux, Langmuir 10 (1984) 1387.
[478] G.J.M. Koper, D. Bedeaux, Physica A 187 (1992) 489.
[479] C. Robertus, W.H. Philipse, J.G.H. Joosten, Y.K. Levine, J. Chem. Phys. 90 (1989) 4482.
[480] P.D.I. Fletcher, A.M. Howe, B.H. Robinson, J. Chem. Soc. Faraday Trans. 1 (1987) 985.
[481] B.W. Ninham, S.J. Chen, D.F. Evans, J. Phys. Chem. 88 (1984) 5855.
[482] V. Chen, D.F. Evans, B.W. Ninham, J. Phys. Chem. 91 (1987) 1823.
[483] O. Abillon, B.P. Binks, D. Langevin, R. Ober, J. Phys. Chem. (and references therein) 92 (1988) 9411.
[484] L. Mukhopadhyay, P.K. Bhattacharya, S.P. Moulik, Colloids Surfs. 50 (1990) 295.
[485] L. Mukhopakhyay, P.K. Bhattacharya, S.P. Moulik, Ind. J. Chem. 32A (1993) 485.
[486] B.K. Paul, M.L. Das, D.C. Mukherjee, S.P. Moulik, Ind. J. Chem. 30A (1991) 328.
[487] R.F. Berg, M.R. Boldover, J.S. Huang, J. Chem. Phys. 87 (1987) 3687.
[488] R.A. Day, B.H. Robinson, J.H.R. Clarke, J.V. Doherty, J. Chem. Soc. Faraday Trans. I (1979) 132.
[489] E. Guth, R. Simha, Kolloid Zh. 74 (1966) 266; G.K. Batchelor, J. Fluid Mech. 93 (1977) 97.
[490] J. Rouviere, J.M. Couret, R. Marrony, J.L. Dejradin, C.R. Hebd, Acad. Sci. Ser. C 286 (1978) 5.
[491] J.B. Peri, J. Colloid Interf. Sci. 29 (1969) 6; J. Am. Oil Chem. Soc. 35 (1958) 110.
[492] Y.K. Pithapurwals, D.O. Shah, J. Am. Chem. Soc. 61 (1984) 1399.
[493] D. Quemada, D. Langevin, J. Theo. Appl. Mech. (1985) 201, special.
[494] K.E. Bennett, J.C. Hatfield, H.T. Davis, C.W. Macosko, L.E. Scriven, in: I.D. Robb (Ed.), Microemulsions, Plenum Press, New York and London, 1982.
[495] J. Peyrelasse, M. Moha-Quchane, C. Boned, Phys. Rev. A 38 (1988) 4155.
[496] C. Boned, J. Peyrelasse, J. Surf. Sci. Technol. 7 (1991) 1.
[497] M. Wong, J.K. Thomas, M. Gratzel, J. Am. Chem. Soc. 98 (1976) 2391.
[498] A.J.W.G. Visser, K. Vos, V.A. Hoek, J.S. Santema, J. Phys. Chem. 92 (1988) 759.
[499] M. Hasegawa, T. Sugimura, Y. Shindo, A. Kitahara, Colloids Surfs. 109 (1996) 305.
[500] Z.J. Nu, N.F. Zhou, R.D. Newman, Langmuir 8 (1992) 1885.
[501] A.T. Papaioannou, H.T. Davis, L.E. Scriven, in: K.L. Mittal, P. Bothorel (Eds.), Surfactants in Solution, Plenum Press, New York, 1987, 1213.
[502] H.T. Davis, J.F. Bodet, L.E. Scriven, W.G. Miller, Physica A 157 (1989) 470.
[503] J.L. Hackett, C.A. Miller, SPE Resevoir Engng. 3 (1989) 791.
[504] C.M. Chen, G.G. Warr, J. Phys. Chem. 96 (1992) 9492.
[505] A.D. Aprano, I.D. Donato, M. Goffredi, V.T. Liveri, J. Soln. Chem. 21 (1992) 323.
[506] D. Ripple, R.F. Berg, J. Chem. Phys. 97 (1992) 7761.
[507] N. Mitra, L. Mukhopadhyay, P.K. Bhattacharya, S.P. Moulik, Ind. J. Biochem. Biophys. 31 (1994) 115.
[508] S. Ray, S.P. Moulik, J. Colloid Interf. Sci. 173 (1995) 28.
[509] D.H. Everett, Basic Principles of Colloid Science, Ch. 11, Royal Chem. Soc., London, 1988.
[510] M. Kotlarchyk, E.Y. Sheu, M. Capel, Phys. Rev. A 46 (1992) 928.
[511] F. Candau, P. Buchert, I. Krieger, J. Colloid Interf. Sci. 140 (1990) 466.
[512] I.M. Krieger, T.J. Dougherty, Trans. Soc. Rheol. 3 (1959) 137.
[513] J. Peyrelasse, C. Boned, Phys. Rev. A 41 (1990) 938.
[514] Z. Saidi, C. Matthew, J. Peyrelasse, C. Boned, Phys. Rev. A 42 (1990) 872; J. Peyrelasse, C. Boned, in: S.H. Chen et al. (Eds.), Structure and Dynamics of Strongly Interacting Colloids and Supramolecular Aggregates in Solution, Kluwer Academic Publisher, The Netherlands, 1992, pp. 801–806.
[515] H.F. Eicke, R. Kubik, Faraday Discuss. Chem. Soc. 76 (1983) 305.
[516] H.F. Eicke, R. Kubik, H. Hammerich, J. Colloid Interf. Sci. 90 (1982) 27.
[517] S.H. Chen, J.S. Huang, Phys. Rev. Lett. 37 (1985) 1888.

[518] R. Zoller, The Physics of Amphorphous Solids, Wiley, New York, 1983.
[519] C.A. Angell, J. Phys, Chem. Solids 49 (1988) 863.
[520] A. D'Aprano, G. D'Arrigo, A. Paparelli, G. Goffredi, V.T. Liveri, J. Phys. Chem. 97 (1993) 3614.
[521] G. D'Arrigo, A. Paparelli, A. D'Aprano, I.D. Donato, M. Goffredi, V.T. Liveri, J. Phys. Chem. 93 (1989) 8367; A. D'Aprano, G.D. Arrigo, M. Goffredi, A. Paparelli, V.T. Liveri, J. Chem. Phys. 95 (1991) 1304.
[522] S. Ray, S.P. Moulik, Langmuir 10 (1994) 2511.
[523] A. Katchalsky, P.S. Curran (Eds.), Nonequillibrium Thermodynamics in Biophyics, Havard University Press, Cambridge, Massachusetts, 1967.
[524] R.C. Baker, A.T. Florescence, R.H. Ottewill, Th.F. Tadros, J. Colloid Interf. Sci. 100 (1984) 332.
[525] T.F. Tadros, in: K.L. Mittal, B. Lindman (Eds.), Surfactants in Solution, Plenum, New York, 1984.
[526] V. Vand, J. Phys. Colloid Chem. 52 (1948) 277.
[527] J.V. Robinson, J. Phys. Colloid Chem. 53 (1949) 1042.
[528] C.A. Miller, R. Hwan, W. Buton, T. Fort, J. Colloid Interf. Sci. 61 (1977) 554.
[529] A.M. Cazabat, D. Langevin, J. Chem. Phys. 74 (1981) 3148.
[530] S. Ray, S.R. Biswal, S.P. Moulik, J. Surf. Sci. Technol. 8 (1992) 191.
[531] H. Eiler, Kolloid Z. 97 (1941) 313; Kolloid Z. 102 (1943) 154.
[532] D.G. Thomas, J. Colloid Sci. 20 (1965) 267.
[533] S.P. Moulik, J. Phys. Chem. 72 (1968) 4682.
[534] H. Erying, D. Henderson, B.J. Stover, E.M. Erying, Statistical Mechanics and Dynamics, Wiley, New York, 1964, 460.
[535] S.P. Moulik, J. Ind. Chem. Soc. 49 (1972) 483; S.P. Moulik, D.P. Khan, Ind. J. Chem. 15A (1977) 267.
[536] A.B. Mandal, S. Ray, A.M. Biswas, S.P. Moulik, J. Phys. Chem. 84 (1980) 856; A.B. Mandal, S. Gupta, S.P. Moulik, Ind. J. Chem. 24A (1985) 670.
[537] W.L. Hinze, Ann. Chim. 77 (1987) 167.
[538] T.A. Hatton, in: J.F. Scamehorn, J.H. Harwell (Eds.), In Surfactant-Based Separation Processes, Marcel Decker, Inc., New York, 1989, p .57.
[539] M.P. Pileni (Ed.), Structure and Reactivity in Reverse Micelles, Elsevier, Amsterdam, 1989.
[540] E.B. Leodidis, T.A. Hatton, J. Phys. Chem. 94 (1990) 6400; E.B. Leodidis, T.A. Hatton, in: D.M. Bloor, E. Wyn-Jones (Eds.), The Structure, Dynamics and Equilibrium Properties of Colloidal Systems, Kluwer Academic Publishers, Netherlands, 1990, p. 201; T.A. Hatton, in: W.L. Hinze, D.W. Armstrong (Eds.), Ordered Media and Chemical Separations ACS Symps. Ser. ACS, Washington, DC, 1987, 342.
[541] M.E. Leser, P.L. Luisi, Biotechnol. Tech. 3 (1989) 149; Chimica 44 (1990) 270.
[542] S. Furusaki, K. Kishi, J. Chem. Eng. Jpn. 23 (1990) 91.
[543] M. Adachi, M. Harada, A. Shioi, Y. Sato, J. Phys. Chem. 95 (1991) 7925.
[544] E.B. Leodidis, T.A. Hatton, J. Colloid Interf. Sci. 147 (1991) 163.
[545] J.H. Fendler, F. Nome, J. Nagyvary, Mol. Evol. 5 (1975) 215.
[546] A. Dossena, V. Rizzo, R. Machelli, G. Cosnati, P.L. Luisi, Biochem. Biophys. Acta 446 (1976) 493.
[547] C. Hansch, A. Leo, Substituent Constants for Correlation Analysis in Chemistry and Biology, Wiley, New York, 1979.
[548] Y. Nozaki, C. Tanford, J. Biol. Chem. 246 (1971) 2211.
[549] H.B. Bull, K. Breese, Arch. Biochem. Biophys. 61 (1974) 665.
[550] P.D.I. Fletcher, J. Chem. Soc. Faraday Trans. 1 (1986) 2651.
[551] E.B. Leodidis, A.S. Bommarius, T.A. Hatton, J. Phys. Chem. 95 (1991) 5493.
[552] P. Plucinski, W. Nitsch, Ber. Bunsenges. Phys. Chem. 93 (1989) 338.
[553] S.R. Dungan, T. Bausch, T.A. Hatton, P. Plucinski, W. Nitsch, J. Colloid Interf. Sci. 145 (1991) 33.
[554] P. Plucinski, W. Nitsch, J. Colloid Interf. Sci. 154 (1992) 104.
[555] P. Plucinski, W. Nitsch, J. Phys. Chem. 97 (1993) 8933.
[556] P. Plucinski, W. Nitsch, Langmuir 10 (1994) 371.
[557] R. Leung, D.O. Shah, J. Colloid Interf. Sci. 120 (1987) 330.
[558] J. Lang, N. Lalem, R. Zana, J. Phys. Chem. 95 (1991) 9533.
[559] A. Caponetti, A. Lizzio, R. Triolo, W.L. Griffith, J.S. Johnson, Jr., Langmuir 8 (1992) 1554.

[560] E.A. Lissi, D. Engel, Langmuir 8 (1992) 452.
[561] P. Plucinski, J. Reitmeir, Colloids Surfs. A 97 (1995) 157.
[562] P.L. Luisi, F.J. Bonner, A. Pellegrini, P. Wiget, R. Wolf, Helv. Chim. Acta 62 (1979) 740.
[563] P. Meier, V.E. Imre, M. Fleschar, P.L. Luisi, in: K.L. Mittal, B. Lindman (Eds.), Surfactants in Solution, Plenum Press, New York, II (1984) 999.
[564] K. Van't Riet, M. Dekker, Proc. 3rd Eur. Congr. Biotechnol. Munich, III (1984) 541.
[565] K.E. Goklen, T.A. Hatton, Biotechnol. Prog. 1 (1985) 69.
[566] M. Decker, K. Van't Riet, S.R. Weijers, J.W.A. Baltussen, C. Laane, B.H. Bijsterbosch, Chem. Eng. J. 33 (1986) B27.
[567] M. Dekker, K. Van't Riet, B.H. Bijsterbosch, R.B.G. Wolbert, R. Hillhorst, AIChE J. 35 (1989) 321.
[568] M. Dekker, J.W.A. Baltussen, K. Van't Riet, B.H. Bijsterbosch, C. Laane, R. Hilhorst, in: C. Laane, J. Tamper, M.D. Lilly (Eds.), Biocatalysis in Organic Media, Proc. Int. Symp., Wageningen, December, 1986, Elsevier, Amsterdam, 1987, p. 285.
[569] M. Dekker, K. Van'Riet, J.J. Van Der Pol, J.W.A. Baltussen, R. Hilhorst, B.H. Bijsterbosch, Chem. Eng. J. 46 (1991) B69.
[570] M. Dekker, K. Van'Riet, B.H. Bijsterbosch, P. Fijneman, R. Hishorst, Chem. Eng. Sci. 45 (1990) 2949.
[571] R.B.G. Wolbert, R. Hilhorst, G. Voskuilen, H. Nachtegal, M. Dekker, K. Van'Riet, B.H. Bijsterbosch, Eur. J. Biochem. 184 (1989) 627.
[572] R. Hilhorst, P. Fijneman, D. Heering, et al., Pure App. Chem. 64 (1992) 1765.
[573] K.E. Goklen, Ph.D. Dissertation, Massachussets institute of Technology, Cambridge, Massachussetts, 1986.
[574] K.E. Goklen, T.A. Hatton, Proc. Int. Solvent Extraction Conf. 3 (1986) 587.
[575] K.E. Goklen, T.A. Hatton, Sep. Sci. Technol. 22 (1987) 831.
[576] T.A. Hatton, in: W.L. Hinze, D.w. Armstrong (Eds.), Ordered Media in Chemical Separations, A.C.S. Symp. Ser., 342 (1987) 170.
[577] J.M. Woll, M.S. Thesis, MIT, Cambridge, Mass, 1987.
[578] J.M. Woll, A.S. Dillon, R.S. Rahaman, T.A. Hatton, in: R. Burgess (Ed.), Protein Purification: Micro to Macro, Alan R. Liss, Inc., New York, 1987, 117.
[579] R.S. Rahaman, J.Y. Chee, J.M.S. Cabral, T.A. Hatton, Biotechnol. Prog. 4 (1988) 218.
[580] J.M. Holl, T.A. Hatton, M.L. Yarmush, Biotechnol. Prog. 5 (1989) 57.
[581] P.L. Luisi, V.E. Mire, H. Jaeckle, A. Pande, in: D.D. Breimer, P. Speiser (Eds.), Topics in Pharmaceutical Sciences, Elsevier, Amsterdam, 1983, p. 243.
[582] M.E. Leser, G. Wei, P.L. Luisi, M. Maestro, Biochem. Biophys. Res. Commum. 135 (1986) 629.
[583] B.D. Kelley, D.J.C. Wang, T.A. Hatton, Biotechnol. Bioeng., 42 (1993) 1119 and 1209.
[584] D.W. Armstrong, W. Li, Annal. Chem. 60 (1988) 88.
[585] G. Marcozzi, N. Correa, P.L. Luisi, M. Caselli, Biotechnol. Bioeng. 38 (1991) 1239.
[586] K. Belafi-Bako, A. Dombi, L. Szabo, E. Nagy, Biotechnol. Tech. 9 (1995) 59.
[587] T. Kingugasa, K. Wantanabe, H. Takeuchi, Ind. Eng. Chem. Res. 31 (1992) 1827.
[588] R. Kuboi, Y. Mori, I. Komasawa, Kagaku Kogoku Ronbonshu 15 (1989) 669.
[589] B.A. Andrew, D.L. Pyle, J.A. Asenjo, Biotechnol. Bioeng. 43 (1994) 1052.
[590] L. Kawakami, S.R. Dungan, Langmuir 12 (1996) 4073.
[591] A Carlson, R. Nagarajan, Biotechnol. Prog. 8 (1992) 85.
[592] M.J. Pires, M.R. Aires-Barros, J.M.S. Cabral, Biotechnol. Prog. 12 (1996) 290.
[593] A. Delahodde, M. Vacher, C. Nicto, M. Waks, FEBS Lett. 172 (1984) 343; A. Delahodde, M. Vacher, M. Vincent, J. Gally, M. Waks, Biochemistry 24 (1985) 7024.
[594] M. Leser, G. Wei, P. Luthi, et al., J. de Chim. Phys. 84 (1985) 1113.
[595] P.L. Luisi, C. Laane, Trends Biotechnol. 4 (1986) 153.
[596] S. Giovenco, C. Laane, R. Hilhorst, Proc. 4th European Congress on Biotechnol., Elsevier, Amsterdam, II (1987) pp. 503–506.
[597] G. Haering, P.L. Luisi, F. Meussdoerffer, Biochem. Biophys. Res. Commun. 127 (1985) 911; G. Haering, A. Pessina, F. Meussdoerffer, S. Hochkoeppler, P.L. Luisi, Ann. N.Y. Acad. Sci. 506 (1987) 334.

[598] C. Laane, S. Boeren, K. Vos, Trends Biotechnol. 3 (1985) 251.
[599] C. Laane, S. Boren, K. Vos, C. Veeger, Biotechnol. Bioeng. 30 (1987) 81.
[600] T.A. Hatton, in: J.F. Scamehorn, J.H. Harwell (Eds.), Surfactant Based Separation Processes, Marcel Dekker Inc., New York and Basel, 1989, p. 55.
[601] L.E. Kawakami, S.R. Dungan, Langmuir 12 (1996) 4073.
[602] K. Osseo-Assare, M.E. Keeney, Sep. Sci. Technol. 15 (1980) 999.
[603] F.J. Ovejero-Escudero, H. Angelino, G. Casamatta, J. Disp. Sci. Technol. 8 (1987) 89.
[604] E.B. Leodidis, T.A. Hatton, Langmuir 5 (1989) 741.
[605] E. Gulari, C. Vijayalakshmi, Paper presented at the ACS symposium, Los Angeles, 1988.
[606] P.A. Winsor, Solvent Properties of Amphiphilic Compounds, Butterworths, London, 1954.
[607] M.L. Robbins, J. Bock, J. Colloid Interf. Sci. 124 (1988) 462.
[608] A. Lampert, R.U. Martinelli, Chem. Phys. 88 (1984) 299.
[609] C.S. Vijayalakshmi, A.V. Annapragada, E. Gulari, Sep. Sci. Technol. 25 (1990) 711.
[610] C.S. Vijayalakshmi, E. Gulari, Sep. Sci. Technol. 26 (1991) 291.
[611] T.E. Bausch, P. Plucinski, W. Nitsch, J. Colloid Interf. Sci. 150 (1992) 226.
[612] R.J. Hunter Foundations of Colloid Science, Clarendon Press, Oxford, 1989.
[613] W. Nitsch, P. Plucinski, J. Ehrlenspiel, J. Phys. Chem. B 101 (1997) 4024.
[614] H.R. Rabie, J.H. Vera, Langmuir 11 (1995) 1162.
[615] A.W. Adamson, J. Colloid Interf. Sci. 29 (1969) 261.
[616] S. Mukherjee, C.A. Miller, T. Fort, J. Colloid Interf. Sci. 91 (1983) 223.
[617] J.F. Jeng, C.A. Miller, Colloids Surfs. 28 (1987) 247.
[618] E. Ruckenstein, R. Krishnan, J. Colloid Interf. Sci. 71 (1979) 321.
[619] J.Th. Overbeek, G.J. Verhoecks, P.L. deBruyn, H.N.W. Lekkerkerker, J. Colloid Interf. Sci. 119 (1987) 422.
[620] R.D. Noble, J.D. Way (Eds.), ACS Symp. Ser., 347 (1987).
[621] S. Schlösser, E. Kossaczky, J. Radio Anal. Nucl. Chem. 101 (1986) 115.
[622] R.M. Izatt, J.D. Lamb, R.L. Bruening, Sep. Sci. Technol. 23 (1988) 1645.
[623] H.L. Rosano, P. Duby, J.H. Schulman, J. Phys. Chem. 65 (1961) 1704.
[624] R. Ashton, L.K. Steinrauf, J. Mol. Biol. 49 (1970) 547.
[625] W.I. Higuchi, A.H. Ghanem, A.B. Bikhazi, Fed. Proc. Fed. Am. Soc. Exp. Biol. 29 (1970) 1327.
[626] K.H. Wong, K. Yagi, J. Smid, J. Membr. Biol. 18 (1994) 379.
[627] J.D. Lamb, J.J. Christensen, S.R. Izatt, K. Bedke, M.S. Astin, R.M. Izatt, J. Am. Chem. Soc. 102 (1980) 3399.
[628] C.F. Reusch, E.L. Cussler, AIChE J. 19 (1973) 736.
[629] Y. Kobuke, K. Hanji, K. Horiguchi, M. Asada, Y. Nakayama, J. Furukawa, J. Am. Chem. Soc. 98 (1976) 7414.
[630] M. Krich, J.M. Lehn, Angew. Chem. Int. Ed. Engl. 14 (1975) 555.
[631] E. Pefferkorn, R. Varoqui, J. Colloid Interf. Sci. 52 (1975) 89.
[632] N.N. Li, A.L. Shrier, in: N.N. Li (Ed.), Recent Developments in Separation Science, CRC Press, Cleveland, I (1972) 163.
[633] N.N. Li, AIChE J. 17 (1971) 459.
[634] N.N. Li, Ind. Eng. Chem. Process Des. Dev. 10 (1971) 215.
[635] J.H. Fendler, A. Romero, Life Sci. 20 (1977) 1109.
[636] R.A. Bartsch, W.A. Charewicz, S.I. Kang, W. Walkowiak, ACS Symp. Ser. 347 (1987) 86.
[637] C. Tondre, A. Xenakis, Colloid Polym. Sci. 260 (1982) 232.
[638] A. Xenakis, C. Tondre, J. Phys. Chem. 87 (1983) 4737.
[639] C. Tondre, A. Xenakis, Faraday Discuss. Chem. Soc. 77 (1984) 115.
[640] A. Xenakis, C. Tondre, J. Colloid Interf. Sci. 117 (1987) 442; Talanta 34 (1987) 509.
[641] A. Derouiche, C. Tondre, J. Chem. Soc. Faraday Trans. 1 (1989) 3301.
[642] A. Derouiche, C. Tondre, Colloids Surfs. 48 (1990) 243.
[643] C. Tondre, M. Boumezioud, J. Phys. Chem. 93 (1989) 846.
[644] M. Boumezioud, A. Derouiche, C. Tondre, J. Colloid Interf. Sci. 128 (1989) 422.
[645] H.S. Kim, C. Tondrer, Sep. Sci. Technol. 24 (1989) 485.
[646] M. Ismael, C. Tondre, J. Membr. Sci. 72 (1992) 181.

[647] J. Wiencek, S. Qutubuddin, Sep. Sci. Technol. 27 (1992) 1407.
[648] J. Wiencek, S. Qutubuddin, Sep. Sci. Technol. 27 (1992) 1211.
[649] W.J. Ward, AIChE J. 16 (1970) 405.
[650] E.L. Cussler, Multicomponent Diffusion, New York, 1976.
[651] K. Larson, J. Wiencek, Environm. Prog. 13 (1994) 253.
[652] K. Larson, B. Raghuraman, J. Wiencek, Ind. Engg. Chem. Res. 33 (1994) 1612.
[653] K. Larson, B. Raghuraman, J. Wiencek, J. Membr. Sci. 91 (1994) 231.
[654] M. Hebrant, P. Mettelin, C. Tondre, J.P. Joly, C. Larpent, X. Chassery, Colloids Surfs. A 75 (1993) 257.
[655] C. Tondre, M. Hebrant, M. Perdicakis, J. Bessiere, Langmuir 13 (1997) 1146.
[656] E. Paatero, J. Sjoblom, S.K. Datta, J. Colloid Interf. Sci. 138 (1990) 388.
[657] D. Bauer, J. Komornicki, Int. Solv. Extr. Conf., 1983, p. 315.
[658] M.L. Robbins, U.S. Patent 3641 (1972) 181.
[659] T. Flaim, S.E. Friberg, ibid 16 (1981) 1467.
[660] K. Osseo-Asare, Colloids Surf. 29 (1988) 403; Sep. Sci. Technol. 23 (1988) 1269.
[661] A.G. Gaonkar, R.D. Neuman, J. Colloid Interf. Sci. 119 (1987) 251.
[662] P. Fourre, D. Bauer, J. Lemerle, Anal. Chem. 55 (1983) 662.
[663] P. Fourre, D. Bauer, Solvent Extr. Ion. Exch. 1 (1983) 463.